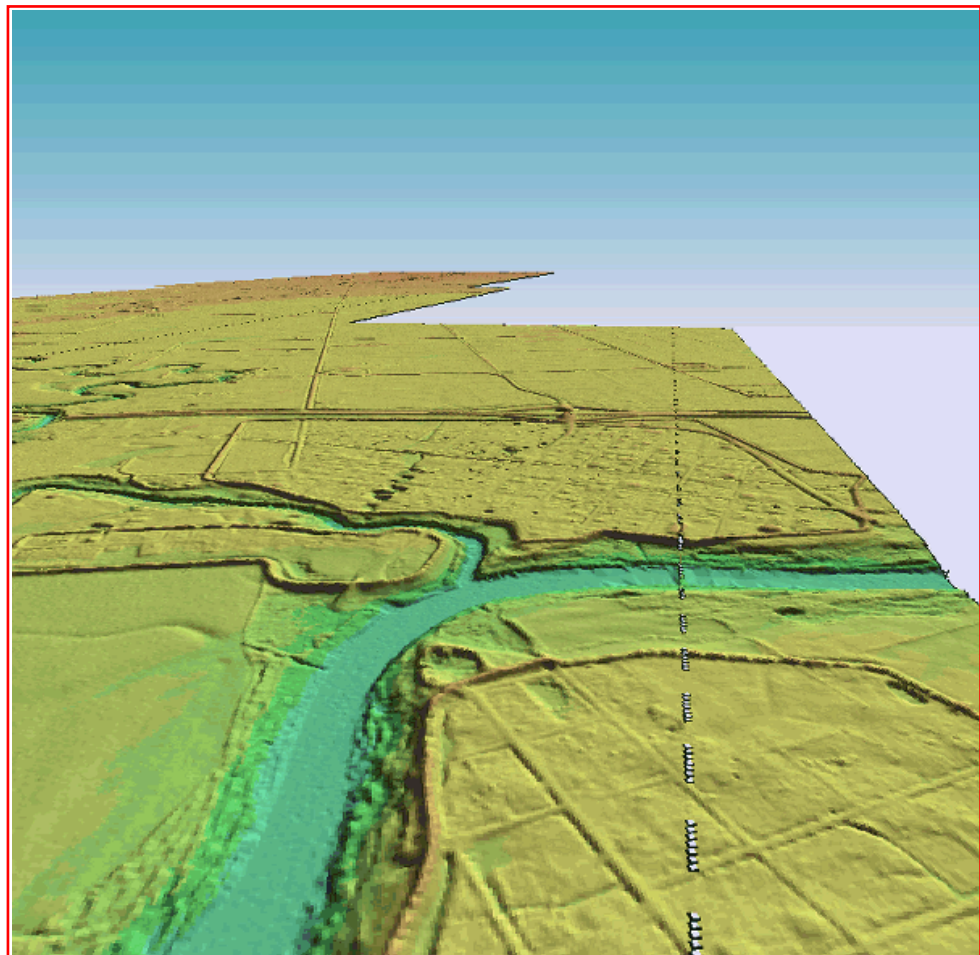Topographic Engineering Center

**US Army Corps
of Engineers ®**

Engineer Research and
Development Center

Evaluating IFSAR and LIDAR Technologies
Using ArcInfo: Red River Pilot Study

July 2000

James J. Damron and Carlton Daniel

REPORT DOCUMENTATION PAGE

Form Approved
OMB No. 0704-0188

1. AGENCY USE ONLY *(Leave blank)*	2. REPORT DATE July 2000	3. REPORT TYPE AND DATES COVERED Technical Report June-October1999,February 2000, May

4. TITLE AND SUBTITLE
Evaluating IFSAR and LIDAR Technologies Using ArcInfo: Red River Pilot Study

5. FUNDING NUMBERS

6. AUTHOR(S)
James J. Damron and Carlton Daniel

7. PERFORMING ORGANIZATION NAME(S) AND ADDRESS(ES)
U.S. Army Engineer Research and Development Center
Topographic Engineering Center
7701 Telegraph Road
Alexandria, VA 22315-3864

8. PERFORMING ORGANIZATION REPORT NUMBER

ERDC/TEC TR-01-2

9. SPONSORING / MONITORING AGENCY NAME(S) AND ADDRESS(ES)

10. SPONSORING / MONITORING AGENCY REPORT NUMBER

11. SUPPLEMENTARY NOTES

12a. DISTRIBUTION / AVAILABILITY STATEMENT
Approved for public release; distribution is unlimited.

12b. DISTRIBUTION CODE

13. ABSTRACT *(Maximum 200 words)*
The 1997 Red River flood resulted in catastrophic damage to residential, commercial, industrial, agricultural, and public properties in large portions of the Red River Valley in Minnesota and North Dakota, and in the Province of Manitoba, Canada. In the aftermath of the flood, the U.S. and Canadian governments asked the International Joint Commission (IJC) to analyze the cause and effects and to recommend ways to reduce the impact of future floods. In support of the IJC study, the U.S. Army Engineer District, Saint Paul, requested assistance from the U.S. Army Engineer Research and Development Center (ERDC), Topographic Engineering Center (TEC) to evaluate emerging airborne remote-sensing technologies for application to crisis management support. A pilot study was conducted using both Interferometric Synthetic Aperture Radar (IFSAR) and LIght Detection and Ranging (LIDAR) collection systems to determine the correct mix of technologies required. The major objectives of the study were to develop and implement a data fusion technique to merge IFSAR and LIDAR DEMs and to test the hydrological flow of water over each respective DEM. The results of this study will provide the Red River task force with a cost comparison for each of the technologies tested during this project and a list of recommendations for performing the remainder of the basin collection.

14. SUBJECT TERMS
IFSAR, LIDAR, ArcInfo, DEM, Arc Interchange File, NAD 83, NAVD 88, FEMA

15. NUMBER OF PAGES
122

16. PRICE CODE

17. SECURITY CLASSIFICATION OF REPORT UNCLASSIFIED	18. SECURITY CLASSIFICATION OF THIS PAGE UNCLASSIFIED	19. SECURITY CLASSIFICATION OF ABSTRACT UNCLASSIFIED	20. LIMITATION OF ABSTRACT

TABLE OF CONTENTS

TABLE OF CONTENTS (Continued)

LIST OF FIGURES

LIST OF TABLES

PREFACE

ACKNOWLEDGMENTS

EVALUATING IFSAR AND LIDAR TECHNOLOGIES
USING ARCINFO: RED RIVER PILOT STUDY

INTRODUCTION

The 1997 Red River flood resulted in catastrophic damage to residential, commercial, industrial, agricultural, and public properties in large portions of the Red River Valley in Minnesota and North Dakota and in the province of Manitoba, Canada. In the aftermath of the flood, the U.S. and Canadian governments asked the International Joint Commission (IJC) to analyze the cause and effects and to recommend ways to reduce the impact of future floods. In support of the IJC study, the U.S. Army Engineer District, Saint Paul, requested assistance from the Topographic Engineering Center (TEC), Alexandria, VA, of the U.S. Army Engineer Research and Development Center (ERDC), to evaluate emerging airborne remote-sensing technologies for application to crisis management support. A pilot study was conducted using both Interferometric Synthetic Aperture Radar (IFSAR) and LIght Detection and Ranging (LIDAR) collection systems to determine the correct mix of technologies required. A major objective of the study was to develop and implement a data fusion technique to merge the IFSAR and LIDAR Digital Elevation Models (DEM).

The Intermap STAR-3i system was used for the IFSAR data collection. For the LIDAR collection, EarthData's AeroScan system was deployed. Both systems collected data over the study area in the fall of 1998 during leaf-off conditions and before the first snowfall. TEC contracted for the Intermap IFSAR collection through the National Aeronautics and Space Administration (NASA), John C. Stennis Space Center, Science Data Buy program. The EarthData LIDAR collection was contracted through a joint effort between the Saint Paul District and the Canadian Government.

TEC developed a detailed evaluation of the DEMs of the Pembina, ND, area using a combination of the IFSAR and LIDAR technologies to provide the IJC Red River study teams with a basis for determining how additional work could be performed, the time and costs involved, and the best technology or technologies to be used. TEC examined how best to combine the IFSAR and LIDAR technologies to obtain the desired accuracy of 15-cm root-mean-square error (RMSE) or 30-cm root-mean-square (RMS) for floodplain mapping. The hydrological flow of water over the IFSAR and LIDAR DEM was assessed prior to the hydrologic modeling group receiving the data to determine what effects the two different DEMs had on surface water.

Because of its cost, LIDAR was flown over the Pembina River from Pembina, ND, to Neche, ND, to test its validity as a collection platform and to verify the DEM product. A way to combine these technologies to improve their robustness and accuracy through the development of routines within the ArcInfo software was explored. The results of this study will provide the Red River task force with a cost comparison for each of the technologies tested during this project and a list of recommendations for performing the remainder of the basin collection.

The Saint Paul District's development of a Geographic Information System (GIS) for the Red River basin emergency response system required these evaluation tasks and data fusion methodology to be executed within a GIS environment. The GIS package used in this study was ArcInfo version 7.2.1 and 8.0.1. In support of the statistical analysis, Minitab 12 and Quattro Pro 9 were used. An attempt was made to document all of the ArcInfo commands, procedures, and utilities used to assure repeatable results and reuse within the Saint Paul District's GIS development.

LIDAR

Airborne LIDAR mapping systems use a combination of three mature technologies: compact laser rangefinders, highly accurate inertial navigation systems (INS), and global positioning systems (GPS). By integrating these subsystems into a single instrument mounted in a small airplane or helicopter, it is possible to rapidly produce accurate digital topographic maps of the terrain beneath the flight path of the aircraft. Airborne LIDAR mapping instruments are active sensor systems, as opposed to passive imagery such as cameras. Current LIDAR systems offer advantages and unique capabilities compared to traditional photogrammetry. For example, airborne LIDAR mapping systems can penetrate forest canopy to map the ground beneath the treetops, accurately map the sag of electrical power lines between transmission towers, or provide accurate elevation data in areas of low relief and contrast, such as beaches.

Commercial airborne LIDAR mapping systems now are available from several instrument manufacturers while many survey companies have designed and built custom systems. Since LIDAR instruments are less sensitive to environmental conditions, such as weather, sun angle, or leaf on/off conditions, the operational range for surveying applications has been expanded. In addition, airborne laser mapping can be conducted at night with no degradation in performance.

AeroScan

The AeroScan LIDAR system is composed of a laser subsystem consisting of the source, scanning assembly, and timing electronics; a positioning and orientation subsystem consisting of the differential GPS and INS; a data storage unit; and processing software (Spencer B. Gross, Inc., 2000). The system develops a scan pattern on the ground with a variable field of view from 10 to 75 degrees. It operates at altitudes from 610 to 6,100 m (2,000 to 20,000 ft) giving a swath width of 350 to 30,000 m (1,148 to 98,425 ft). The achievable point density may vary between 1.5-m and 12-m with a horizontal range of 15-cm to 1-m and a vertical accuracy of 15- to 60-cm. Once the GPS positions are determined, the scanner position and sensor orientation are used to compute the position of the laser spot on the ground. Appropriate transformations are employed to derive the final data product in the user-specified horizontal and vertical datums. Obstructions and vegetation can be removed during the postprocessing phase, if required, to produce a bare earth DEM. The final DEM can be formatted to any user-defined system, or may be delivered as ASCII point data (x, y, z).

IFSAR

The state of the art in exploiting IFSAR for terrain information is advancing rapidly, and provides significant potential for use in crisis support operations. Unlike conventional Synthetic Aperture Radar (SAR) imagery, IFSAR data permit the generation of rectified SAR images co-registered with an accurate DEM. In addition, this imagery can have an absolute geographic accuracy of 1-m RMS or less. The rapidity with which IFSAR data can be collected and processed over wide areas and its all-weather, day-night capabilities offer significant potential for providing direct support to crisis situations.

Cognizant of expanding capabilities in radar interferometry, the U.S. Department of Defense began an aggressive program to pursue the acquisition of highly accurate computerized terrain data using IFSAR in 1992 under the sponsorship of the Defense Advanced Research Projects Agency (DARPA) with ERDC TEC as the executive agent. This program, titled Interferometric Synthetic Aperture Radar for Elevations (IFSAR-E), has been executed by the Environmental Research Institute of Michigan (ERIM), and resulted in the fabrication of an interferometric radar integrated with a GPS and INS on a Learjet 36A. The NASA Jet Propulsion Laboratory (JPL), at the California Institute of Technology, Pasadena, CA, developed processing software and the ground-processing environment. The software and ground-processing capabilities have been transitioned to Intermap Technologies Inc., Englewood, CO, and are referred to as STAR-3i.

The STAR-3i System

Traditional SAR systems gave two-dimensional (2-D) views of the earth and included geometric distortions inherent in slant-range SAR data. IFSAR was developed to provide an elevation component to SAR imagery. The additional information from interferometric techniques provides a three-dimensional (3-D) view of the earth and removes some of the geometric distortions.

Three files are generated from the IFSAR instrument: a magnitude file, correlation file, and elevation file. The magnitude file is a backscatter image that provides information on the shape of features, as well as terrain texture. The correlation image provides information on a surface or volume backscatter. The elevation data, or DEM, provides information on terrain elevation and height of features.

The STAR-3i system consists of two X-band radar antennae mounted in a Learjet 36A. Data are collected from the twin antennae simultaneously. The sets of acquired data are "interfered" by a digital correlation process to extract terrain height data used to geometrically correct the radar image. STAR-3i uses postprocessed differential GPS data, together with onboard laser-based inertial measurement data, to obtain highly accurate positioning control. Terrain height and positioning data are enhanced by calibration of the baseline (the distance between the two antennae). The accuracy of the positioning information and calibration is such

that no in-scene control points are required. The only requirement is that a ground-based GPS receiver must be located within 200 km of the data collection site so that differential GPS processing can take place.

The STAR-3i is typically flown at 12,000-m and acquires a 10-km-wide swath of 2.5-m resolution on the ground. The system has been designed to collect DEMs at a rate of 100 km^2 per minute with 1- to 3-m vertical accuracy. Improved DEM accuracy is achieved by reducing the aircraft altitude to 6,000-m, which reduces the swath width to 6 km. At this lower aircraft height, ground resolution stays the same; however, the signal-to-noise ratio is one-half that of the higher altitude, thereby improving precision in the vertical direction.

IFSAR and LIDAR PRODUCTS

The study area shaded in Figure 1 was located on the upper limb of the United States side of the Red River near the city of Pembina, ND, and included most of the Pembina River. The IFSAR and LIDAR products were delivered in a Universal Transverse Mercator (UTM) projection, Zone 14, North American Datum of 1983 (NAD 83) horizontal datum, and North American Vertical Datum of 1988 (NAVD 88) with all units in meters. The areal extents of the IFSAR and LIDAR data sets are shown in Figure 2. The orientation of the LIDAR collection was from the northwest to southeast and orientation of the IFSAR collection was from east to west.

A color-shaded relief in Figure 3 is used to show the extent of the IFSAR DEM data with an approximate area of 371 square miles (mi^2) or 960 square kilometers (km^2). Three data sets were delivered from Intermap Technologies, Inc., through the Saint Paul District for this study, GLOBAL Terrain 1 (GT1) and GT2 DEM products and magnitude images. The major difference between the GT1 and GT2 products is their vertical accuracy. The GT1 product has an approximate vertical accuracy of 1-m and the GT2 product has an approximate vertical accuracy of 1.5-m. The magnitude image is a reflective intensity image of the radar return, a sample of which is shown in Figure 4. The tiling scheme used is based on an overlarge U.S. Geological Survey (USGS) 7.5-min DEM. The Intermap GT1, GT2, and magnitude image products all were delivered at the cost of $83 per km^2 for a total cost of approximately $80,000.

In Figure 5, a color-shaded relief is used to show the extent of the LIDAR DEM data with an approximate area of 59 mi^2 or 152 km^2. Four data sets were delivered from EarthData through a Canadian contract for this study: full and separate strips in an Arc GRID format, ASCII x,y,z bare-earth surface, and ASCII x,y,z reflective surface. The full and separate strip DEMs were delivered as bare-earth products, where most of the vegetation and building structures have been removed to create a flat, smooth surface. The defined EarthData products were all delivered at the cost of $789 per km^2 for a total cost of approximately $120,000.

North

Dakota

Figure 1. Shaded Study Area
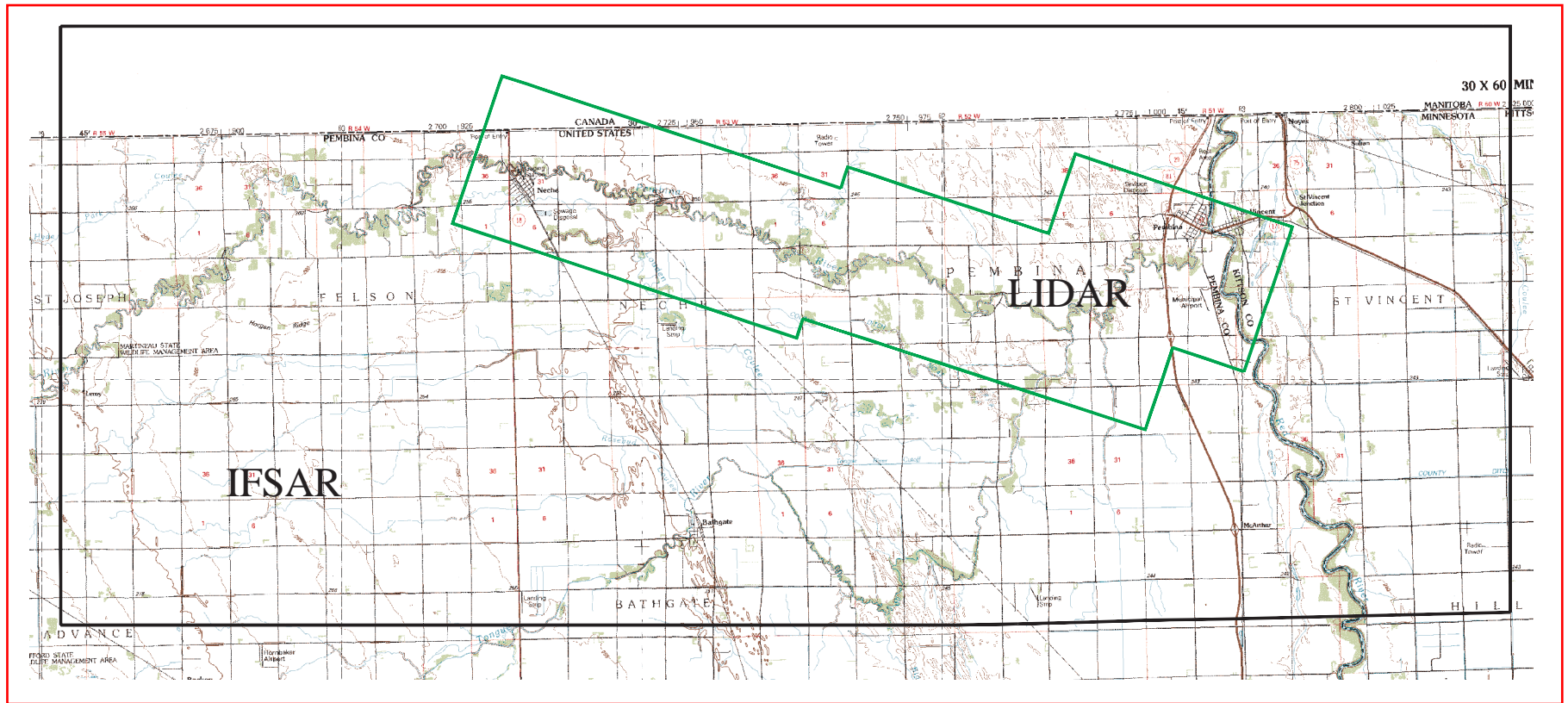
Figure 2. Extents of LIDAR and IFSAR DEMs
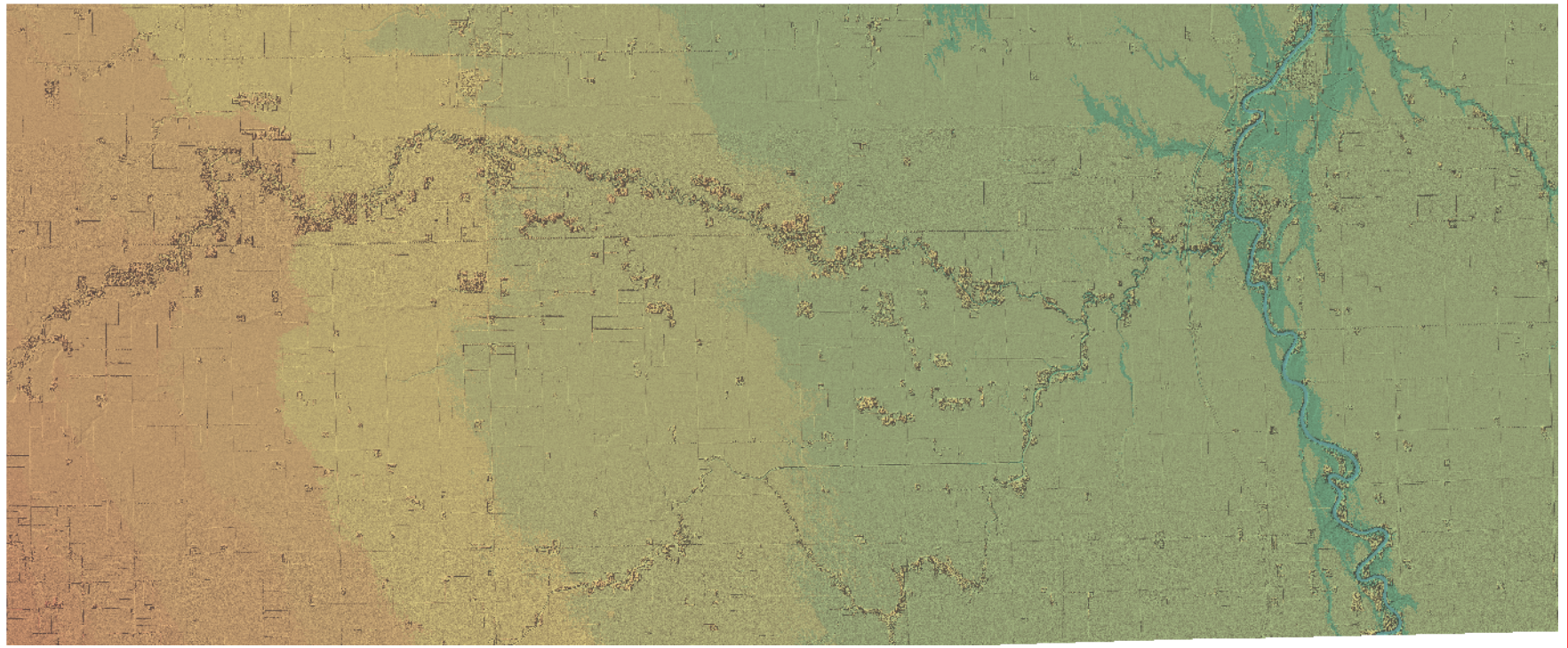
Figure 3. IFSAR Color-Shaded Relief
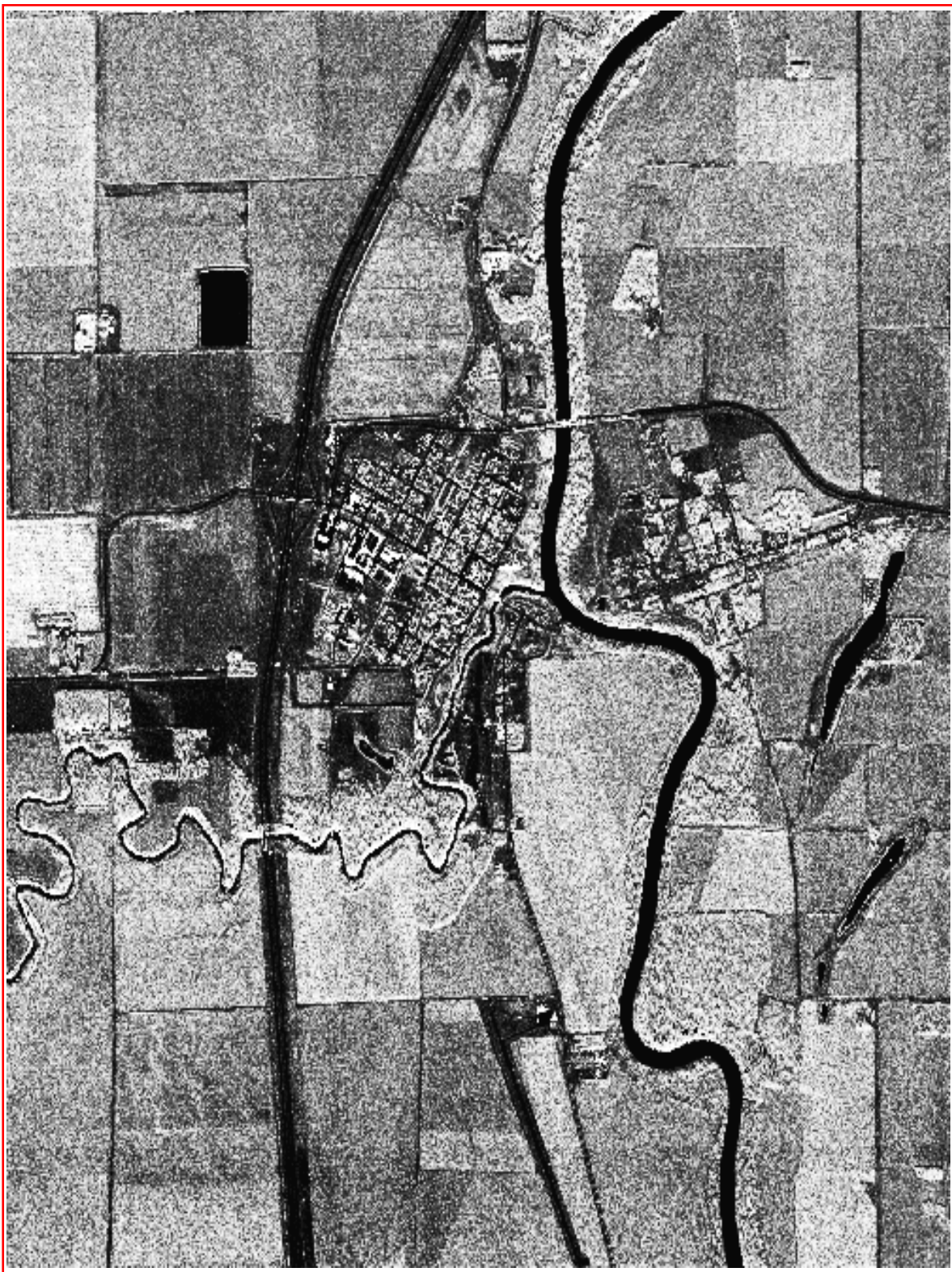
Figure 4. IFSAR Magnitude Image near Pembina, ND
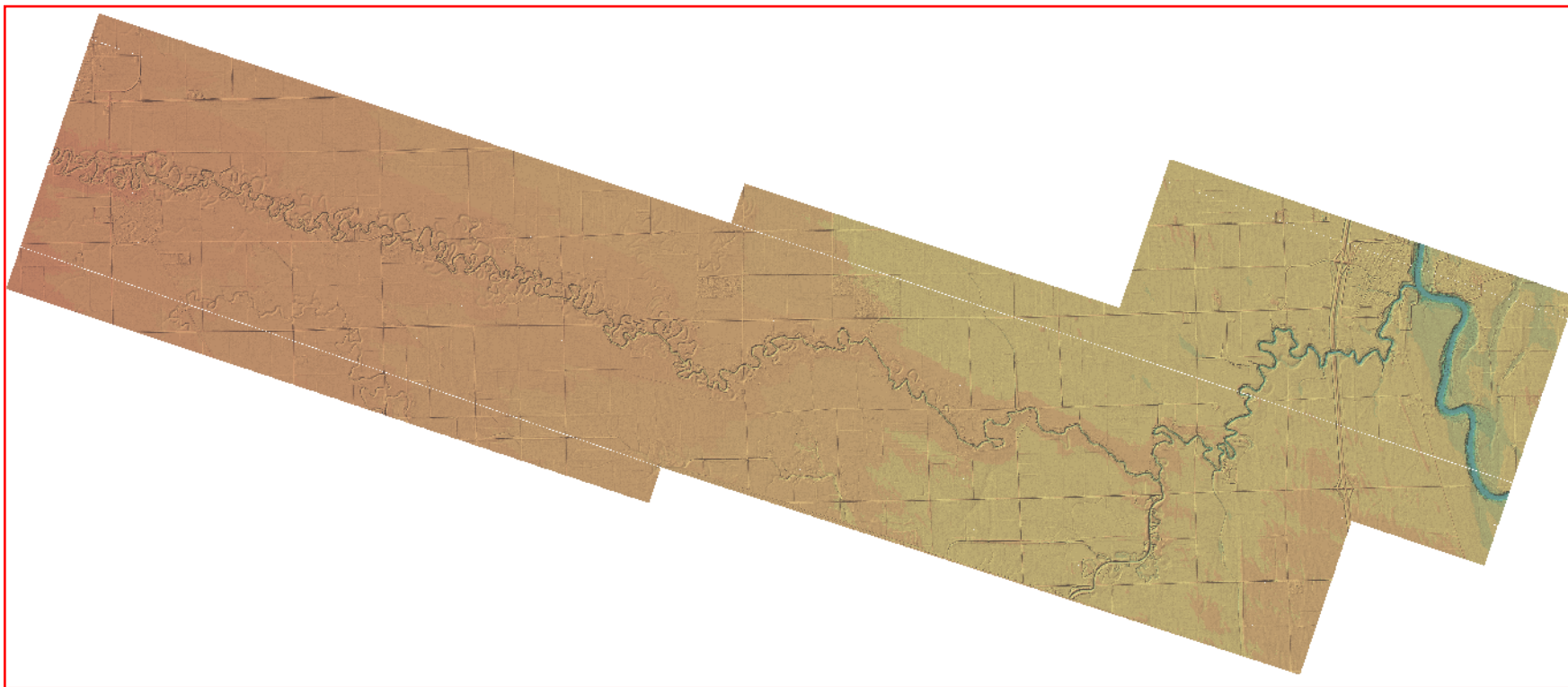
Figure 5. LIDAR Color-Shaded Relief

Data Formats

The format of the IFSAR DEM data had an IEEE floating point, 32-bit signed binary format and a 5-m post spacing with a .bil extension. The .bil extension was dropped before the IFSAR DEM data were imported into ArcInfo using the *FLOATGRID* command. The header files with .txt extensions were used as a reference, and new header files were created to import the data correctly into ArcInfo. A single DEM header file has the Intermap header parameters for file gt1n48w097h2m1.txt in Appendix A. The last two letters of IFSAR header file names are m1, which differ from the DEM files, which end with a v1. A full file listing of the delivered DEM products is shown in Table 1 except for their extensions and header files. There were a total of five files each for the GT1 and GT2 DEM products. The GT1 DEMs were merged together and used for the analysis because of the 1-m vertical accuracy.

Table 1. IFSAR DEMs

GT1 DEM	GT2 DEM
gt1n48w097h2v1	gt2n48w097h2v1
gt1n48w097h3v1	gt2n48w097h3v1
gt1n48w097h4v1	gt2n48w097h4v1
gt1n48w097h5v1	gt2n48w097h5v1
gt1n48w097h6v1	gt2n48w097h6v1

The IFSAR magnitude images were delivered in a TIFF format with a .tif extension and a 2.5-m pixel resolution. A single magnitude header file has the Intermap header parameters for file im2n48w097h2m1.txt in Appendix B. A world header file with a .tfw extension in Figure 6 was created to reference each TIFF image using parameters found in Appendix B. The *IMAGEGRID* command was used to import five magnitude images. In Table 2, a full file listing of the delivered magnitude images is shown except for their extensions and world header files.

2.50000000000000
0.00000000000000
0.00000000000000
-2.50000000000000
627729.50000000000000
5431751.00000000000000

Figure 6. TIFF World File for File im2n48w097h2v1.tfw

Table 2. Magnitude Images

gt1n48w097h2v1
gt1n48w097h3v1
gt1n48w097h4v1
gt1n48w097h5v1
gt1n48w097h6v1

The LIDAR DEM data had Arc GRID and ASCII x,y,z as the two basic formats. The Arc GRID files were easily copied from the two CD-ROMs to an ArcInfo work space using the *COPY* command. The Arc GRID files had a 3-m post spacing for the full DEM and separate strip DEMs. The ASCII x,y,z data can be imported using a number of different routines within ArcInfo. There were a total of 12 files each for the ASCII x,y,z bare-earth and reflective surfaces. A full file listing of the delivered DEM products is shown in Table 3 except for their extensions and directory structures.

Table 3. LIDAR Data Set

Reflective	Bare-earth	Arc GRID	Arc GRID
183921	183921c	l183921	full_dem
185701	185701c	l185701	
190710	190710c	l190710	
191555	191555c	l191555	
192522	192522c	l192522	
193616	193616c	l193616	
194633	194633c	l194633	
195349	195349c	l195349	
195932	195932c	l195932	
200359	200359c	l200359	
200946	200946c	l200946	
201423	201423c	l201423	

DEM Anomalies

DEM anomalies or artifacts, which are similar to a commonly seen USGS 7.5-min DEM artifact known as a corn row, can best be seen by using a shaded-relief technique. A color-shaded-relief technique is applied to the IFSAR and LIDAR DEMs for this study. A black and white method of shading is accomplished by using the *HILLSHADE* command with the following string *ifsarshade = hillshade(ifsardem, 315, 45, all)*. Anomalies not noticeable before can easily be detected when performing this type of visual quality assurance.

The IFSAR DEM had one major flaw associated with its delivery. The flaw was introduced by editing the DEM prior to delivery. It is visible in Figures 7 and 8 with rough patches running north to south. Three areas near the far northern edge of the delivered IFSAR DEM have rough patches in the DEM. Similar areas can be found in the IFSAR DEM near tree lines following the flight path caused by a shadowing created by the trees and the IFSAR sensor. The IFSAR magnitude images had no visible anomalies, but the areas were different for the combined IFSAR DEM and magnitude image data sets.

The LIDAR DEM had two major flaws associated with its delivery, deep depressions and data voids visible in Figure 9. Most of the data voids are areas of adjoining seams, but other areas of the LIDAR DEM have many linear patches of data voids running throughout the LIDAR DEM visible as white areas in Figures 10, 11, and 12. The deep depressions can be found throughout the LIDAR DEM as shown in Figures 9, 10, 11, and 12, and can be found mainly near urban areas. The minor flaw is not easily seen and appears to have curved linear cuts in the terrain running along the collection path visible in Figures 11 and 12. These areas do not appear to be ground scars as with glacial terrain of the area.
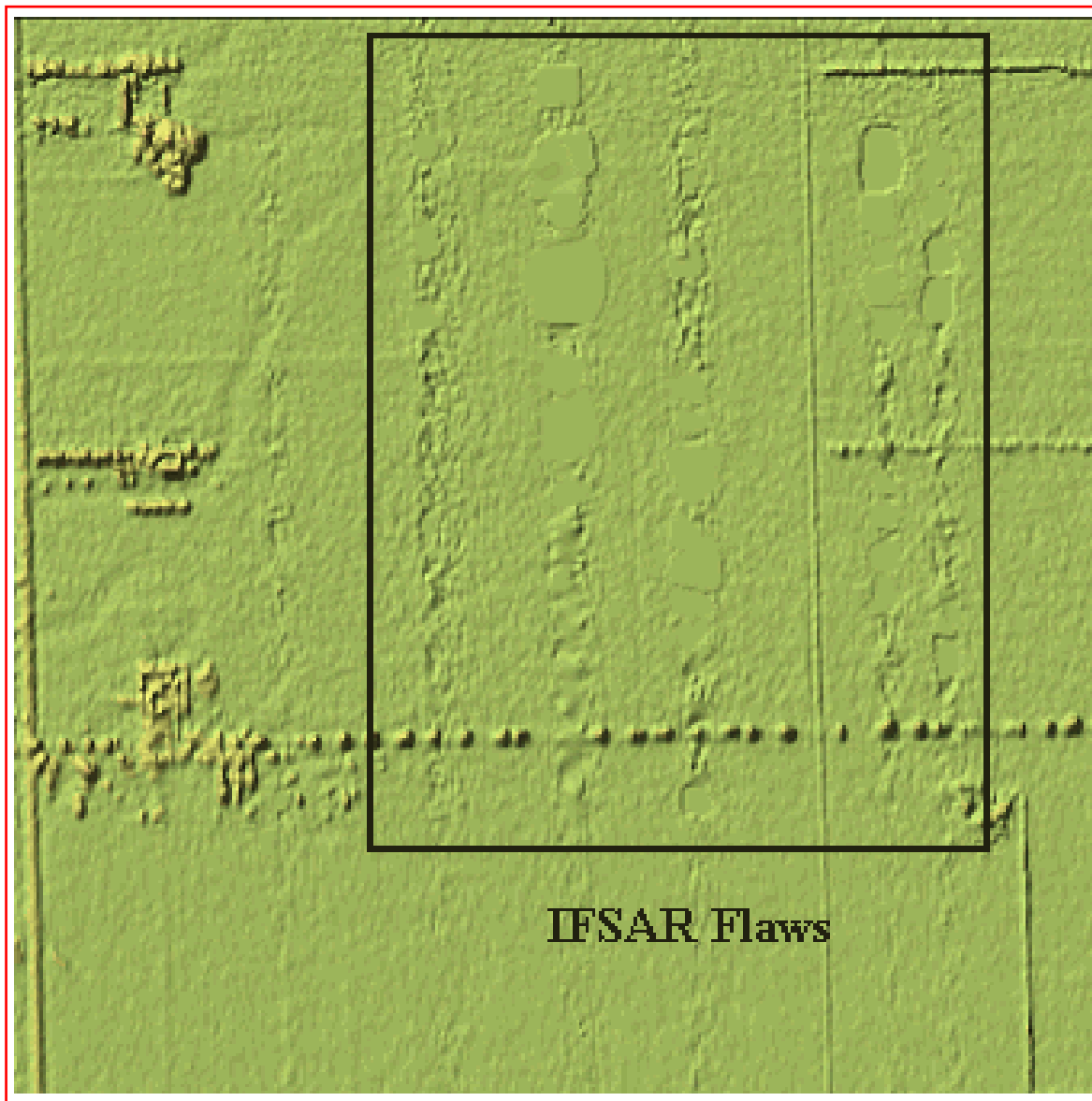
Figure 7. IFSAR DEM Flaws

13
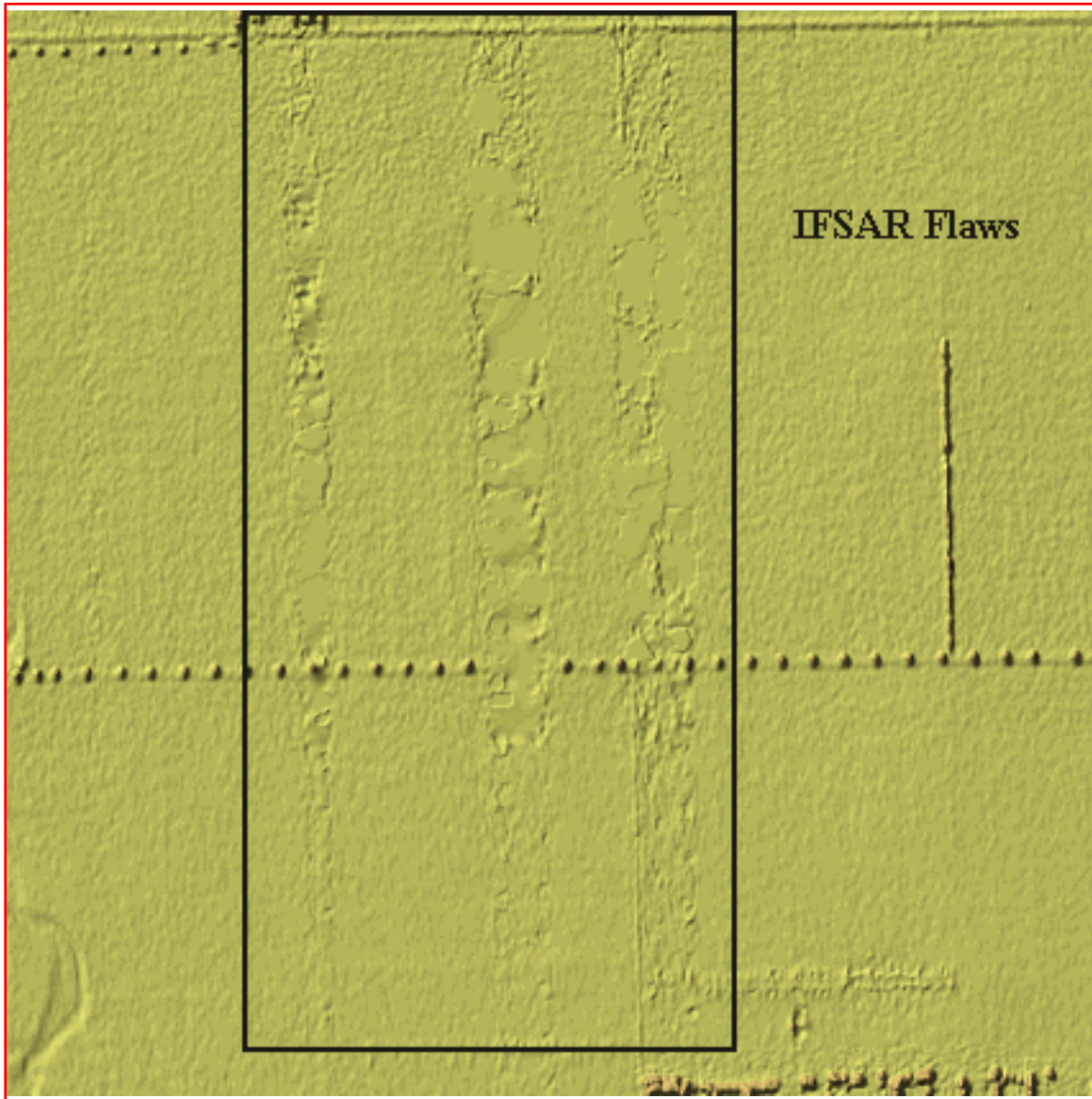
Figure 8. IFSAR DEM Flaws
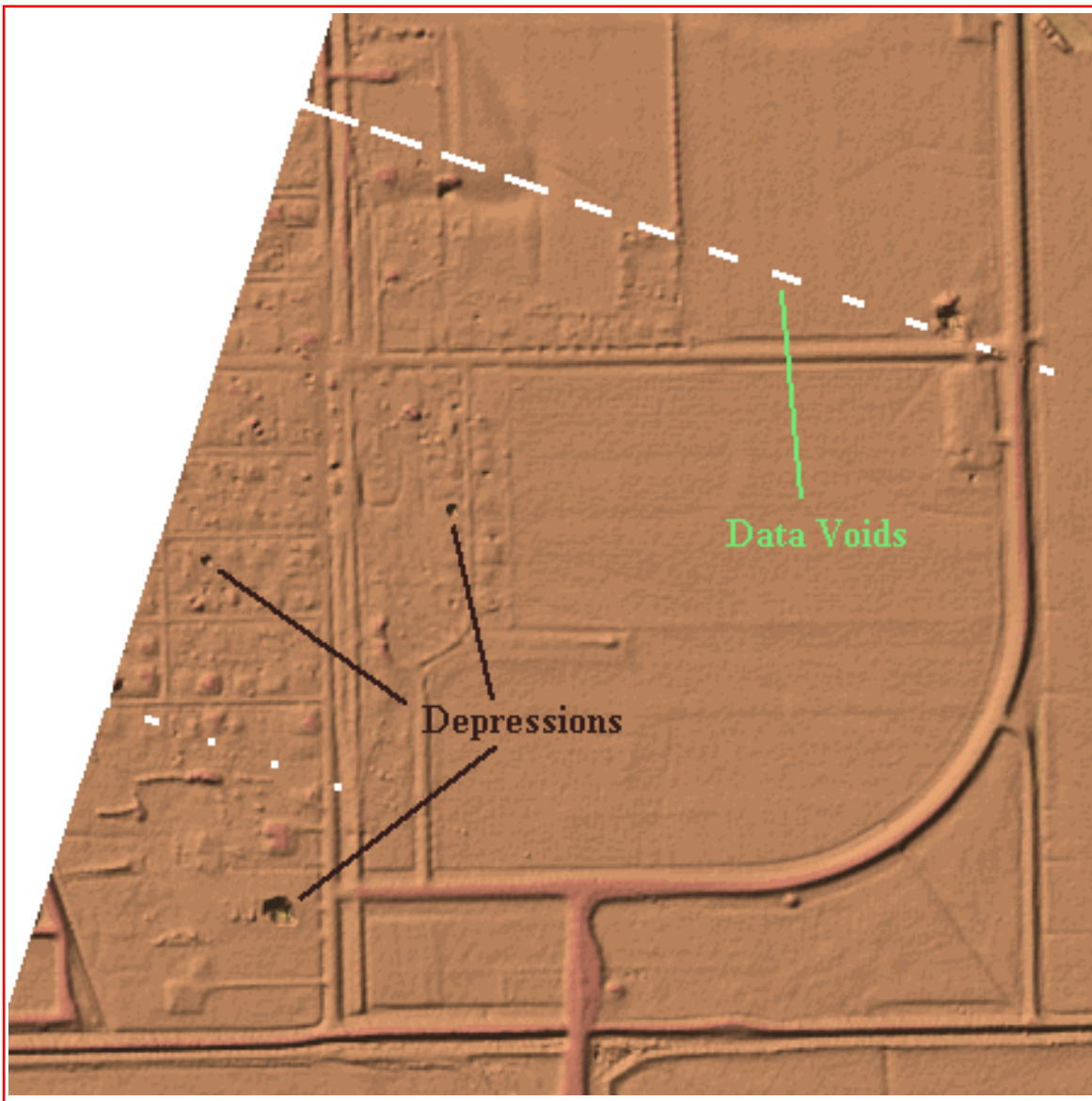
Figure 9. LIDAR DEM Flaws - Depressions and Data Voids
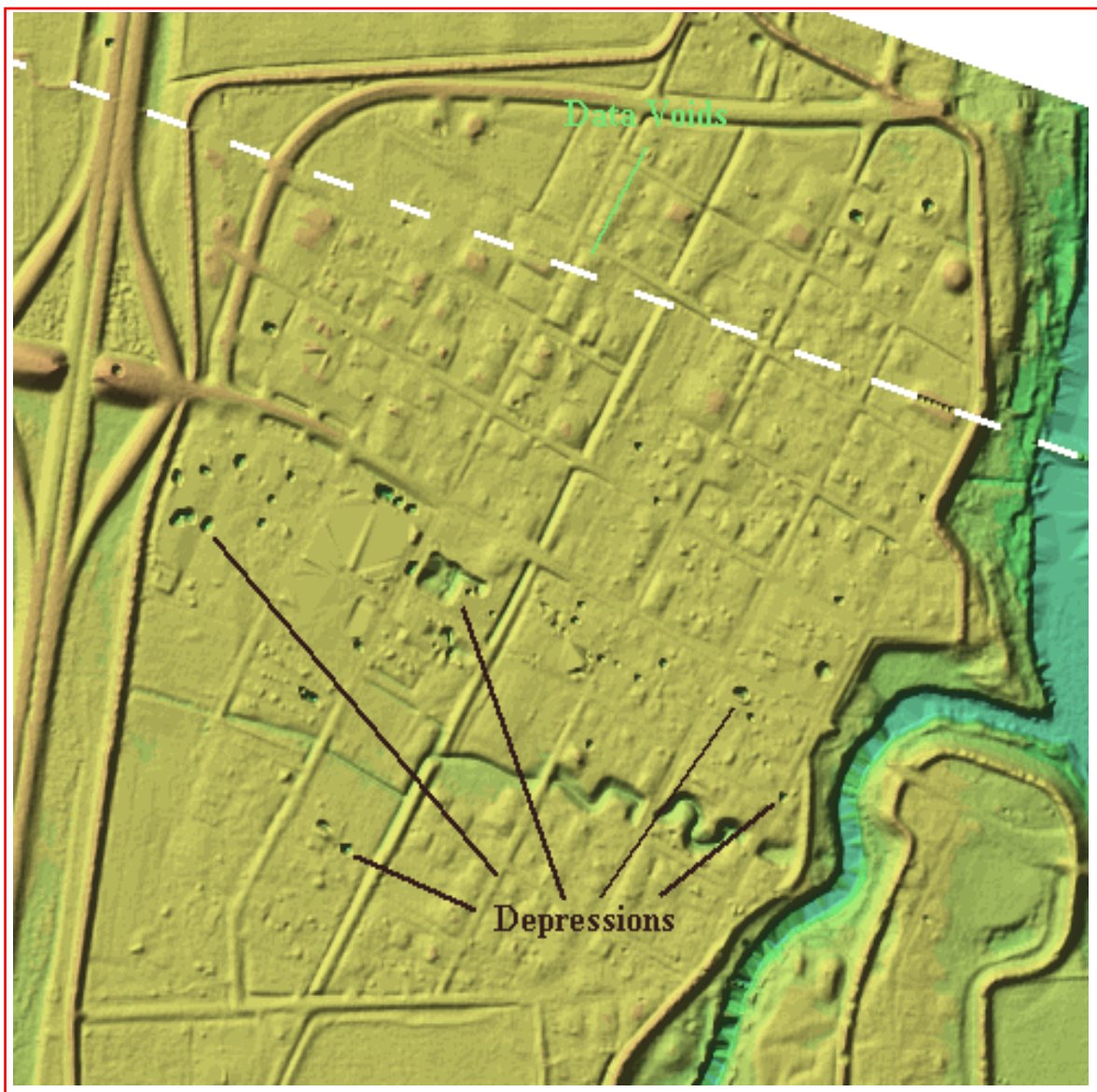
Figure 10. LIDAR DEM Flaws - Depressions and Data Voids
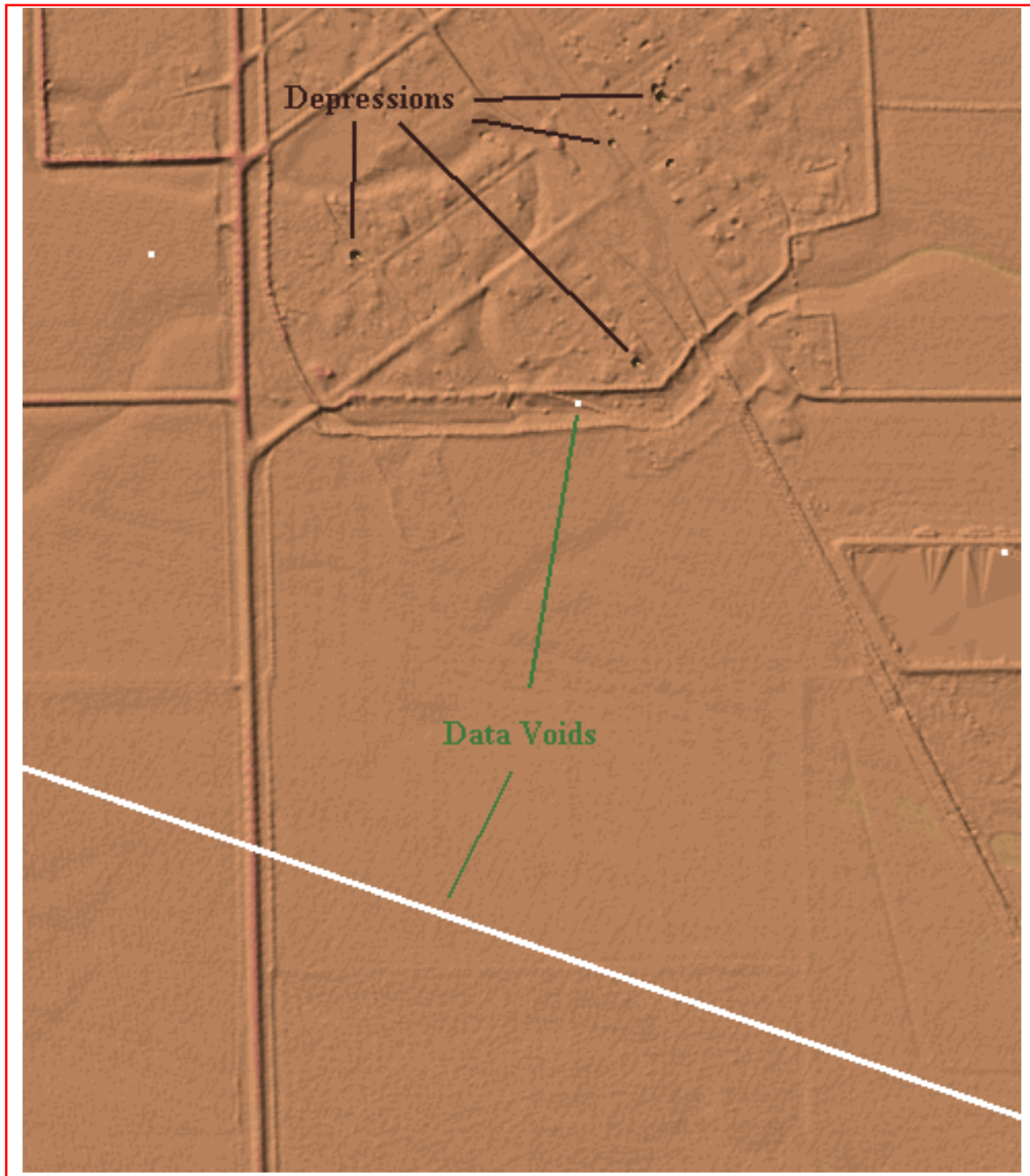
Figure 11. LIDAR DEM Flaws - Depressions and Data Voids
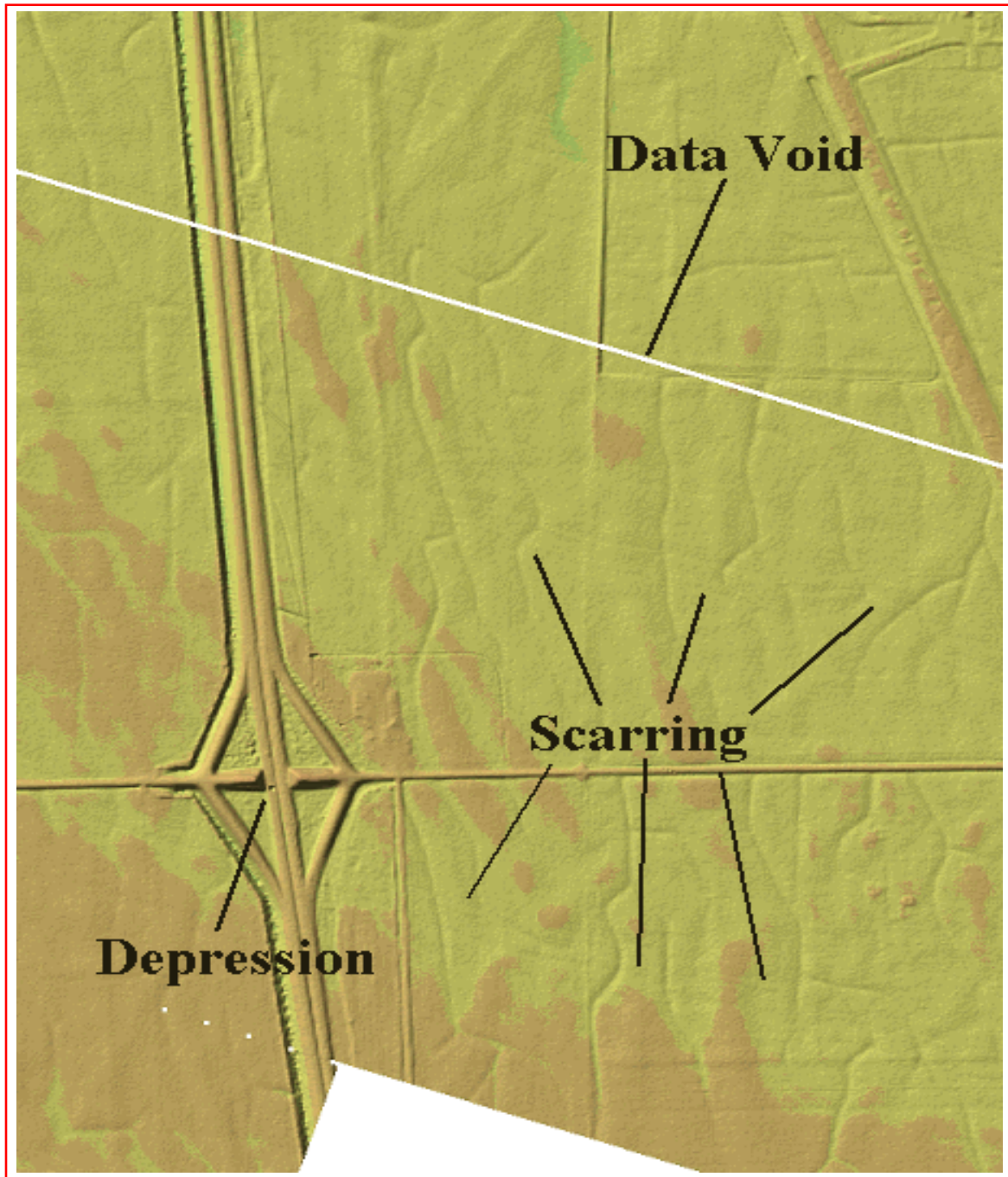
Figure 12. LIDAR DEM Flaws - Depressions, Data Voids, and Scarring

DEM PREPARATION: HYDROLOGIC MODELING

To apply hydrologic modeling to a DEM surface effectively, depression filling and surface smoothing routines are needed. IFSAR and LIDAR DEMs are not an exception to this process. Both IFSAR and LIDAR DEMs require smoothing and filling routines to produce a useable DEM for hydrologic modeling. In Figure 13, the original 5-m IFSAR DEM without any filter routines is shown. It is apparent that the surface needs filtering to achieve the type of condition needed for hydrologic modeling after examining the zoomed-in area of the IFSAR DEM in Figure 14. The terrain is rough and bumpy with many small depressions. This does not allow water to flow correctly across the DEM. ArcInfo 7.2.1 was used to perform the depression and surface smoothing routines found at the Arc prompt and in the Arc GRID.

Vegetation Removal

One of the problems encountered with IFSAR DEMs is the vegetation cover in the data. The second problem is the near- and far-range areas where elevation data appear rough. Some tools in ArcInfo 7.2.1, although primitive, can be used to edit a DEM to eliminate features such as forested areas. In Figure 15, forest areas have been edited out by a three-step process. First, forest areas were digitized and elevation attributes added to each polygon. Second, the polygons were converted to a grid with elevation values using the *POLYGRID* command. Third, the *GRIDINSERT* command was used to merge the two grids together. The drawback to this process and traditional photogrammetric editing is the lack of tools that will help to adjust the slope of the inserted DEM to the surrounding edge of the old DEM. This is why the inserted grid appears flat and the surrounding slope is not captured well.

The *LATTICETIN* command also can be employed to interpolate a new surface. The same procedure as *POLYGRID* can be used with the addition of a nodata value of -9999 added to the polygon attribute field. The *SELECTMASK* command in Arc GRID can be used to blank out the vegetated areas. The new DEM surface will appear to have blank holes. The *LATTICETIN* command will be used to interpolate across the nodata values created earlier. The *TINLATTICE* command can be used to convert the *TIN* back to a gridded surface. This process was not performed and is provided as guidance to eliminate forest canopies in the IFSAR DEM.

Creating a Hydrologic DEM

DEM smoothing is accomplished by using low-pass and averaging filters. Low-pass filters can be used to smooth DEMs by the number of iterations the filter is run across a surface using the *FILTER* command at the Arc prompt. An example of a low-pass filter being used is shown in Figure 16 using a 3 by 3 filter with two iterations with the low-pass option, and in Figure 17 using five iterations. This type of filter averages the surrounding values using the *FOCALMEAN* command at the GRID prompt with varying window sizes. The result of a *FOCALMEAN* filter is shown in Figure 18 using a 5 by 5 filter. The following string was used for the DEM in Figure 18 and in Figure 19 using a 7 by 7 filter: *demfocmn = focalmean*

Figure 13. Original IFSAR DEM

Figure 14. Zoomed-In Area of IFSAR DEM

Figure 15. Forest Removal

Figure 16. Two Iterations Using the *FILTER* Command with a Low-Pass Option

Figure 17. Five Iterations Using the *FILTER* Command with a Low-Pass Option

Figure 18. *FOCALMEAN* with a 5 x 5 Window

Figure 19. *FOCALMEAN* with a 7 x 7 Window

(ifsardemclp, rectangle, 5, 5) . The effects of the low-pass filter with five iterations are similar to these using the *FOCALMEAN* 5 by 5 filter. The drawbacks to this type of smoothing are that features disappear slowly and the DEM is lowered based on the type of filters employed in the process.

Depressions are filled using the *FILL* command in Arc GRID. This fill process was run on the entire IFSAR DEM data set but continued to crash. The technical support of Environmental Systems Research Institute (ESRI), Redlands, CA, stated the problem was due to the embedded limitation of 100,000 records and 500 unique values. The *FILL* command does not support floating point data over large areas, but one solution was to multiply the DEM by 1,000 or more to eliminate the decimal places, convert the data to integer values, and use *BUILDVAT* on the integer DEM. The GRID module also has not been updated since 1995. The *FILL* command was used on a smaller area with the option to fill everything within a 0.5-m range, and results are shown in Figure 20.

Other tools in ArcInfo can be employed to help determine how acceptable a surface is to water flow. The *SURFACEPROFILE* and *STACKPROFILE* commands can be used in ArcPLOT to display surface cross sections. The *SURFACEPROFILE* command will display a single DEM, while the *STACKPROFILE* command will display multiple DEMs. The *FLOWDIRECTION* and *FLOWACCUMULATION* commands in ArcGRID can be used to determine how water will flow across a DEM. ArcInfo's documentation can further clarify the commands used in this section and other sections of this study. The *FLOWDIRECTION* and *FLOWACCUMULATION* commands were used on the LIDAR and IFSAR DEM. Stream segments were disjointed in the IFSAR DEM, and the LIDAR DEM seemed to have other problems discussed in the next chapter.

The LIDAR DEM with many depressions posed a special problem. Each depression would have to located and edited manually to correct the problem. This is needed for surface runoff modeling and possibly hydrologic modeling. The hydrologic modeling group will best determine the use of the LIDAR and IFSAR DEM. If IFSAR and LIDAR DEMs are used for other purposes, no smoothing or filling routines need to be applied.

Recommendations

The off-the-shelf commercial GIS software packages require further enhancement for DEM editing and improved hydrologic processing. ArcInfo versions 7.2.1 and 8.0.1 presently are deficient in several areas of DEM editing and creating hydrologic DEMs. Primitive DEM editing capabilities exist in ArcInfo but are similar to photogrammetric techniques that do not take the slope of a surface into account while editing the terrain. A more robust true 3-D approach could achieve the desired solution by allowing a user to rotate the DEM in space for better editing. Filtering techniques work but are not effective on near- and far-range areas of the IFSAR DEM. Surface water does not flow across the IFSAR DEM surface due to the noise and, with further filtering, achieves a poor hydrologic DEM. Surface elevations are reduced, by as much as 0.1 to

Figure 20. *FILL* Command

0.5-m, and elevated roads disappear from the DEM. The sink-filling limit is reached at 100,000 records and 500 unique values using *SINK* and *FILL* commands to create a hydrologic DEM. This deficiency is due to the out-of-date Arc GRID module, which has not been updated since 1995. A bug report was submitted as CQ00116633 to GRID by ESRI's technical support on the request of TEC. The bug was for *FILL* to handle integer and floating point data of any size. The outcome of the bug is pending ESRI's review of worthiness for a fix.

FIRST LIDAR DELIVERY

The vertical comparison focused on the overlap area between the LIDAR and IFSAR DEMs. The area of overlap was the extent of the LIDAR DEM. The basic investigation used simple differencing *diffdem = LIDARdem - IFSARdem* as the first step to finding the greatest deviation in elevation between the LIDAR and IFSAR DEMs and is shown in Table 4 in the "Before" column. The simple differencing results can be viewed in Figure 21. The orange and yellow in Figure 21 point to a problem with the collection or production process with the LIDAR DEM. The green is mostly vegetation found in the IFSAR DEM. The red is the sides of the Pembina River channel.

Statistical Tools

A regression analysis was run in ArcInfo using the *SAMPLE* and *REGRESSION* commands at the GRID prompt. The *SAMPLE* command used the string *oldcompare1 = sample (baredem, gt1dem)* to calculate the data table used for the regression analysis. The *REGRESSION* command was then used with the string *regression oldcompare1 linear brief* to find the RMSE for the LIDAR and IFSAR DEMs. The results of the regression analysis are shown in Table 5. This analysis considered all of the overlap area including vegetated areas found in the IFSAR DEM. The high RMSE value of 1.78-m and coefficient value of 38 is attributed to vegetation in the IFSAR DEM.

Other spatial analysis tools are available in ArcInfo, such as the *CORRELATION*, *GEARY*, and *MORAN* commands. The *CORRELATION* command provides information on cross correlation between two grids. The *GEARY* and *MORAN* commands provide spatial autocorrelation indexes for a grid, which can be applied to DEMs. Spatial autocorrelation is a measure of simularity of each object within an area (ArcInfo Help). More information is provided by ArcInfo's online help under GRID statistical functions and commands.

Table 4. LIDAR and IFSAR Elevation Differences in Meters

Before	Count	After	Count
-31	2	-30	2
-29	1	-28	1
-28	1	-27	1
-27	2	-26	2
-25	1	-24	1
-24	2	-23	2
-23	5	-22	5
-22	7	-21	7
-21	17	-20	17
-20	20	-19	20
-19	42	-18	42
-18	94	-17	94
-17	166	-16	166
-16	488	-15	488
-15	1541	-14	1541
-14	4316	-13	4316
-13	8925	-12	8925
-12	13863	-11	13863
-11	20259	-10	20259
-10	28266	-9	28266
-9	37855	-8	37855
-8	47818	-7	47818
-7	56663	-6	56663
-6	62627	-5	62627
-5	66805	-4	66805
-4	71226	-3	71226
-3	78196	-2	78196
-2	100523	-1	100523
-1	1271498	0	5318248
0	4201024	1	154274
1	18530	2	18530
2	6978	3	6978
3	3313	4	3313
4	1610	5	1610
5	627	6	627
6	82	7	82
7	14	8	14
8	7	9	7
9	3	10	3

Legend

- 🟩 -31 to -2
- 🟨 -1 to -1
- 🟧 0 to 0
- 🟥 1 to 9
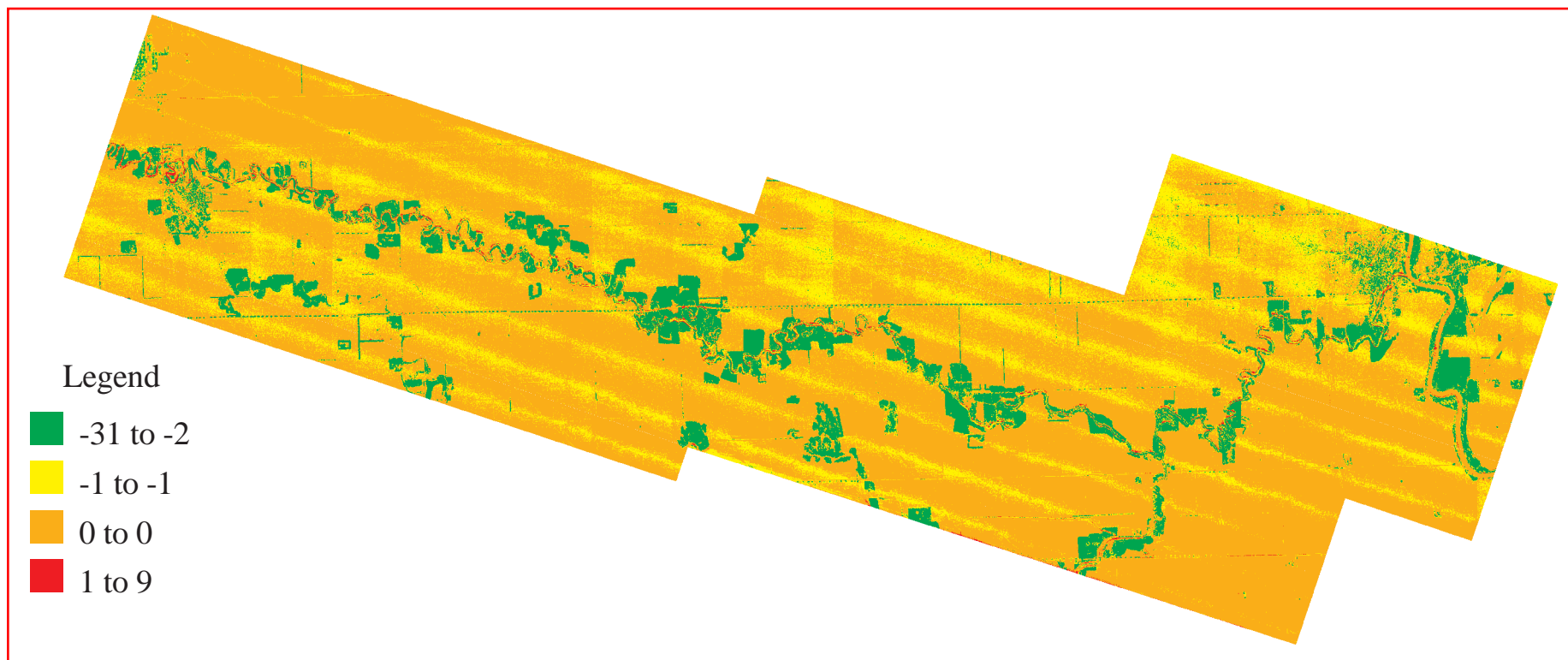
Figure 21. Elevation Difference Image of the LIDAR and IFSAR DEM

Table 5. Regression Analysis Using ArcInfo

Coef #	Coef
0	38.284
1	0.839
RMS Error	1.779
Chi-Square	19313105.407

Analysis

A regression analysis and a t-test were run using 415 random points collected away from vegetation found in the IFSAR DEM and away from structures not found in the LIDAR DEM. Three points were found to be near or over low-level vegetation in the IFSAR DEM and were eliminated. Points near transportation structures were eliminated from the total number of points. The IFSAR DEM lacks accurate definition of transportation structures in the area and would not provide a fair comparison of the two data sets. This brought the sample points down to 412 points for the analysis. An Arc Macro Language (AML) script was written to take elevation values from the LIDAR and IFSAR DEMs as a stacked grid seen in Appendix C. The x- and y-coordinates of the 412 points were put into an ASCII text file, and the AML was run to extract the elevation data for the analysis. The first calculations were made using Quattro Pro and checked using Minitab version 12 software. A one-tail and two-tail paired t-test were run to check the mean values of the LIDAR and IFSAR DEMs. In Table 6, the first t-test conclusion is that the null hypothesis is rejected and the differences are significant with a p-value of .00 for the one- and two-tail paired t-test. This means that the data sets have a significantly different mean. In Table 6, the r-squared value of 99.2 percent in the "Before Correction" section shows a strong relationship between the two DEMs with a RMSE value of 0.36-m.

Cross sections can play an important role in checking the differences between DEMs. Several cross sections were used to check the LIDAR and IFSAR DEMs. The *STACKPROFILE* and *SURFACEPROFILE* commands can be used to produce cross-section graphs in ArcPlot, and a sample AML is seen in Appendix D. The *SCREENSAVE* command was used to capture the cross-section graphs as an image for this report. In Figure 22, an approximate 1-m offset is seen in one of several cross-sections used to view the LIDAR and IFSAR DEMs. Cross sections helped to evaluate and confirm the approximate 1-m offset and provided supporting information to apply a 1-m correction to the IFSAR DEM. The effects of the correction can be seen in Table 4 by the reduction of 1,117,224 elevation points to category 0 in the "AFTER" column. Visual results are shown in Figures 23 and 24.

The second one- and two-tail paired t-test was run to check the mean difference of the LIDAR and newly corrected IFSAR DEM with a p-value of 0.00 shown in Table 6. The second t-test conclusion is that the null hypothesis is rejected. The means of the data sets are significantly different. The final regression analysis was run with results listed in the Table 6 "After

Table 6. Regression Analysis Using Corrected IFSAR DEM

		Before Correction	
		Regression Output:	
t-test	Paired	Constant	1.4618
One Tail	0.0000	Std Err of Y Est	0.3641
Two Tail	0.0000	R Squared	0.9922
		No. of Observations	412
		Degrees of Freedom	410
		X Coefficient(s)	0.9909
		Std Err of Coef.	0.0043

		After Correction	
		Regression Output:	
t-test		Constant	2.4527
One Tail	0.0000	Std Err of Y Est	0.3641
Two Tail	0.0000	R Squared	0.9922
		No. of Observations	412
		Degrees of Freedom	410
		X Coefficient(s)	0.9909
		Std Err of Coef.	0.0043

Figure 22. LIDAR and IFSAR Cross Section

Legend

■ -30 to -4
■ -3 to -1
■ 0 to 0
■ 1 to 10
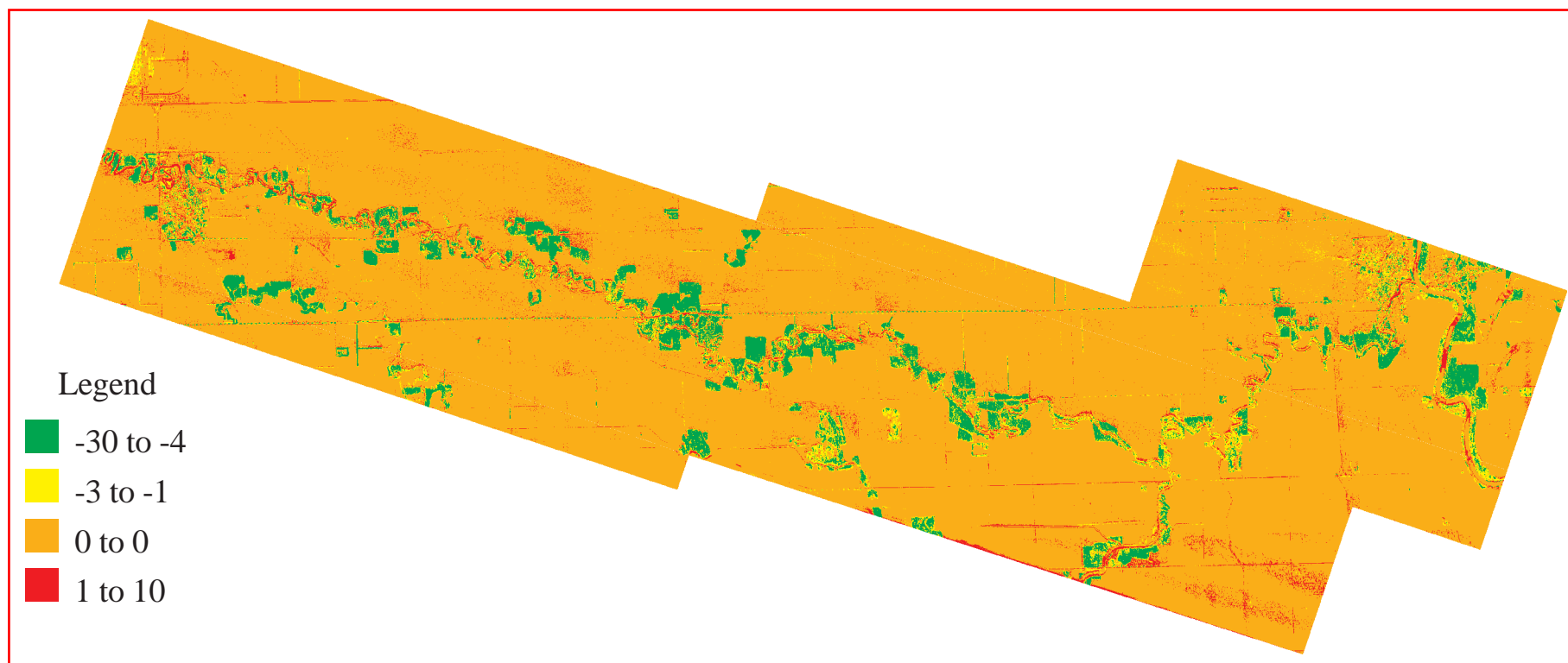
Figure 23. Elevation Difference Image of the LIDAR and Corrected IFSAR DEM
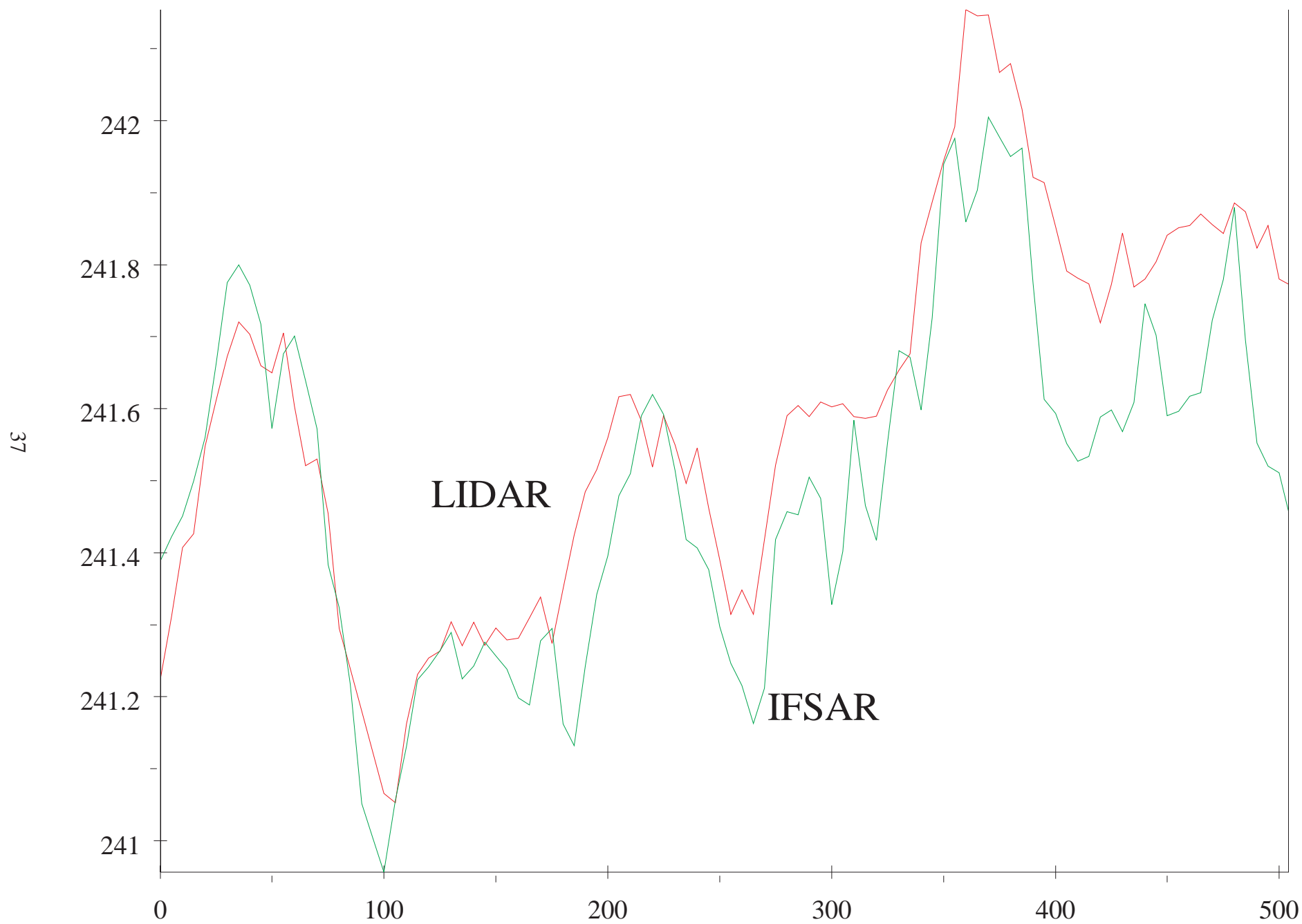
Figure 24. Corrected IFSAR DEM and LIDAR Cross Section

Correction" section. In Figure 25, a plot of the residuals versus the order of data does not show significant deviation from normality. The normal probability plot of residuals in Figure 26 shows no significant deviation. The regression plot in Figure 27 shows most all of the residuals falling withing the 95 percent range with a few outliers. Graphs in Figures 28 (IFSAR) and 29 (LIDAR) show significant deviation from normality; a K-S test for normality gives a p-value of 0.01, which confirms the non-normality. Because of this, the assumptions of the t-test are violated and the p-values may be inaccurate. Further testing will be done upon redelivery of the LIDAR DEM.

Recommendation

EarthData needs to redeliver the LIDAR bare-earth DEM to eliminate the wave or roll effect visible in Figure 21 and fill data voids found in the DEM. EarthData has been contacted and a delivery date is unknown. EarthData confirmed there was a systematic error in the LIDAR DEM in July of 1999 and they were working to correct the problem. Man-made transportation structures and vegetated areas do not lend themselves to be useful for accessing the accuracy of the two DEMs due to the differences in two collection devices. IFSAR is capable of capturing man-made transportation structures, but as the structure decreases in size the structure in less defined in the DEM. This may be due to processing of the IFSAR DEM from 2.5- to 5-m and other processing techniques. LIDAR seems to be better in the capture of man-made transportation features. High accuracy GPS control should be collected across the actual terrain of the study area at the 2-cm level would provide a more accurate comparison and analysis of the LIDAR and IFSAR DEMs.
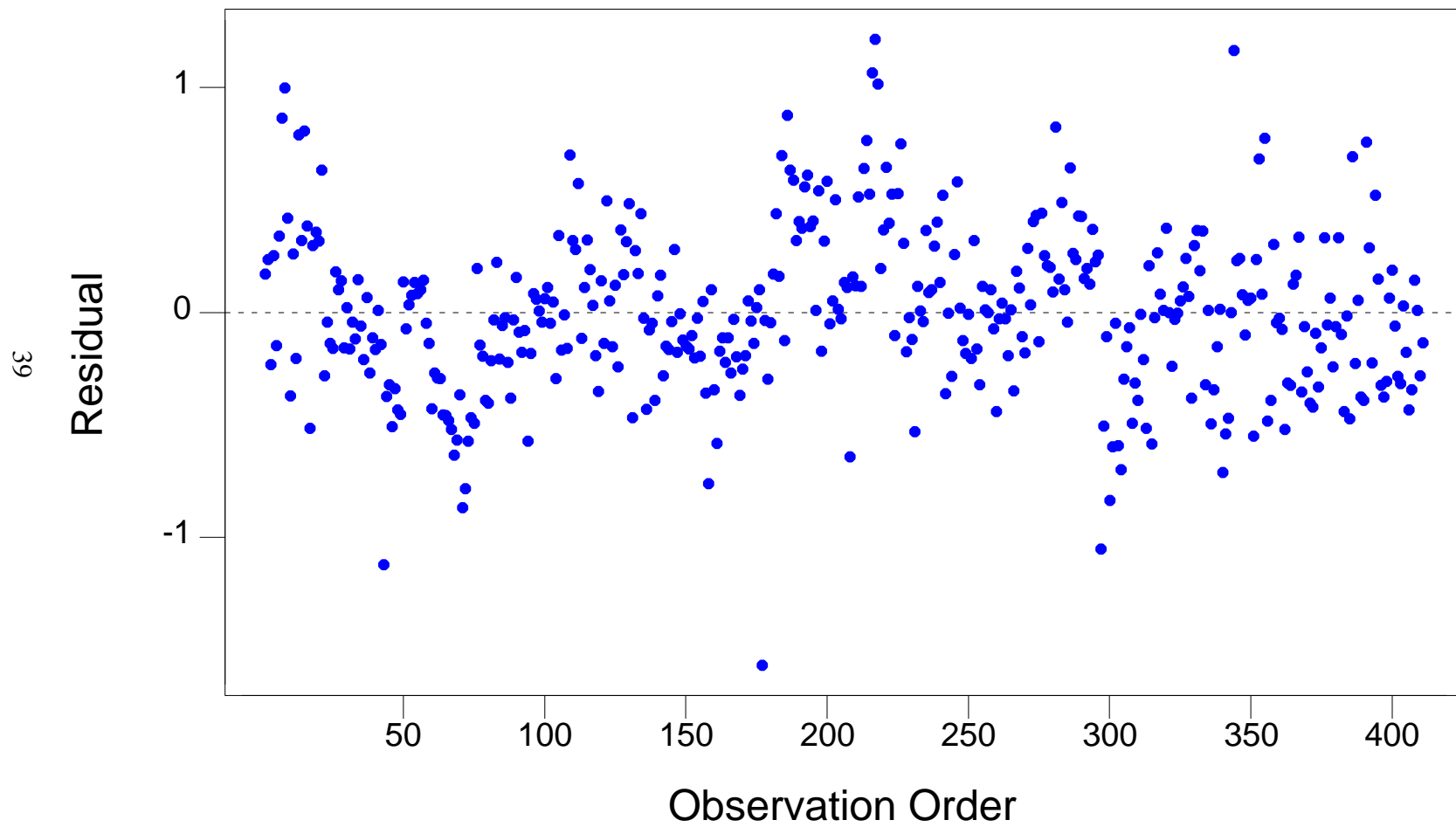
Figure 25. Residuals Versus the Ordered Data for the Corrected IFSAR and LIDAR DEM
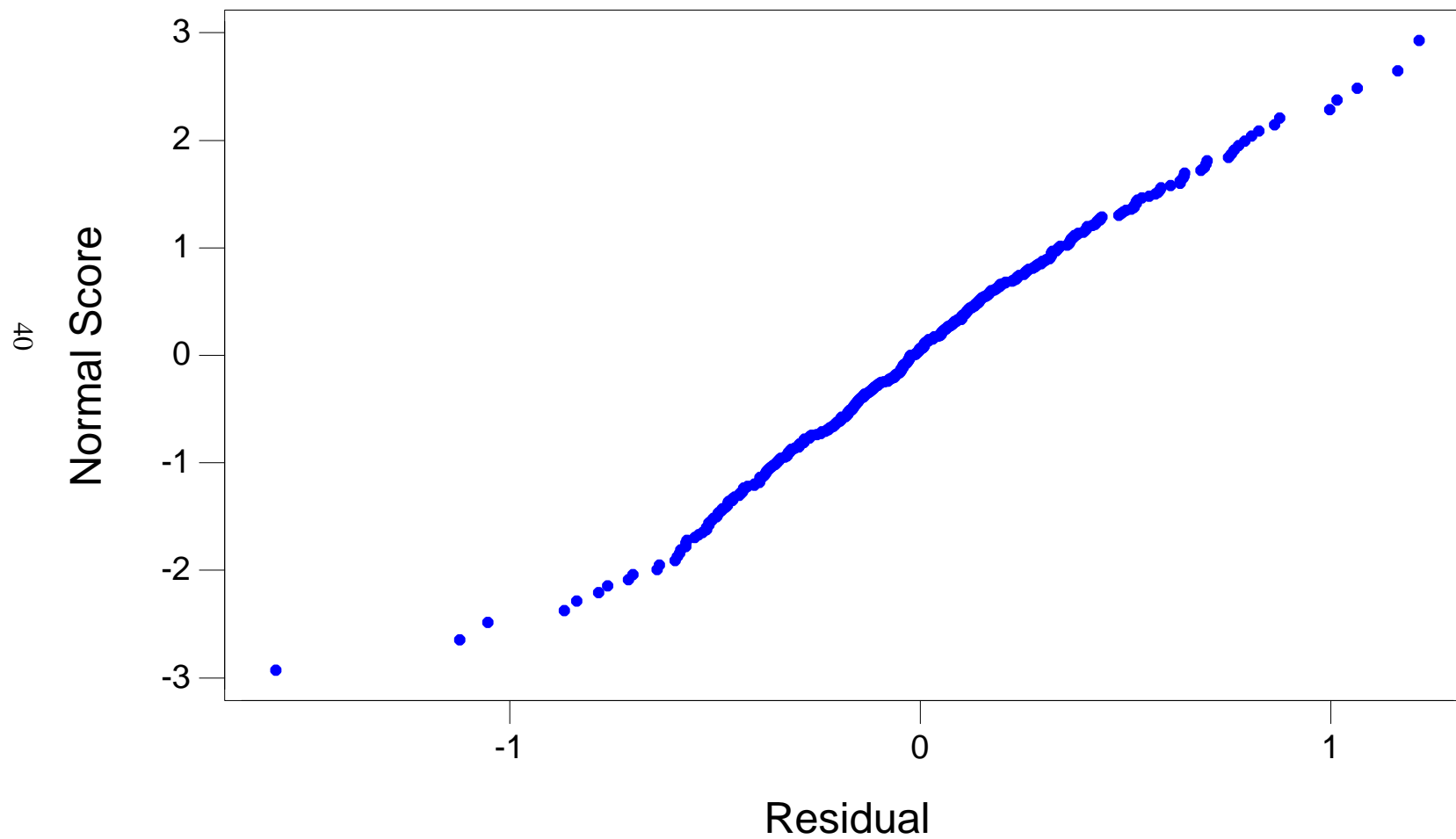
Figure 26. Normal Probability Plot of the Residuals

$$Y = -6.5E\text{-}01 + 1.00168X$$
$$R\text{-}Sq = 99.2\ \%$$
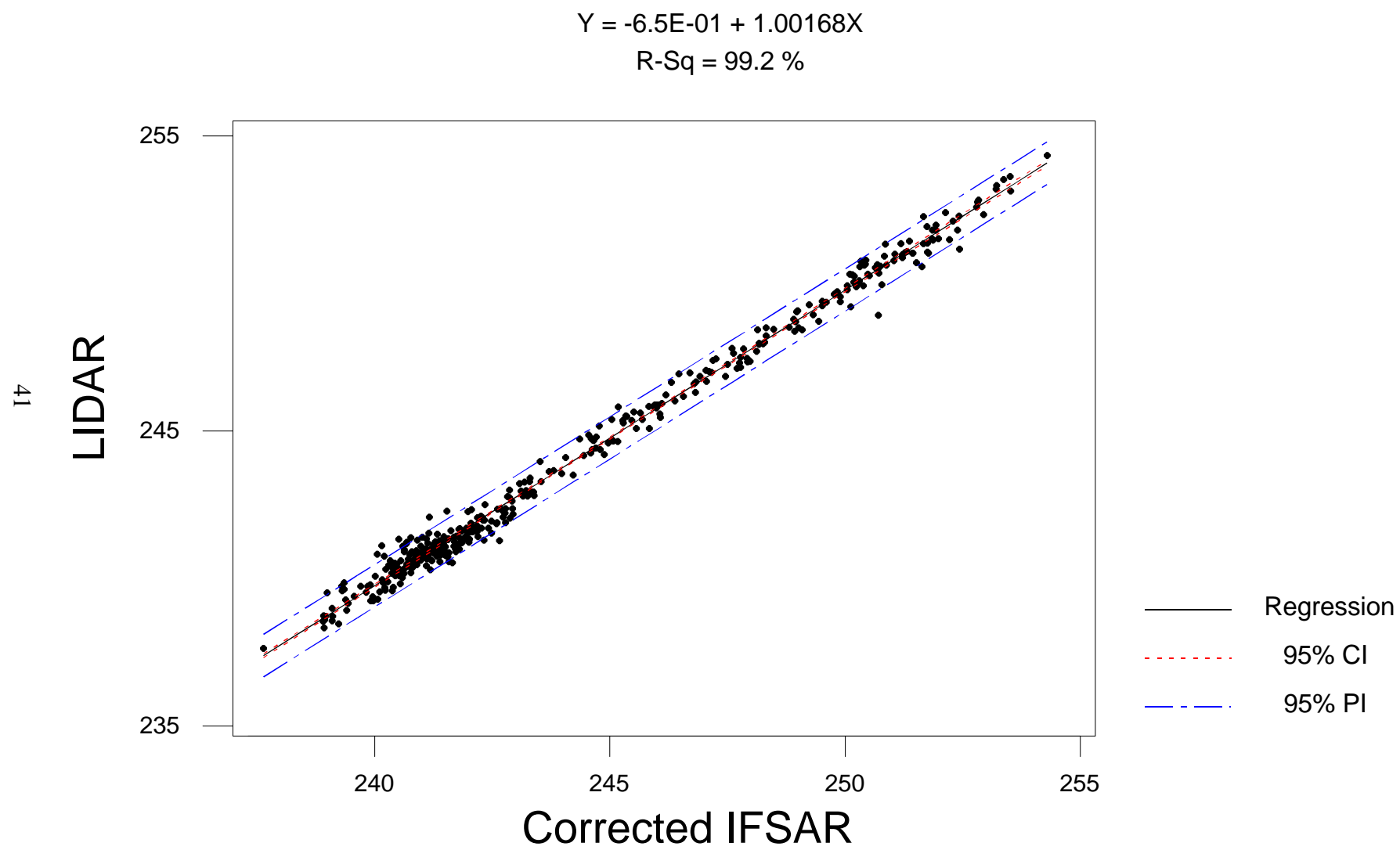
Figure 27. Regression Plot
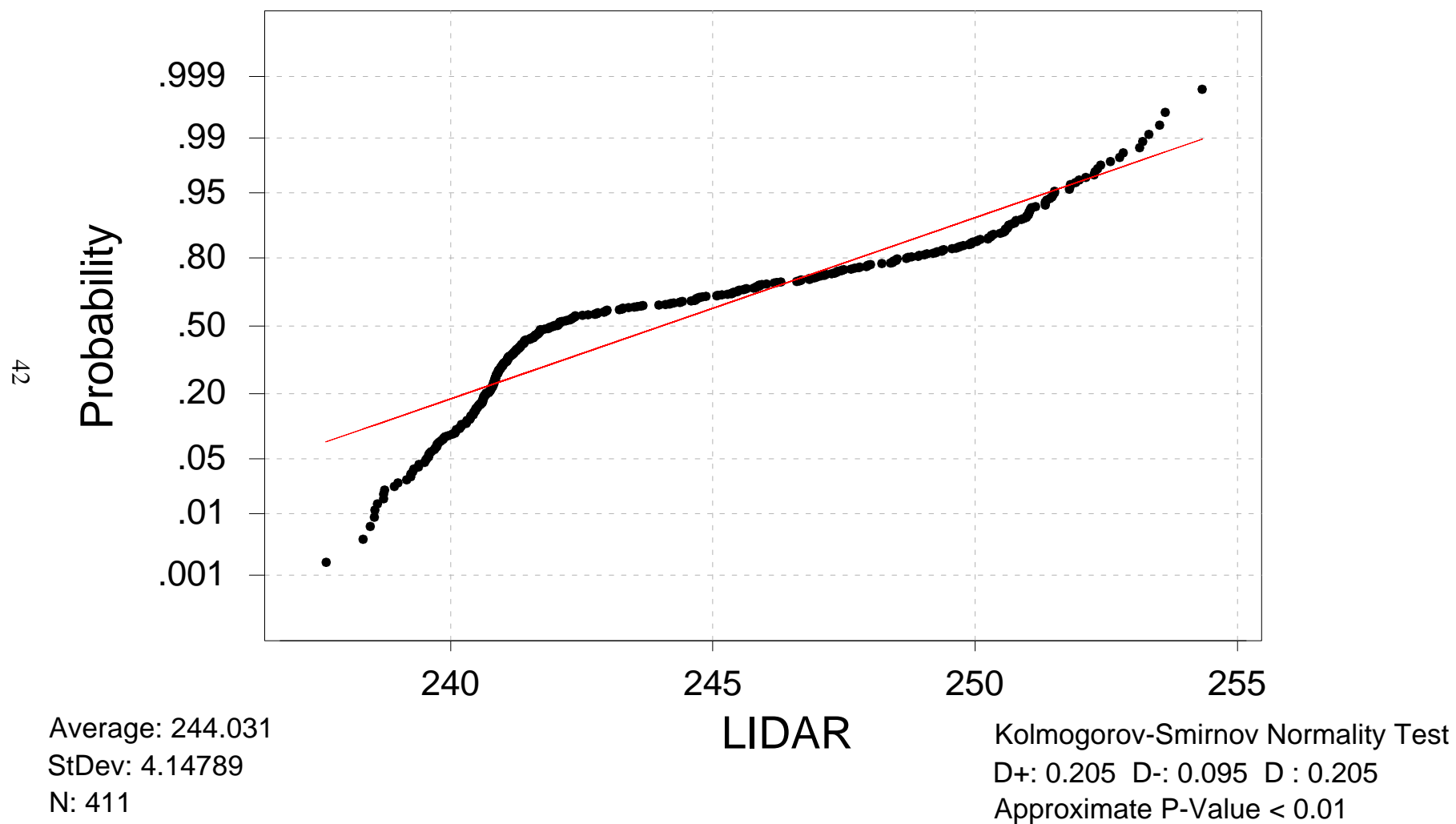
Figure 28. Normal Probability Plot for the IFSAR DEM Data

Average: 244.031
StDev: 4.14789
N: 411

Kolmogorov-Smirnov Normality Test
D+: 0.205 D-: 0.095 D : 0.205
Approximate P-Value < 0.01

Average: 244.266
StDev: 4.12494
N: 411

Kolmogorov-Smirnov Normality Test
D+: 0.191 D-: 0.094 D : 0.191
Approximate P-Value < 0.01
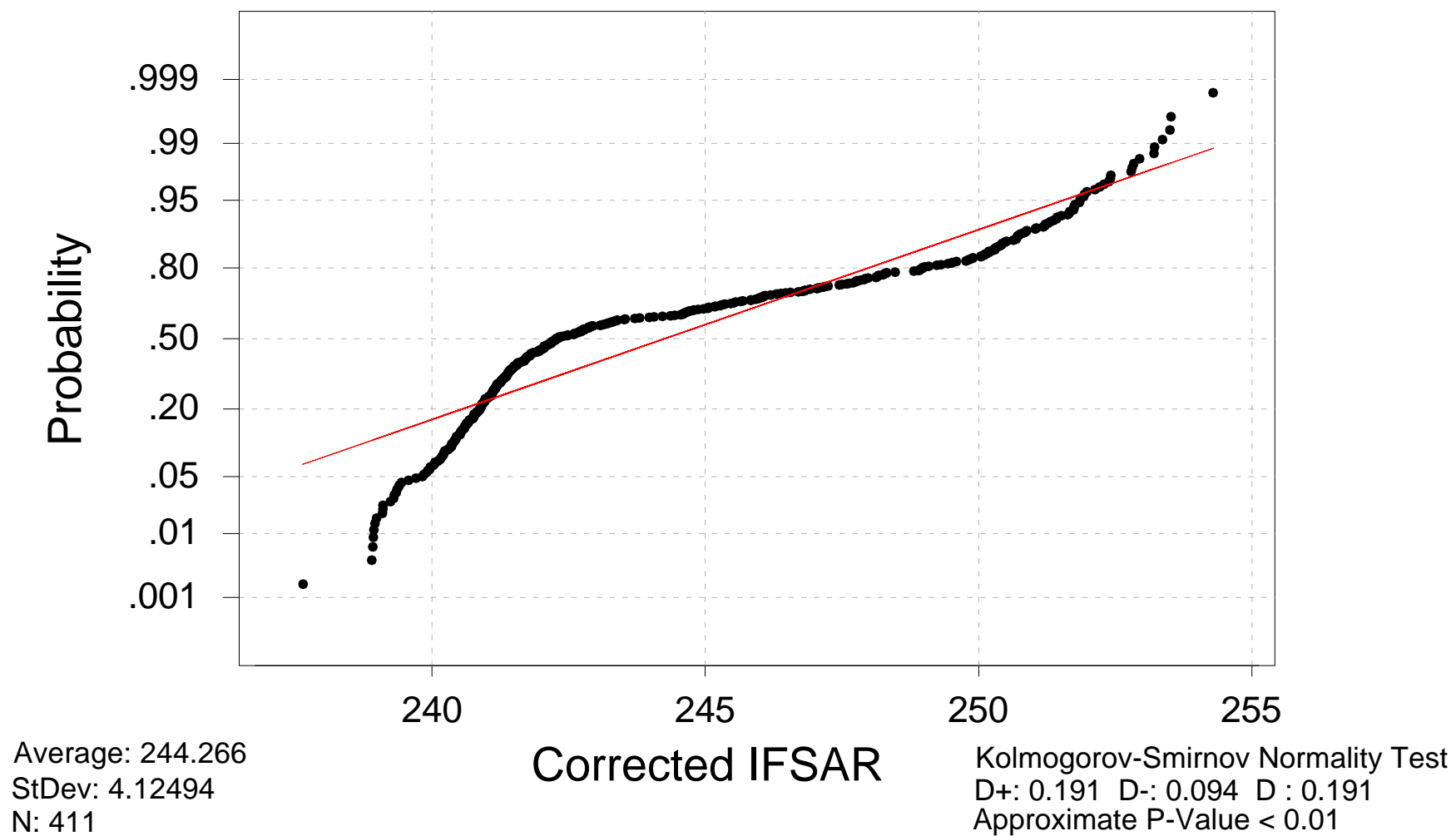
Figure 29. Normal Probability Plot for the LIDAR DEM Data

DATA FUSION

The purpose of performing a data fusion or merging DEMs is to find the best economy of data types and resolutions. The concept of data fusion is not new and has been around for years. The purpose of this section is to explain how data fusion can work to provide a robust new DEM from two or more different resolution DEMs for floodplain mapping. The data fusion methodology can be accomplished with any raster-based GIS as long as it supports masking and merging routines within the software package. ArcInfo and ERDAS Imagine software packages provide support for masking and merging. ArcInfo was used for the data fusion process for the study area. The seven-step process (Damron 1999) presented in Figure 30 can be used in any raster-based GIS. In ArcInfo, the *GRIDINSERT* command was used to perform the same process as the seven-step process:

1. *ifsarres2 = resample (ifsarclp, 2)*

2. *Convert IFSAR or LIDAR data from NAVD88 to Ellipsoid heights if needed*

3. *output1 = con (isnull(nasalidar), 100, nasalidar)*

4. *output2 = setnull (output1 < 50, output1)*

5. *output3 = (output2 - 100)*

6. *outmask1 = selectmask (ifsarres2 , output3)*

7. *mosaic1 = mosaic (outmask1, nasalidar)*

Figure 30. Seven-Step DEM Fusion Technique

The fusion process was run twice using the LIDAR and IFSAR DEMs. The first process was run to see what the LIDAR and IFSAR DEMs looked like with no vertical corrections. The fusion or merging process was accomplished at the Arc prompt using the *GRIDINSERT* command, which will resample the LIDAR DEM to 5-m post spacing and apply the masking routine to the IFSAR DEM. In Figures 31 and 32, the 1-m offset observed earlier is visible by the appearance of a clean and sharp lip between the LIDAR and IFSAR DEMs. Vertical checks using cross sections made it possible to correct the 1-m offset found in the IFSAR DEM. The results of the 1-m correction to the IFSAR DEM can be seen in Figures 33 and 34 with the second run of the data fusion process to the LIDAR and corrected IFSAR DEM. The systematic error can be seen along the eastern edge of the DEM, which appears slightly higher and then lower than the rest of the DEM. In Figure 35, the edge of the fused DEM is clearly seen in the before and after fusion with the old IFSAR DEM 1-m above the corrected IFSAR. A fused LIDAR and corrected IFSAR DEM was delivered to the Saint Paul District, and the Canadian contractor performed the

analysis for the hydrologic modeling.

TEC should work with the Canadian contractor to determine the best level of variation in the smoothing and filling routines for the IFSAR and LIDAR DEMs. TEC and the Canadian contractor should determine the most efficient format for distribution of the fused DEM based on software and size limitations of hydrologic software being used for the study.
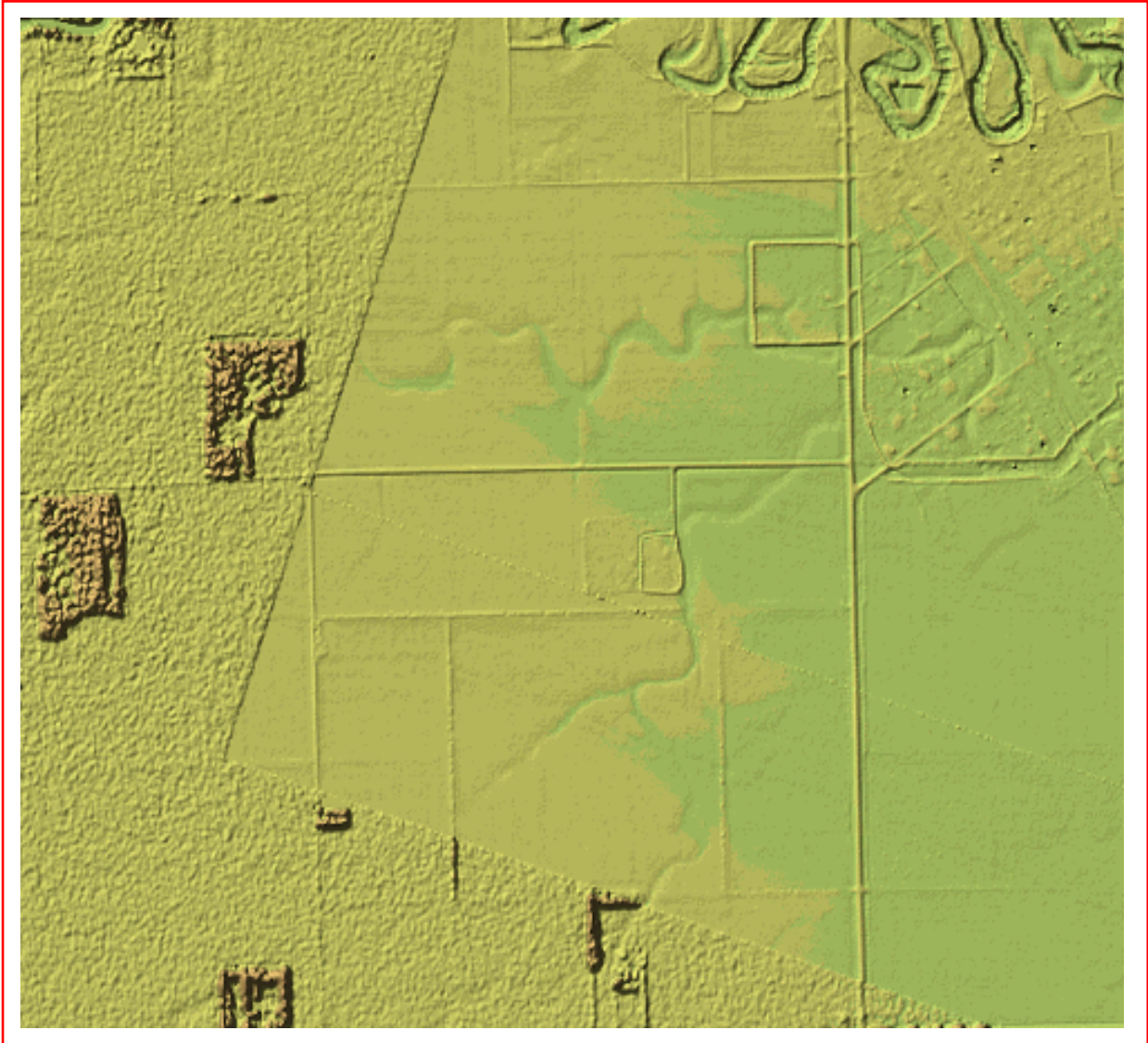
Figure 31. IFSAR DEM 1-m Offset Fused with LIDAR DEM
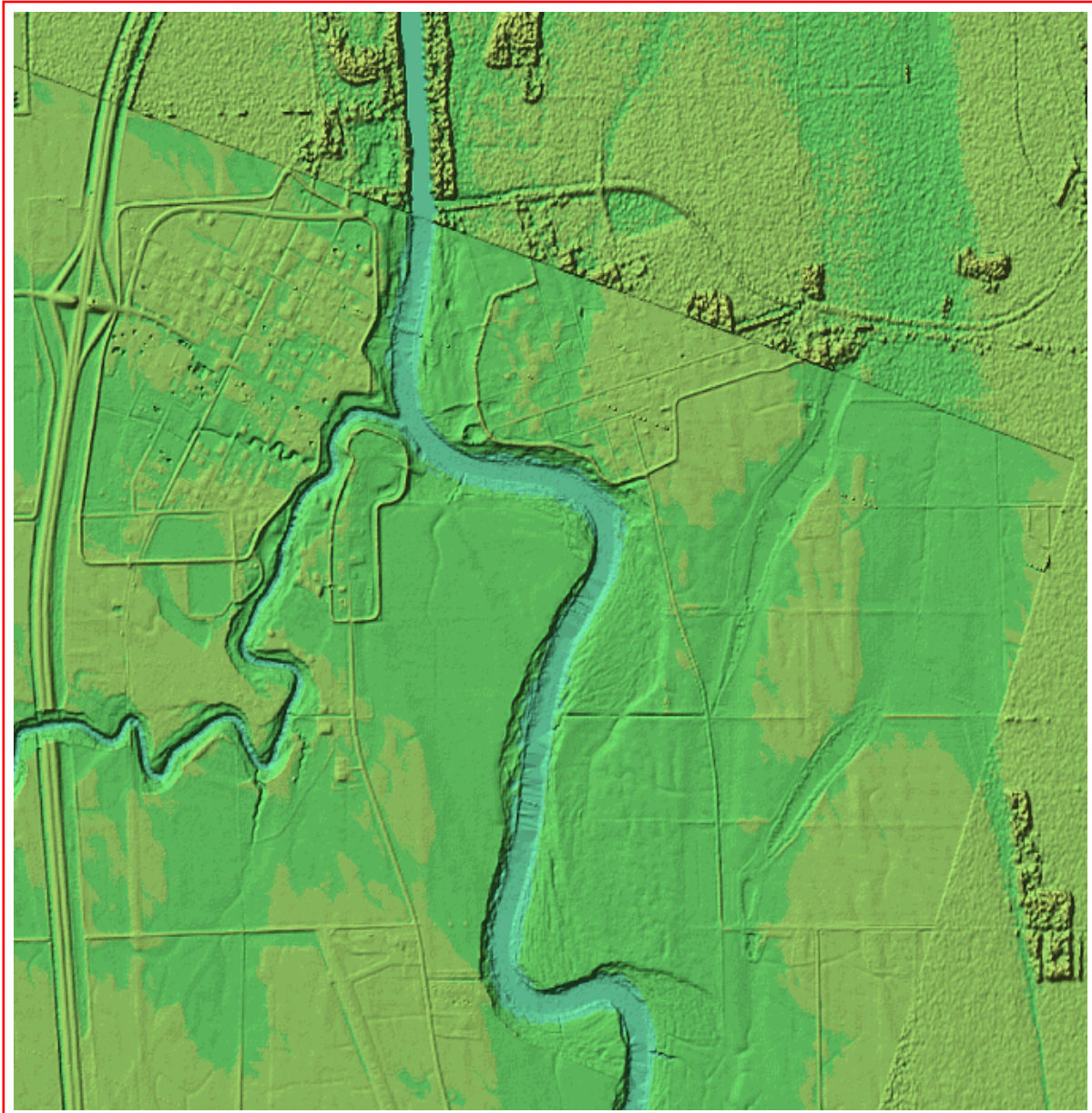
Figure 32. IFSAR DEM 1-m Offset Fused with LIDAR DEM

Figure 33. Corrected IFSAR DEM Fused with the LIDAR DEM
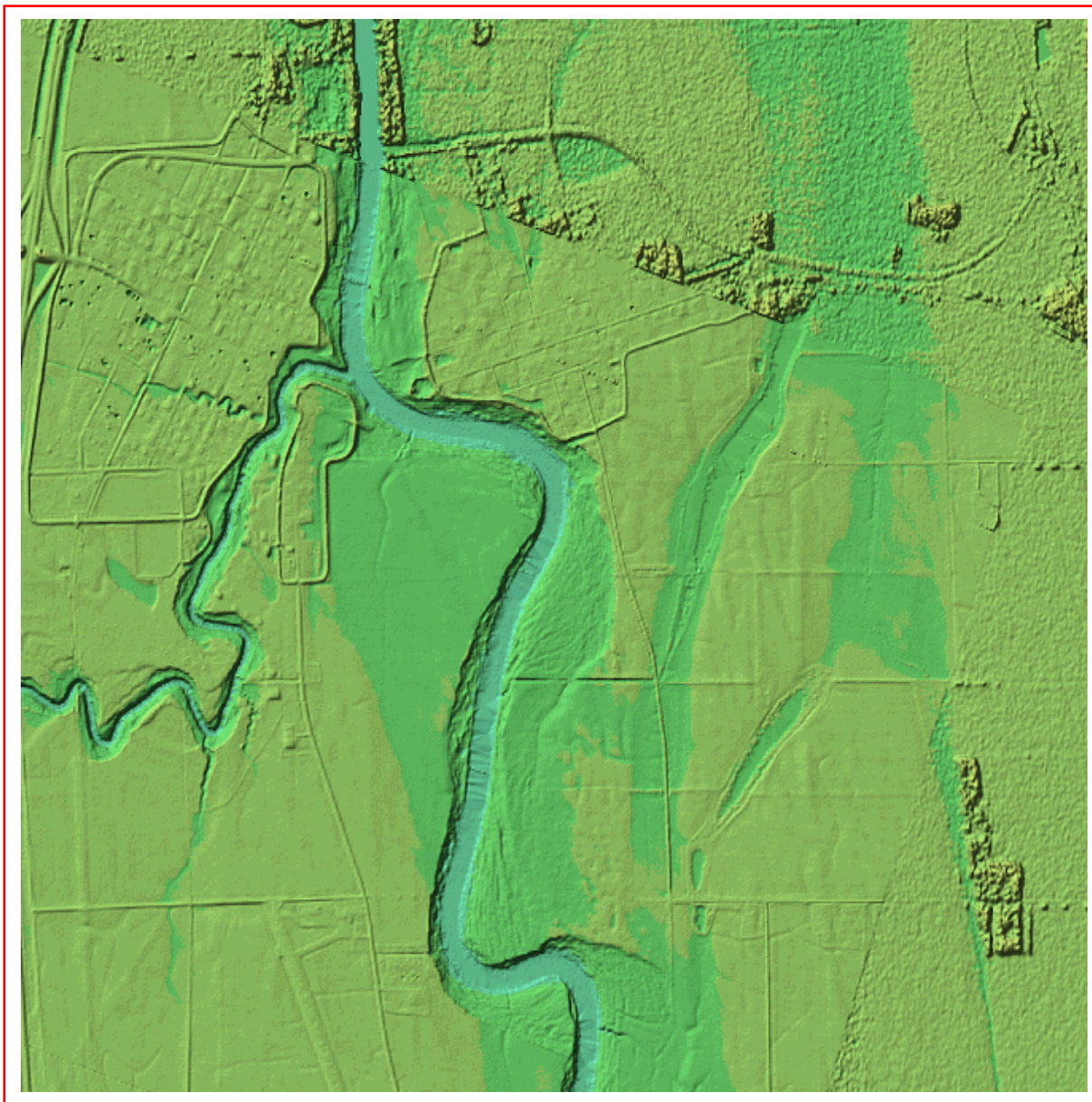
Figure 34. Corrected IFSAR DEM Fused with the LIDAR DEM
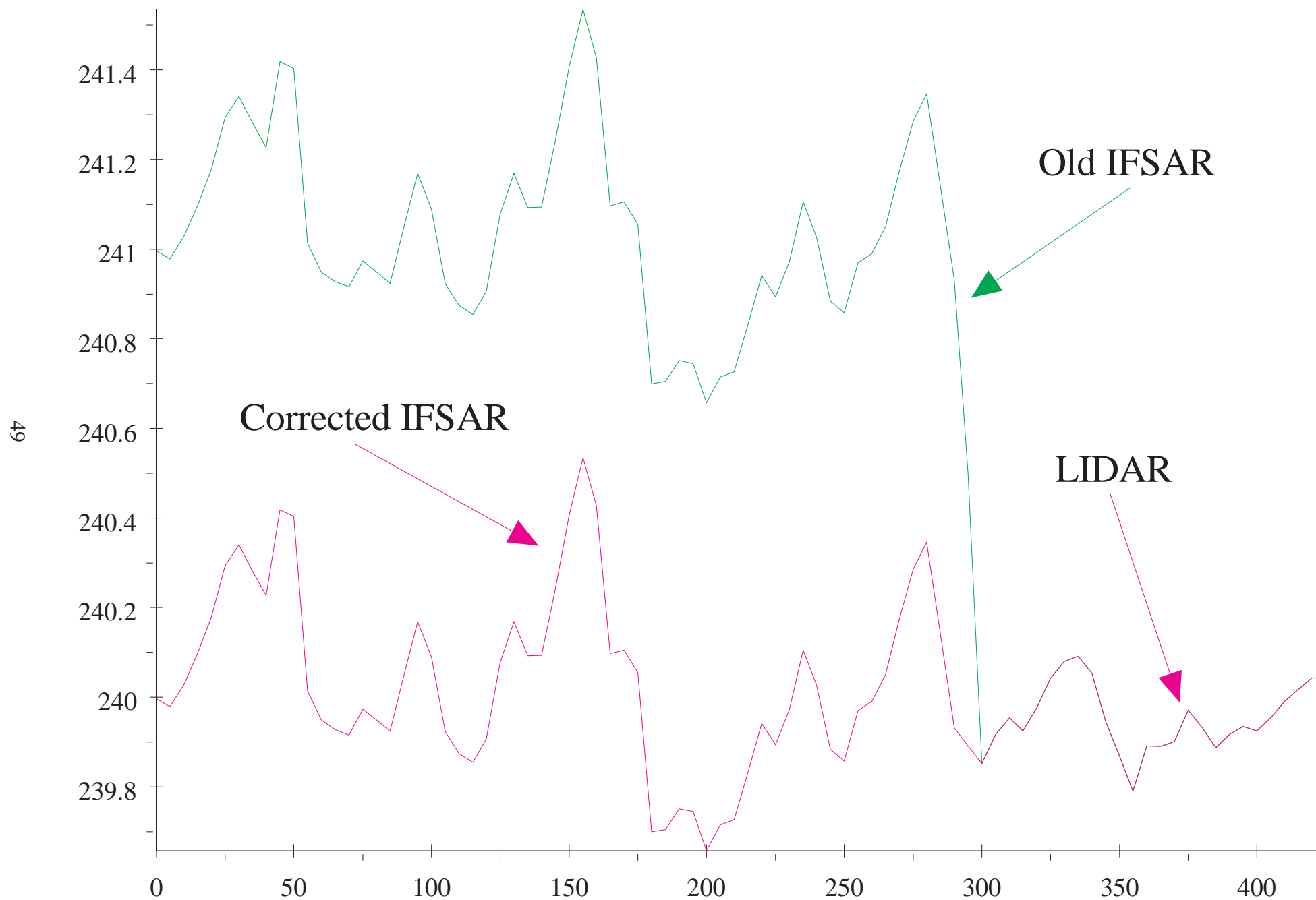
Figure 35. Cross Section Along an Edge of the Merged DEMs

SECOND LIDAR REDELIVERY

The second LIDAR DEM was delivered to TEC in February 2000. EarthData notified TEC in early July 1999 that a systematic error was present in the first LIDAR delivery. TEC reported their initial findings of several errors found in the first LIDAR delivery at a meeting with the Saint Paul District in August 1999.

DEM Anomalies

Three major anomalies were associated with the LIDAR second delivery. The first anomalies were data voids found throughout the entire LIDAR DEM. In Figure 36, data voids are seen in the northeast corner of the database. Another large data void is shown in Figure 37 south of the Pembina River. In Figure 38, data voids are found along the entire length of the Pembina River, which includes the Red River. The total area coverage of the second LIDAR delivery is approximately 59 mi^2 or 153 km^2. The total area represented by data voids is approximately 0.61 mi^2 or 1.58 km^2, which represents 1 percent of the collected area.

The second anomaly was found along the flight line paths of the collection. The seaming anomaly was not found in the prior delivery of the LIDAR DEM. In Figure 39, the seaming anomaly is apparent along edges of the collection area. The seams can be found in all of the flight line paths. Figure 40 shows another example of the flight line seaming anomaly. The third anomaly was introduced by the seaming problem and is associated with elevated road structures and the terrain surface. Elevated road structures and the terrain surface appear broken in many places, as seen in Figures 37 and 39.

Vertical Comparison

The vertical accuracy was assessed with the methods used during the first comparison. Simple differencing was performed using Arc GRID. The same comparisons were performed on the first and second LIDAR deliveries. The second LIDAR delivery was 25- to 26-m below the surface of the first LIDAR delivery. This is shown in Figure 41 with the yellow and orange showing the locations of the major differences. Further analysis is unwarranted at this time due to the extreme vertical offset in the second LIDAR delivery.
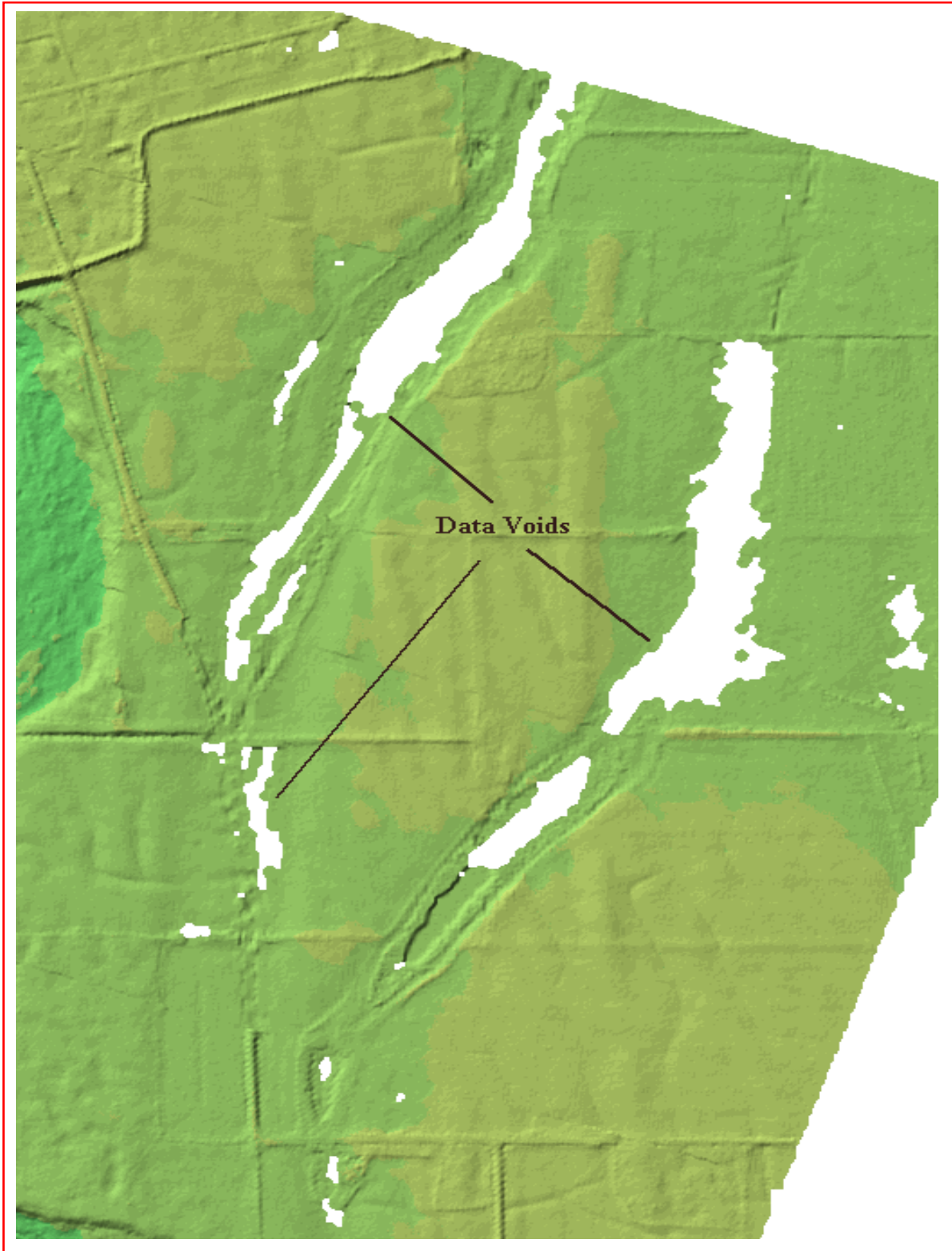
Figure 36. Data Voids in Second LIDAR Delivery

Figure 37. Data Voids in Second LIDAR Delivery and Seam Anomaly

Figure 38. Data Voids in Second LIDAR Delivery

Figure 39. Seaming Anomaly
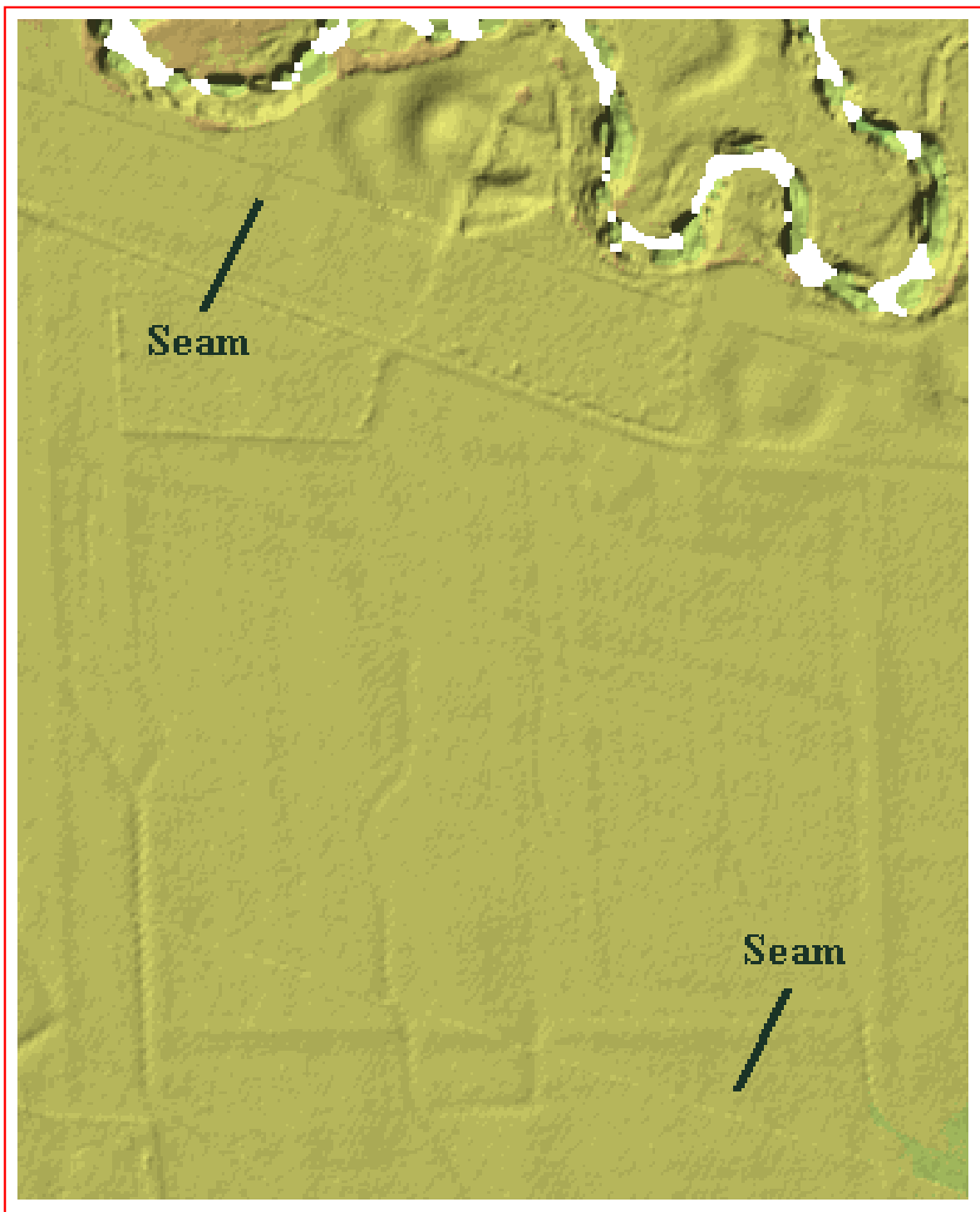
Figure 40. Seaming Anomaly

Legend

■ 7 to 24
■ 25 to 25
■ 26 to 26
■ 27 to 32
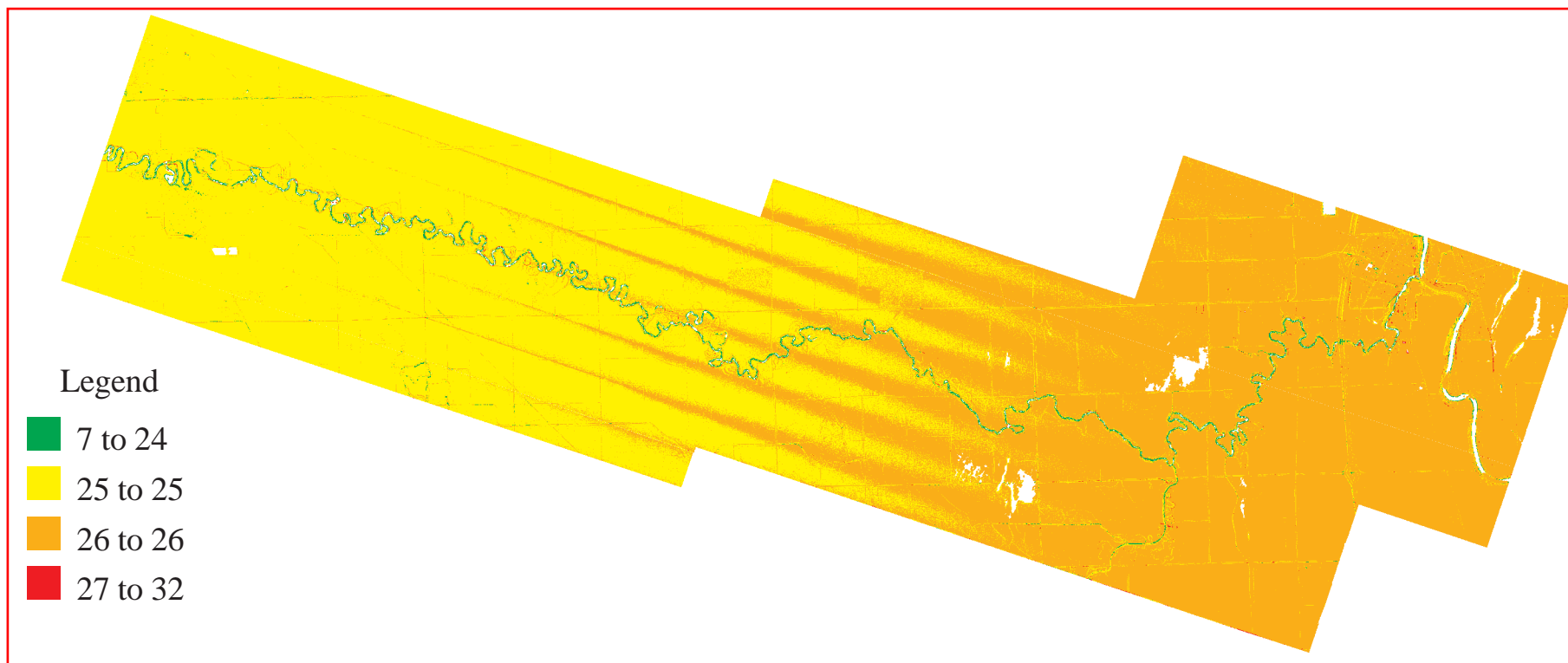
Figure 41. First LIDAR and Second LIDAR Delivery Difference

A comparison of the second LIDAR delivery to the corrected IFSAR DEM shows that the second LIDAR delivery is approximately 25- to 26-m below the IFSAR DEM surface. In Figure 42, the yellow and orange show a similar pattern to that found in the first investigation in Figure 21. The red is mainly vegetation found in the IFSAR DEM.

Cross sections were used to view the elevation differences. In Figure 43, the corrected IFSAR DEM and first LIDAR delivery are above the second LIDAR delivery with an apparent 20-m plus elevation difference using the *STACKPROFILE* command. A 25-m correction was made to the second LIDAR delivery, shown in Figure 44. The second LIDAR delivery should have been at the similar elevation levels as the first LIDAR delivery. Further analysis is unwarranted at this time due to the extreme vertical offset.

Recommendation

Earthdata was notified of the discrepancy in the data and confirmed the offset. The second LIDAR delivery was not processed to orthometric heights but was delivered in ellipsoidal heights. The 20-m plus difference in the second LIDAR redelivery will prevent the hydrologic group from using the second LIDAR redelivery to complete their study. Because of the inconsistencies in reprocessing the second LIDAR redelivery to non-orthometric heights, the introduction of more extensive data voids, and the distortion of topographic features from seams, using the first fused data set in the hydrologic study is recommended.

Legend

- 🟩 7 to 24
- 🟨 25 to 25
- 🟧 26 to 26
- 🟥 27 to 56
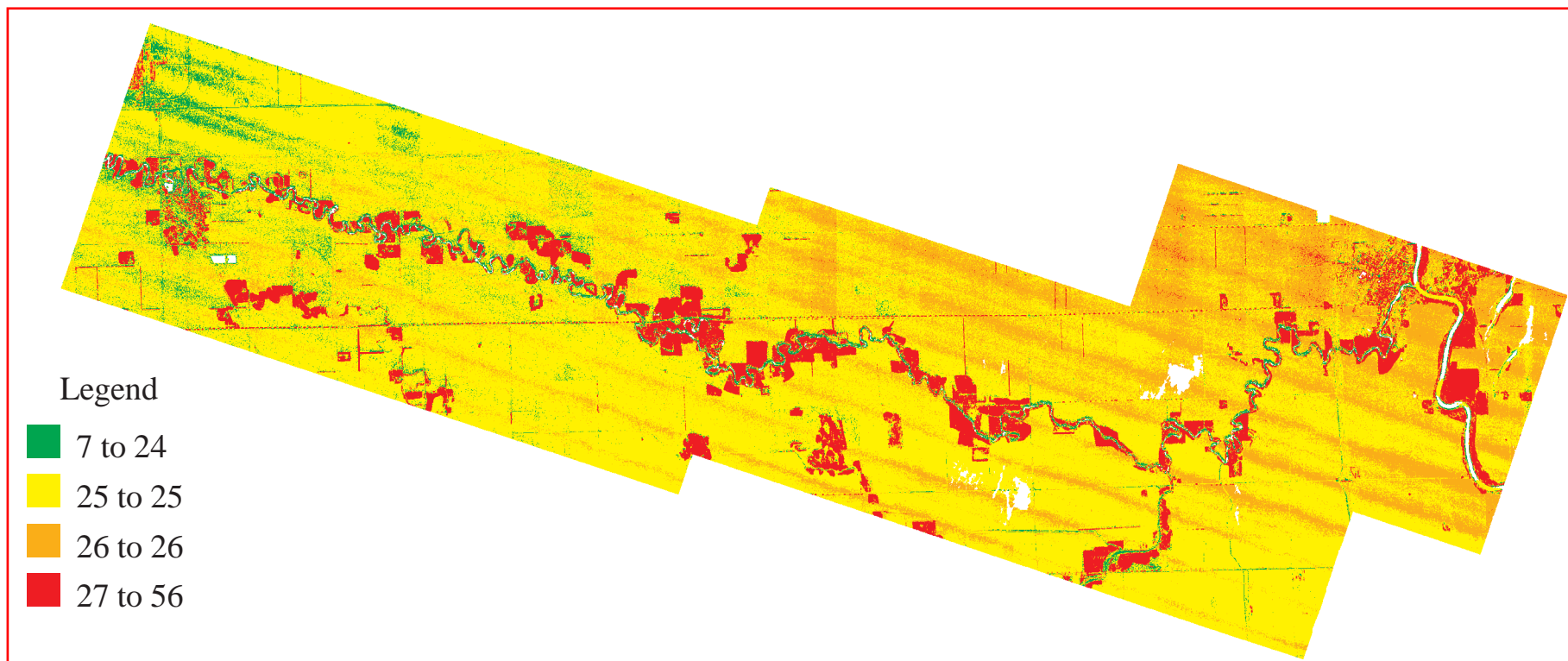
Figure 42. Corrected IFSAR and Second LIDAR Delivery Difference
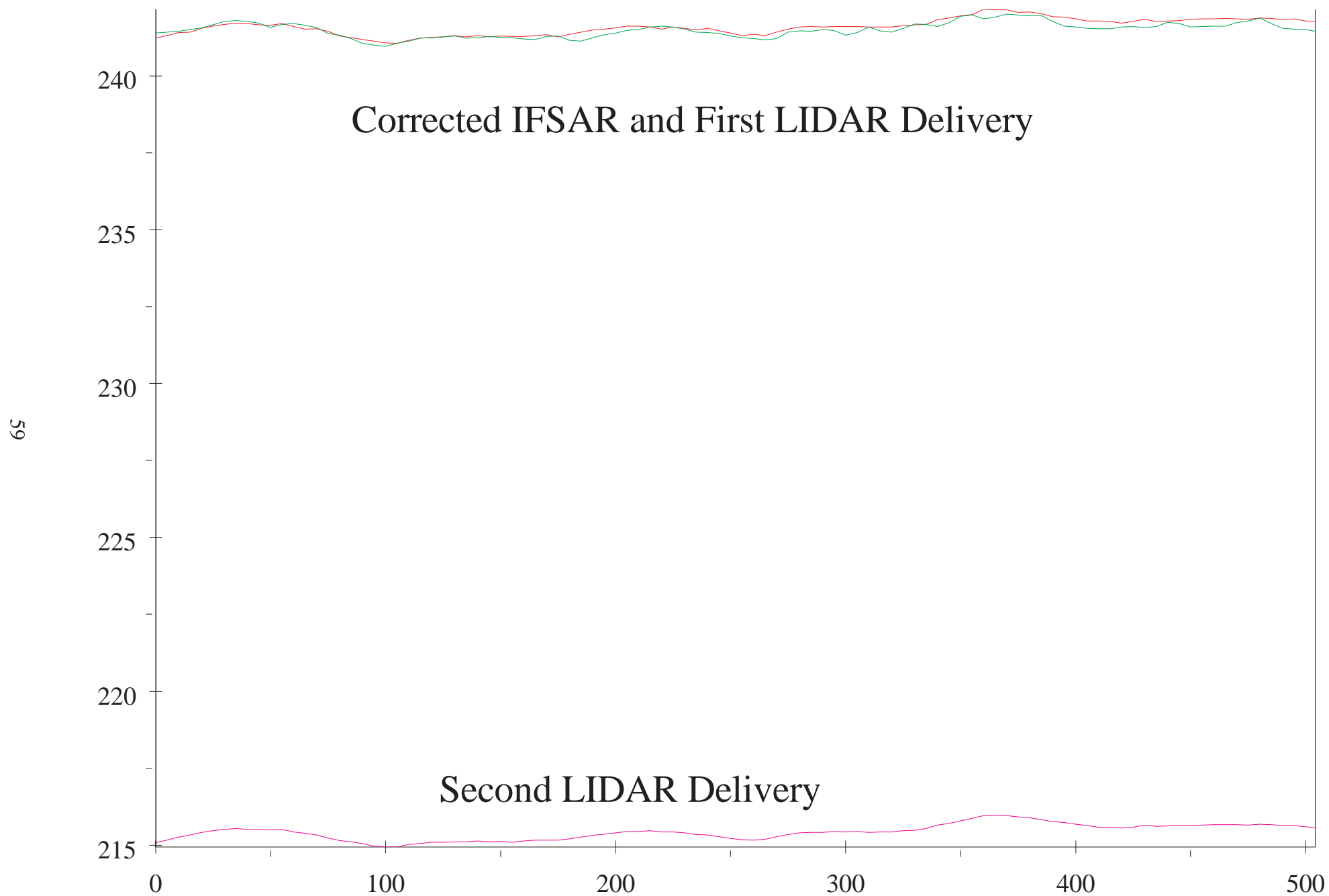
Figure 43. Cross-section of the Corrected IFSAR, First LIDAR, and Second LIDAR Delivery
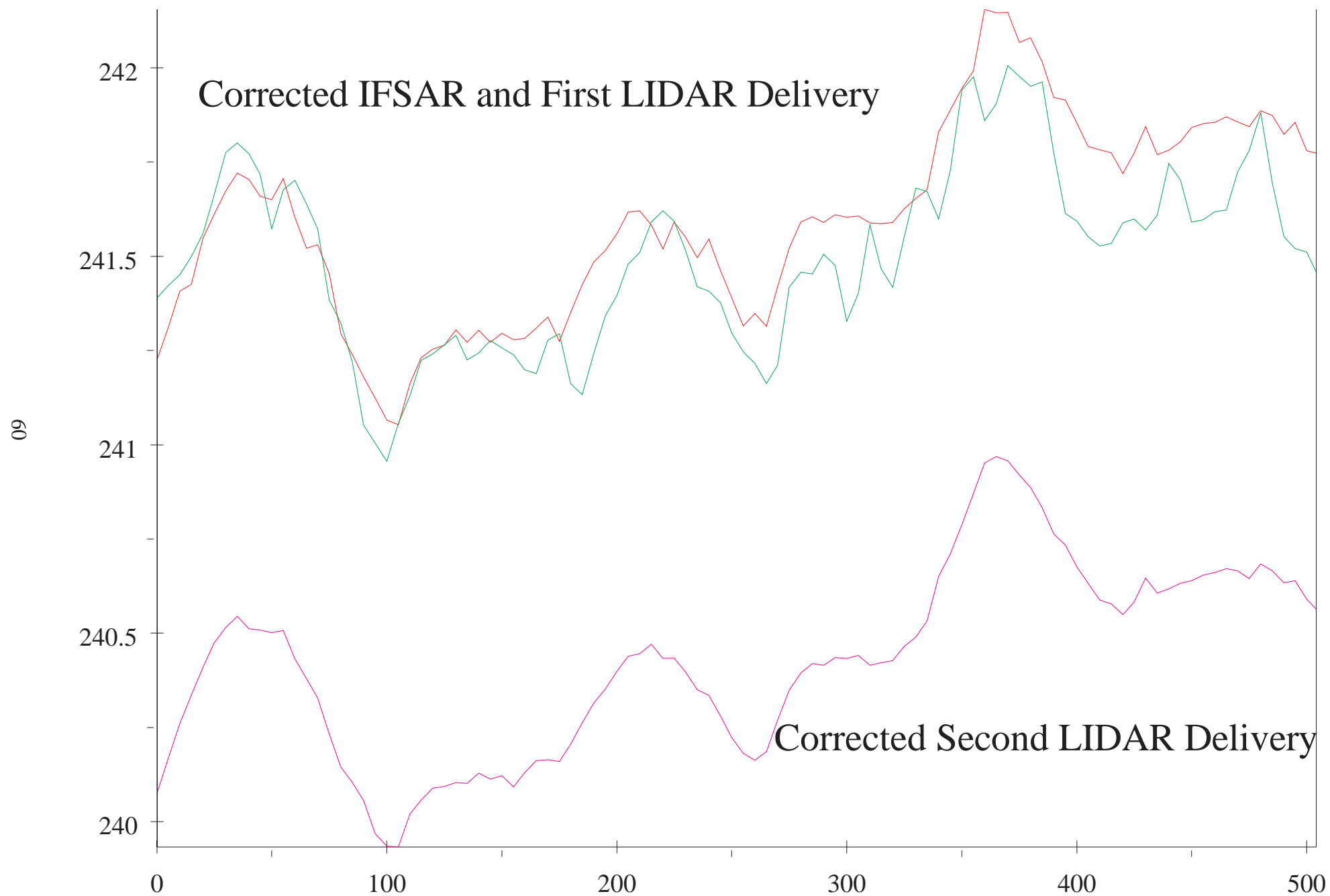
Figure 44. Cross-section of the Corrected Second LIDAR Delivery, Corrected IFSAR, and First LIDAR Delivery

THIRD LIDAR REDELIVERY

TEC informed EarthData of the offset in the second LIDAR delivery. EarthData confirmed that the geoid heights were not processed for the second LIDAR delivery and agreed to reprocess and deliver a third LIDAR data set to TEC within 2 weeks.

DEM Anomalies

The same three anomalies associated with the second LIDAR delivery were present in the third LIDAR delivery. Large areas of the data set still had data voids and the seaming problems were still present. The total area delivered was approximately 58 mi^2 or 150 km^2. The total area representing data voids was approximately 1 mi^2 or 2.6 km^2, which represents 1.73 percent of the total area. The seaming anomaly also introduced problems with elevated road structures and the physical terrain. The elevated road seen in Figure 45 clearly is not intact at the bend due to the seaming anomaly. The oxbows and roads appear to have problems along the seams in Figures 45, 46, and 47.

Vertical Comparison

A regression analysis was run on the first and third LIDAR DEMs to determine their correlation. The *SAMPLE* function was issued at the Grid prompt with the string *lidarsamp = sample (lidard1, lidar3, bilinear)*. The *REGRESSION* command was used to analyze the two LIDAR DEMs with the string *regression lidarsamp linear brief*. The results of the ArcInfo regression are shown in Table 7 with a RMSE of 0.235-m. Next, all three DEMs were clipped to a smaller area seen in Figure 48 to eliminate vegetation from the IFSAR DEM for a combined regression analysis in ArcInfo. The *SAMPLE* function was used with the string *lidarifsarsamp = sample (gt1clp, lidardclpl, lidarclp3, bilinear)*. The *REGRESSION* command was run again with results seen in Table 8. The *CORRELATION* command was used to look at the relationship of the first and third LIDAR DEMs and the corrected IFSAR DEM. The *CORRELATION* command used the example string *correlation gt1clip lidarclp1* for each of the three combinations with results seen in Table 9.

Table 7. ArcInfo Regression Analysis for the First and Third LIDAR DEMs

Coef #	Coef
0	-0.490
1	1.001
RMS Error	0.235
Chi-Square	916337.333
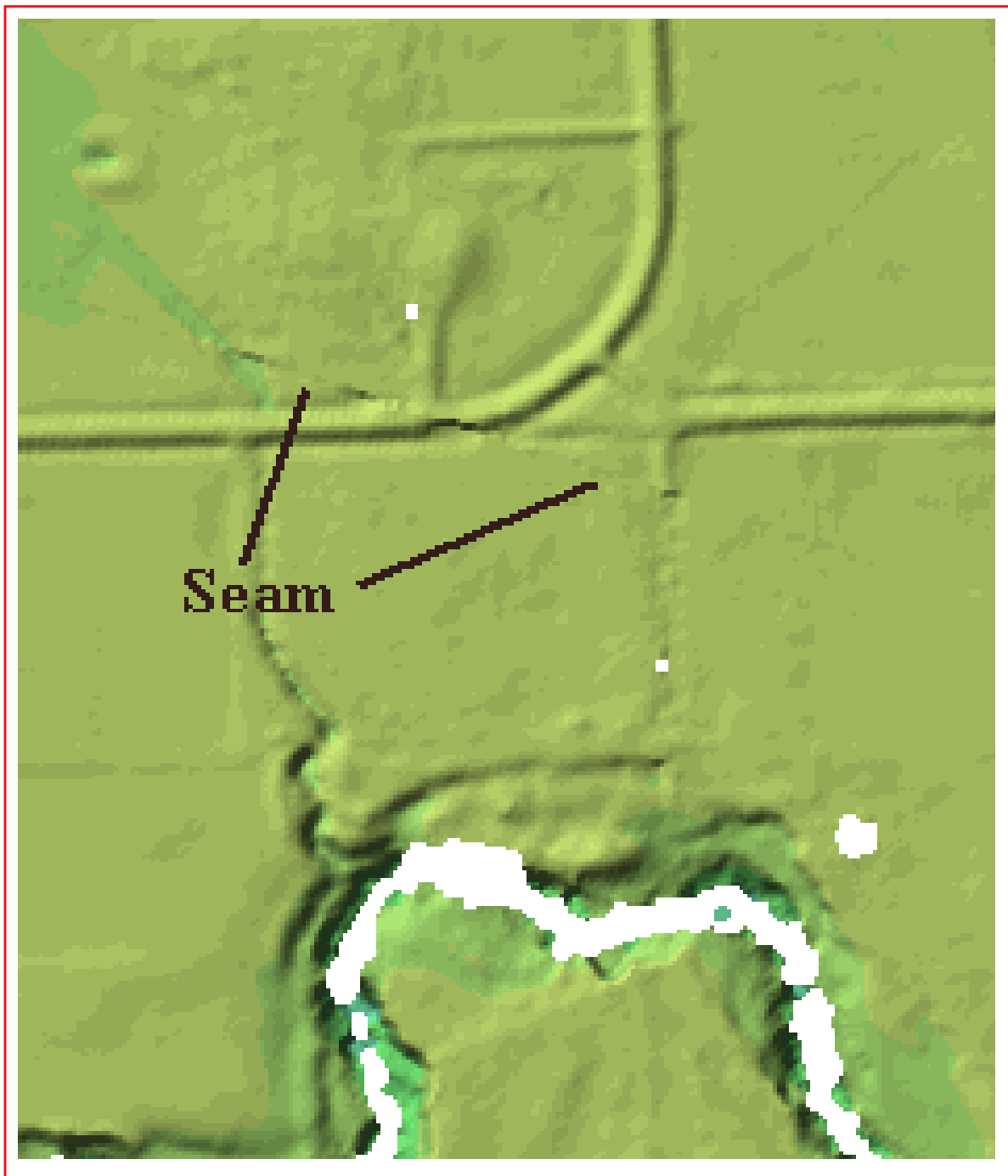
Figure 45. Third LIDAR Delivery Seaming Anomaly

Figure 46. Third LIDAR Delivery Seaming Anomaly
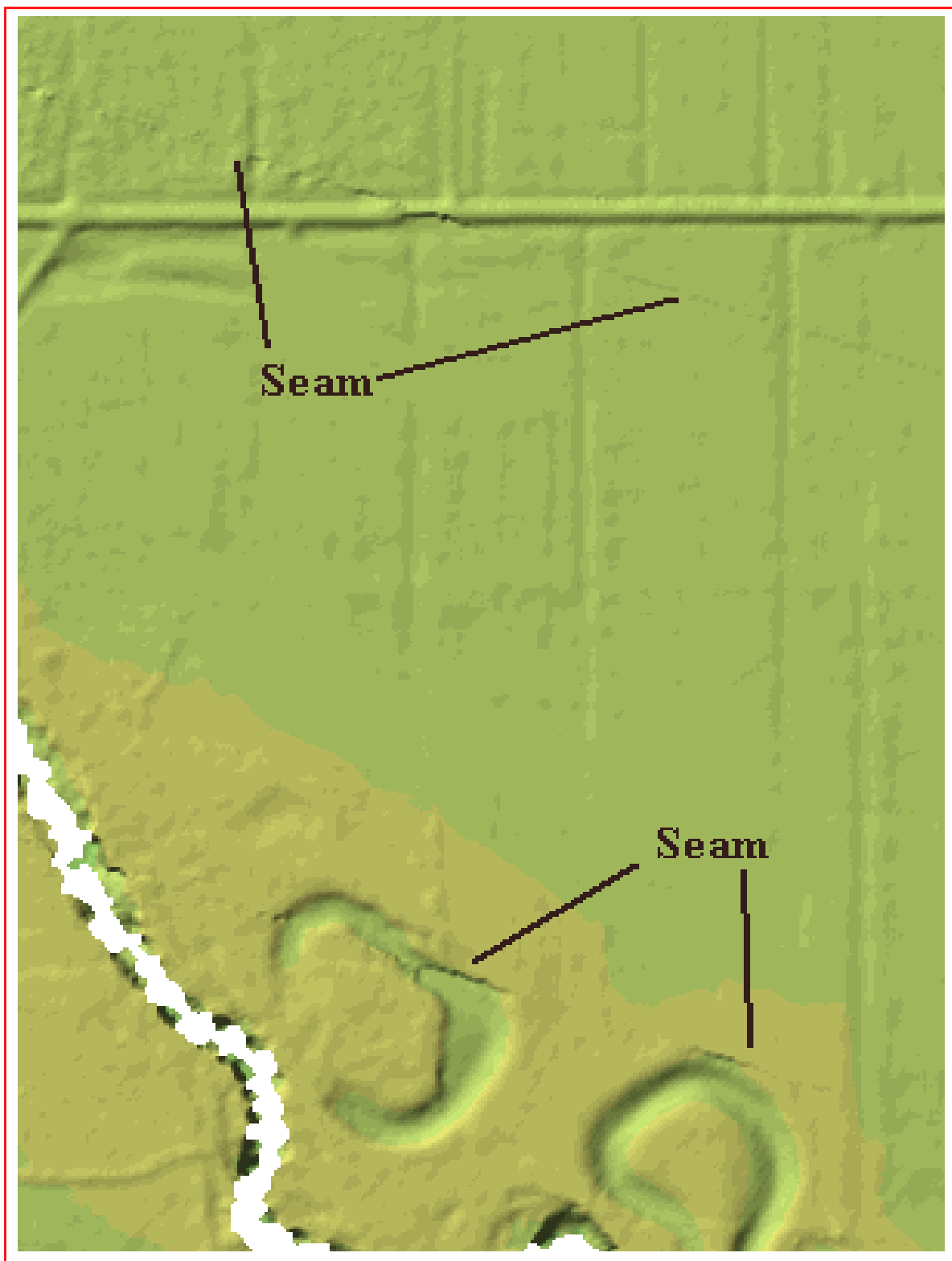
Figure 47. Third LIDAR Delivery Seaming Anomaly
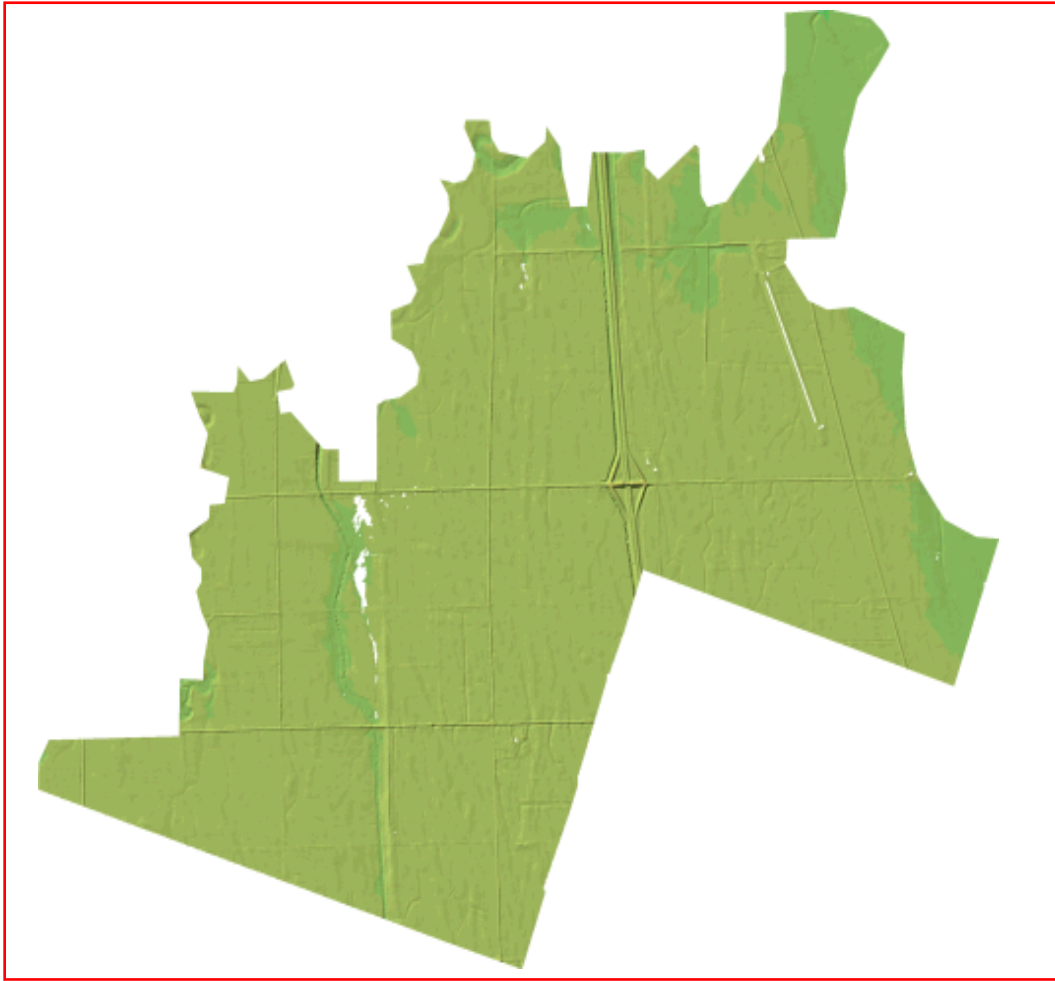
Figure 48. Clipped Area

Table 8. ArcInfo Regression Analysis

Coef #	Coef
0	31.99
1	-0.147
2	1.011
RMS Error	0.281
Chi-Square	66280.091

Table 9. ArcInfo Correlation Analysis

Correlation Corrected GT1 and 1st LIDAR DEM	0.925185
Correlation Corrected GT1 and 3rd LIDAR DEM	0.936569
Correlation 1st and 3rd LIDAR DEM	0.988297

The *MAKESTACK* command with the *LIST* option was used to put the corrected IFSAR and first and third LIDAR deliveries into an associated file. Elevation data were extracted from the stacked file using the same AML used earlier. The AML placed the extracted data into an ASCII text file for analysis. The entire list of the extracted data is shown in Appendix E. One point was dropped from the analysis because it was over a data void in the third LIDAR delivery. The basic statistics were computed using 411 points with results seen in Table 10.

Table 10. Basic Statistics

	GT1	1st LIDAR	3rd LIDAR
Mean	244.0366	244.2683	244.5250
Max	254.3342	254.2984	254.6667
Min	237.6239	237.6307	237.8957
STD	4.1382	4.1174	4.1274

Analysis was performed using Quattro Pro 9, Minitab version 12, and S-Plus. One- and two-tail paired t-tests were performed using the 411 elevation points. The one-tail paired t-test was run for three combinations of the corrected IFSAR, the first LIDAR, and third LIDAR deliveries and concluded the null hypothesis was rejected in all 3 cases. The two-tail paired t-test was run for three combinations of the corrected IFSAR, first, and third LIDAR deliveries and concluded the null hypothesis was rejected. The results of the one- and two-tail paired t-test are seen in Table 11 with p-values of 0.00 and in Appendix F.

Nonparametric tests were performed that do not depend on normality for accuracy. Three common nonparametric tests were used: the Kolmogorov-Smirnov (K-S) test, the Mann-Whitney (M-W) test, and the Runs test. All of these tests are distribution-free, so the non-normality of the data is irrelevant. The K-S test, M-W test, and Runs test were performed. Results are shown in Table 11 and in Appendices F and G. The K-S test for the GT1-first LIDAR and first-third LIDAR combinations concluded the null hypothesis was not rejected with p-values of 0.08 and 0.15. The K-S test for GT1-third LIDAR concluded the null hypothesis was rejected with p-values of 0.00. The M-W test GT1-first LIDAR and first-third LIDAR combinations concluded the null hypothesis was not rejected with p-values of 0.13 and 0.15. The M-W test for GT1-third LIDAR concluded the null hypothesis was rejected with p-values of 0.00. The Runs test with p-values of 0.00 concluded the null hypothesis was rejected. Regression analysis was run for

completeness with results shown in Table 12.

Table 11. Analysis

		GT1-1st	GT1-3rd	1st-3rd
t-test	One Tail	0.0000	0.0000	0.0000
Paired	Two Tail	0.0000	0.0000	0.0000
K-S	p-value	0.0754	0.0001	0.1481
	ks	0.0876	0.1557	0.0779
M-W	p-value	0.1340	0.0029	0.1450
Runs	p-value	0.0000	0.0000	0.0000

Table 12. Regression Output

	GT1-1st	GT1-3rd	1st-3rd
Constant	2.4049	1.9207	-0.2747
Std Err of Y Est	0.3643	0.3338	0.0908
R Squared	0.9922	0.9935	0.9995
Number of Observations	411	411	411
Degrees of Freedom	409	409	409
X Coefficient(s)	0.9911	0.9941	1.0022
Std Err of Coef.	0.0043	0.0040	0.0011

The second comparison involved the use of a large and several small cross sections to evaluate the first and third LIDAR deliveries and the corrected IFSAR DEM. The comparison used only the area of overlap between the three DEMs. The cross-section seen as a black line in Figure 49 was used because of the lack of data voids and is approximately 5,000-m across. The graph in Figure 50 is a cross-section of the difference grid of the first LIDAR delivery and the corrected IFSAR DEM. The presence of the systematic error can be seen as a wave in the graph starting on the left side moving across to the far right side.

In Figure 51, the difference grid of the third LIDAR delivery and the corrected IFSAR shows the systematic error is still present. The cross-section in Figure 52 shows the systematic error is slightly reduced but is still present in the third LIDAR Delivery. The difference grid of the first and third LIDAR deliveries shows the height difference between the two deliveries in Figure 53. The cross-section of the difference grid for the first and third LIDAR deliveries in
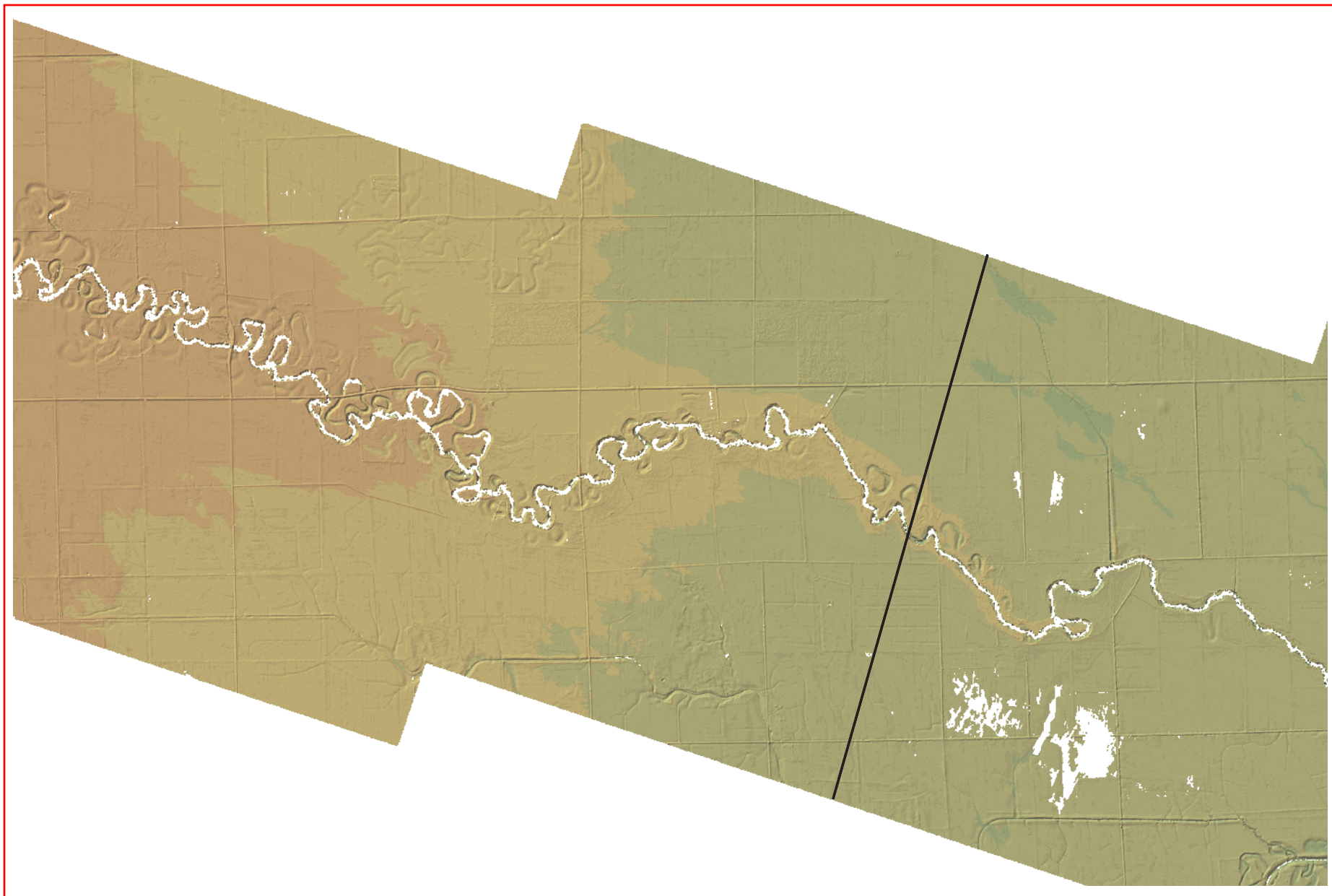
Figure 49. 5,000-m Cross-section Line
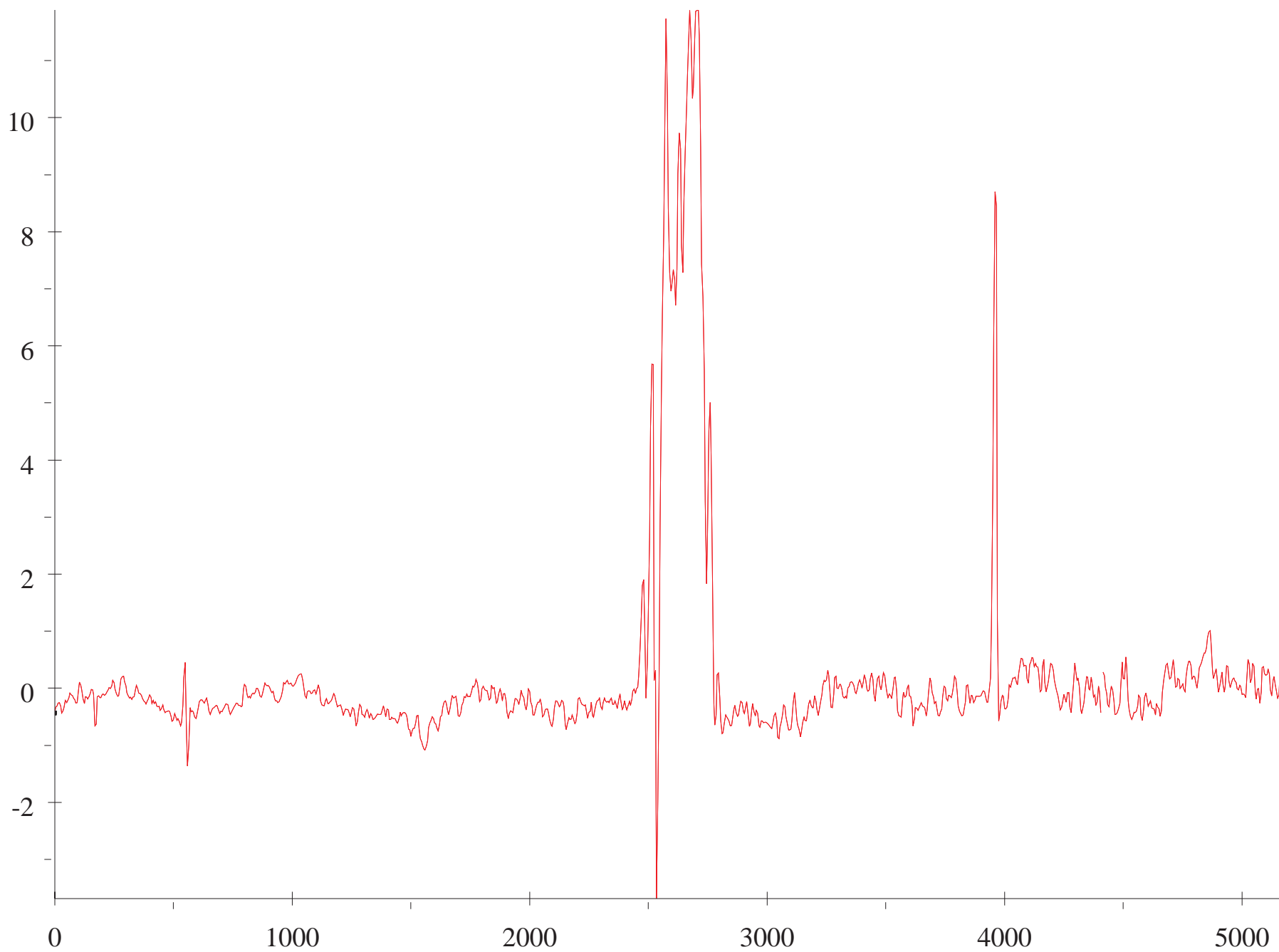
Figure 50. Difference Cross-section of the First LIDAR Delivery and Corrected IFSAR

69
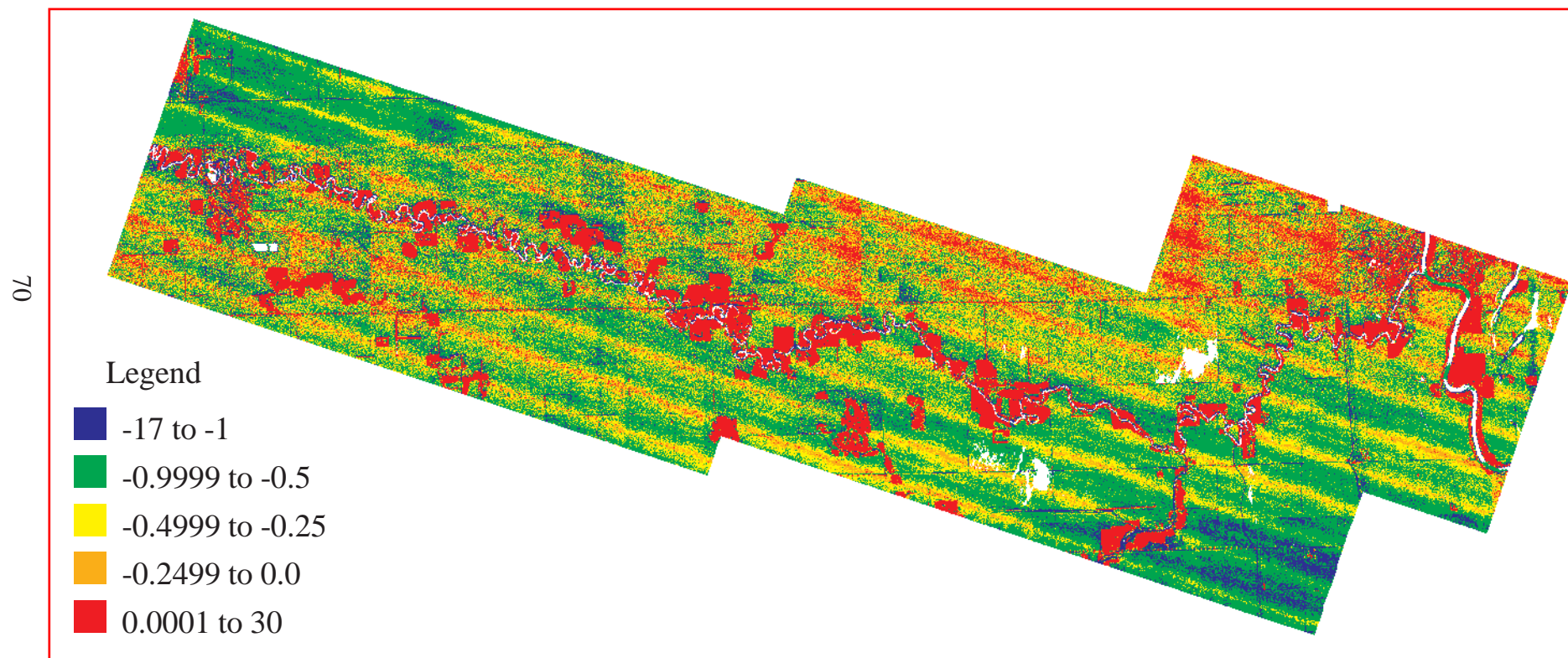
Figure 51. Difference Grid of the Third LIDAR Delivery and Corrected IFSAR
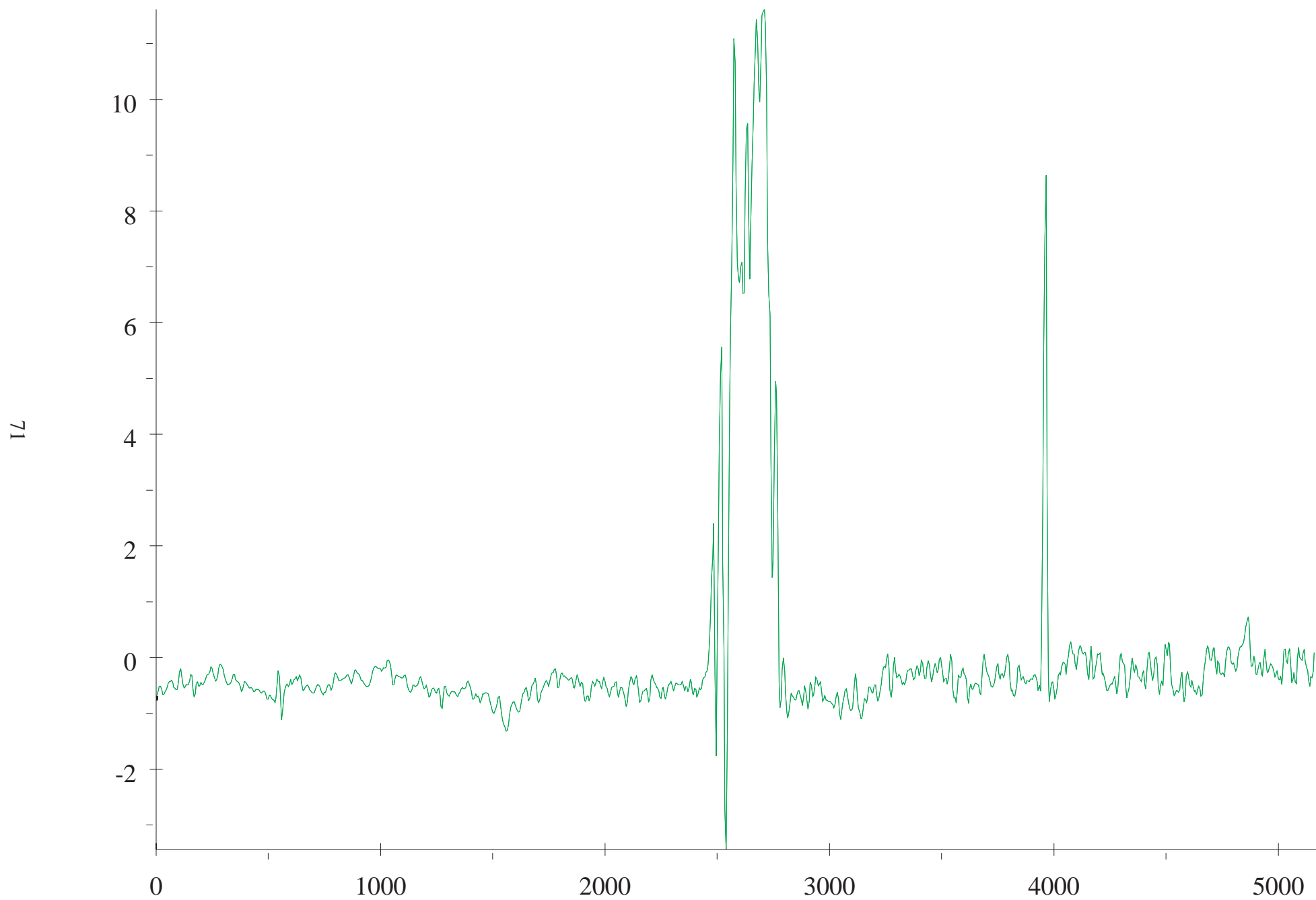
Figure 52. Difference Cross-section of the Corrected IFSAR and the Third LIDAR Delivery

Legend

- ■ -18 to -1
- ■ -0.9999 to -0.5
- ■ -0.4999 to -0.25
- ■ -0.2499 to 0.0
- ■ 0.0001 to 6
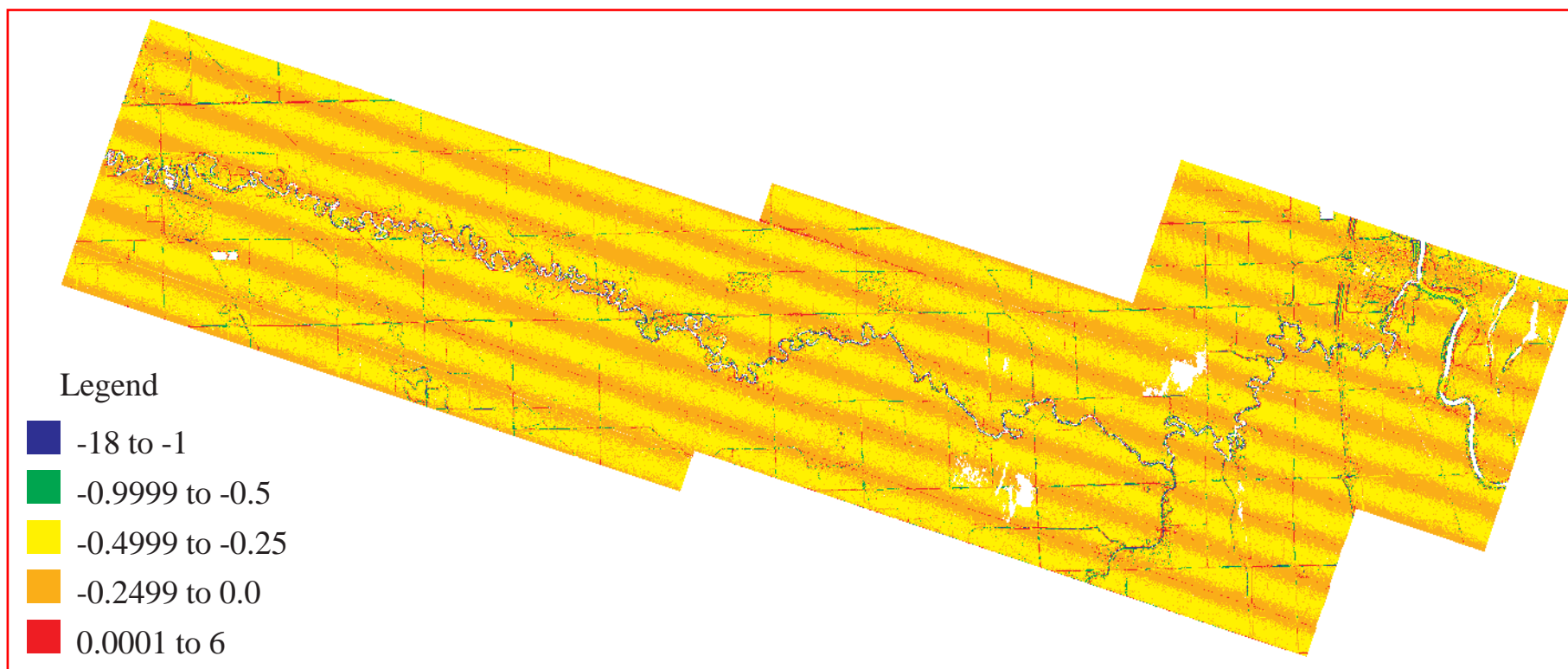
Figure 53. Difference Grid of the First and Third LIDAR Delivery

Figure 54 show the total difference in height as well as the systematic error in the LIDAR data set. In Figure 55, the cross-section of the first and third LIDAR deliveries and corrected IFSAR DEM illustrates the height differences between the three DEMs. The Pembina River in the center of Figure 56 is higher than the surrounding terrain and could be one of the many causes of flooding in the area. In Figure 57, the differences between the three DEMs is apparent and illustrates how variable the differences are in height along the cross-section.

Recommendations

TEC recommends the use of the first LIDAR delivery for the hydrologic modeling because of the large data voids and the unsuccessful elimination of the systematic error in the second and third LIDAR data sets. The cross sections provided proof of the difference in heights, and the systematic error was still present in the data.
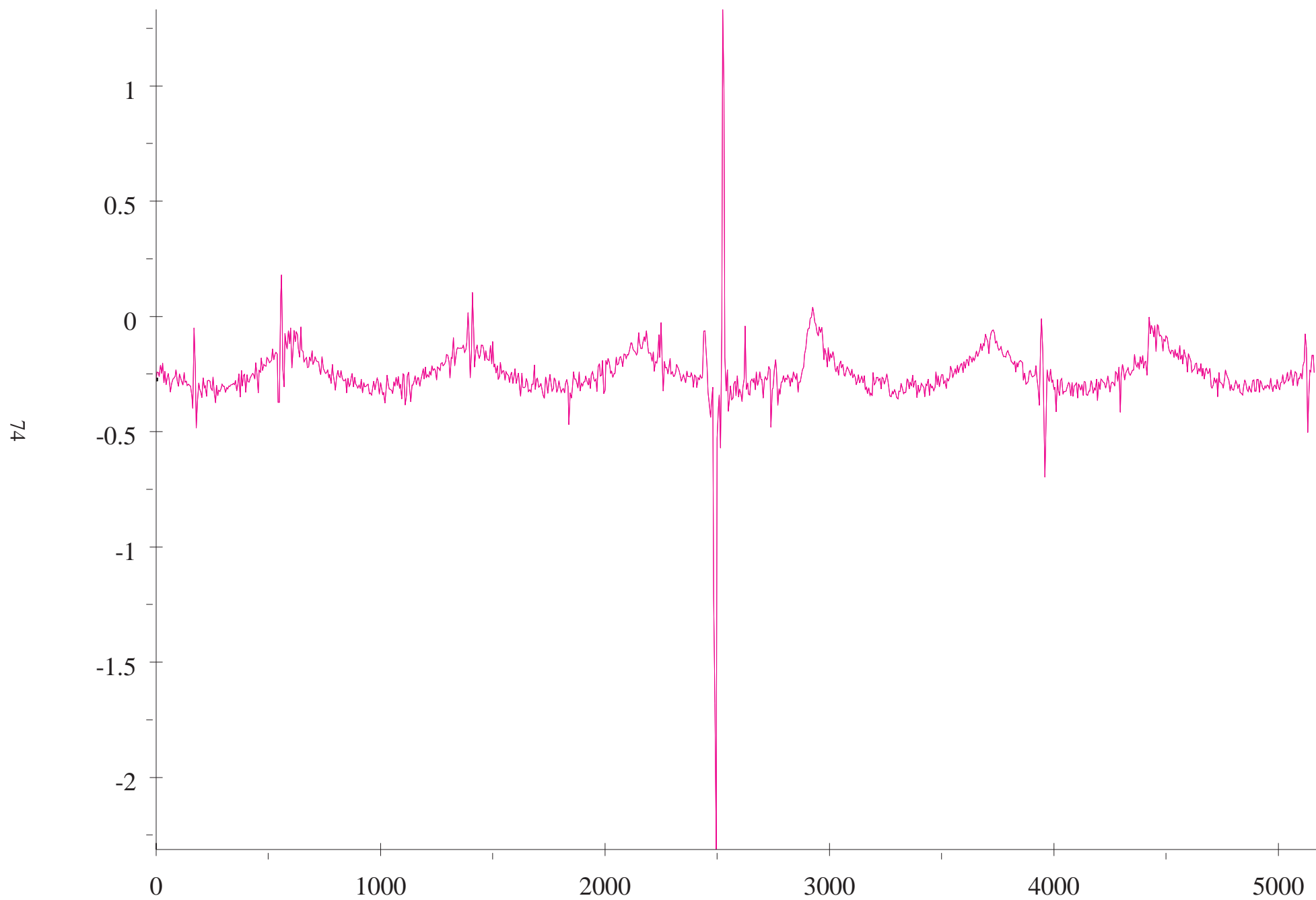
Figure 54. Difference Cross-section of the First and Third LIDAR Deliveries
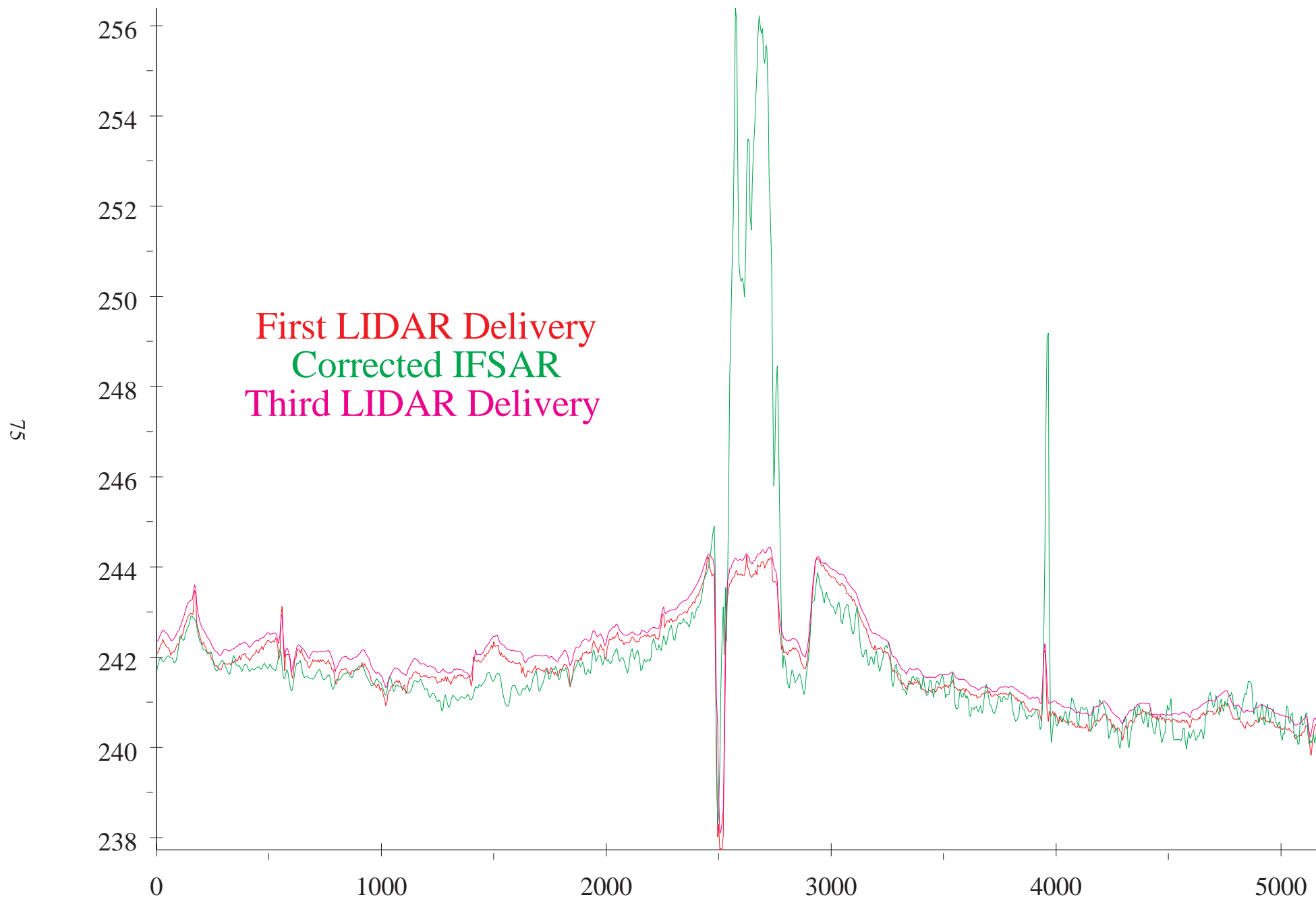
Figure 55. Difference Cross-section of the First and Third LIDAR Deliveries and Corrected IFSAR
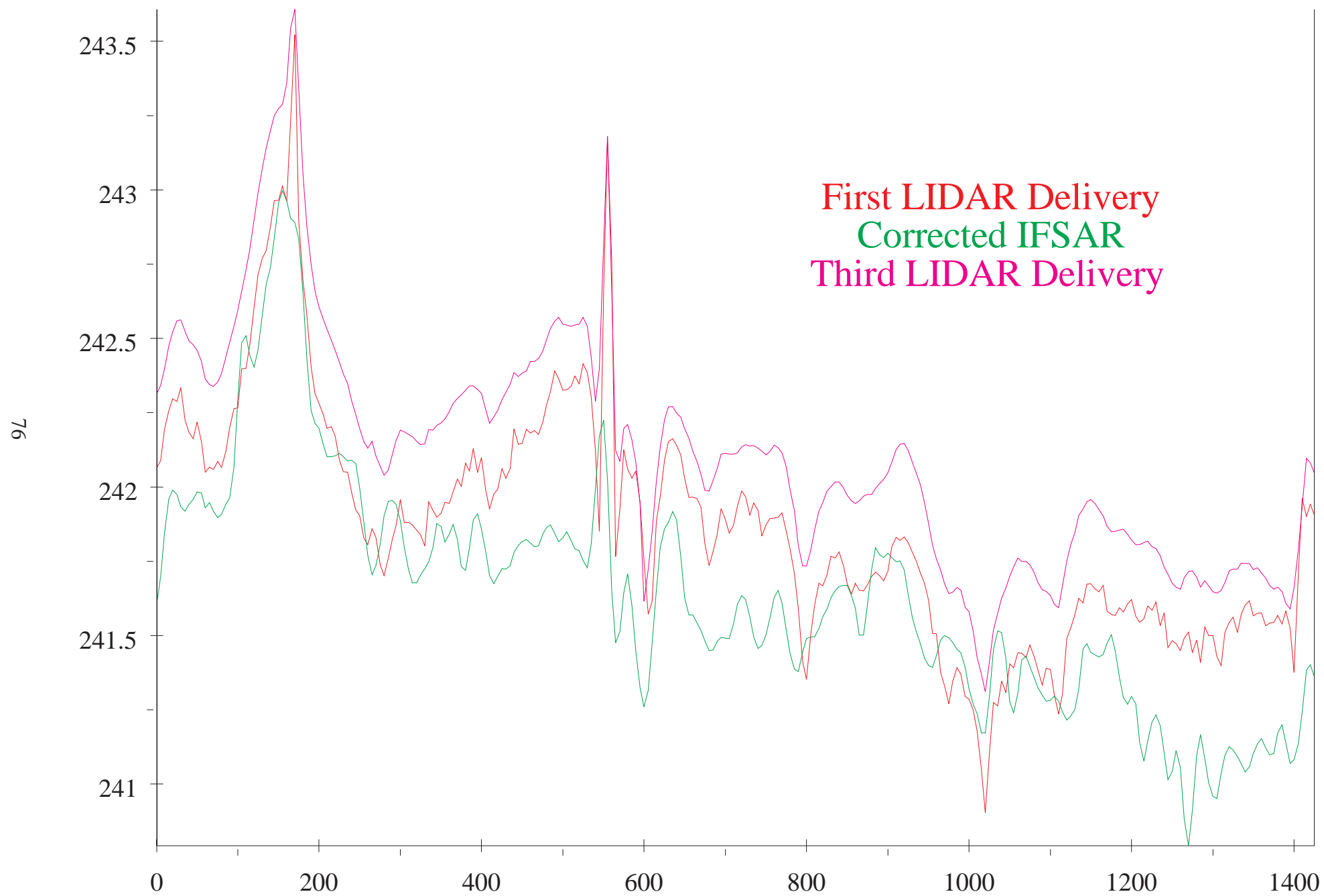
Figure 56. Closer View of Figure 55
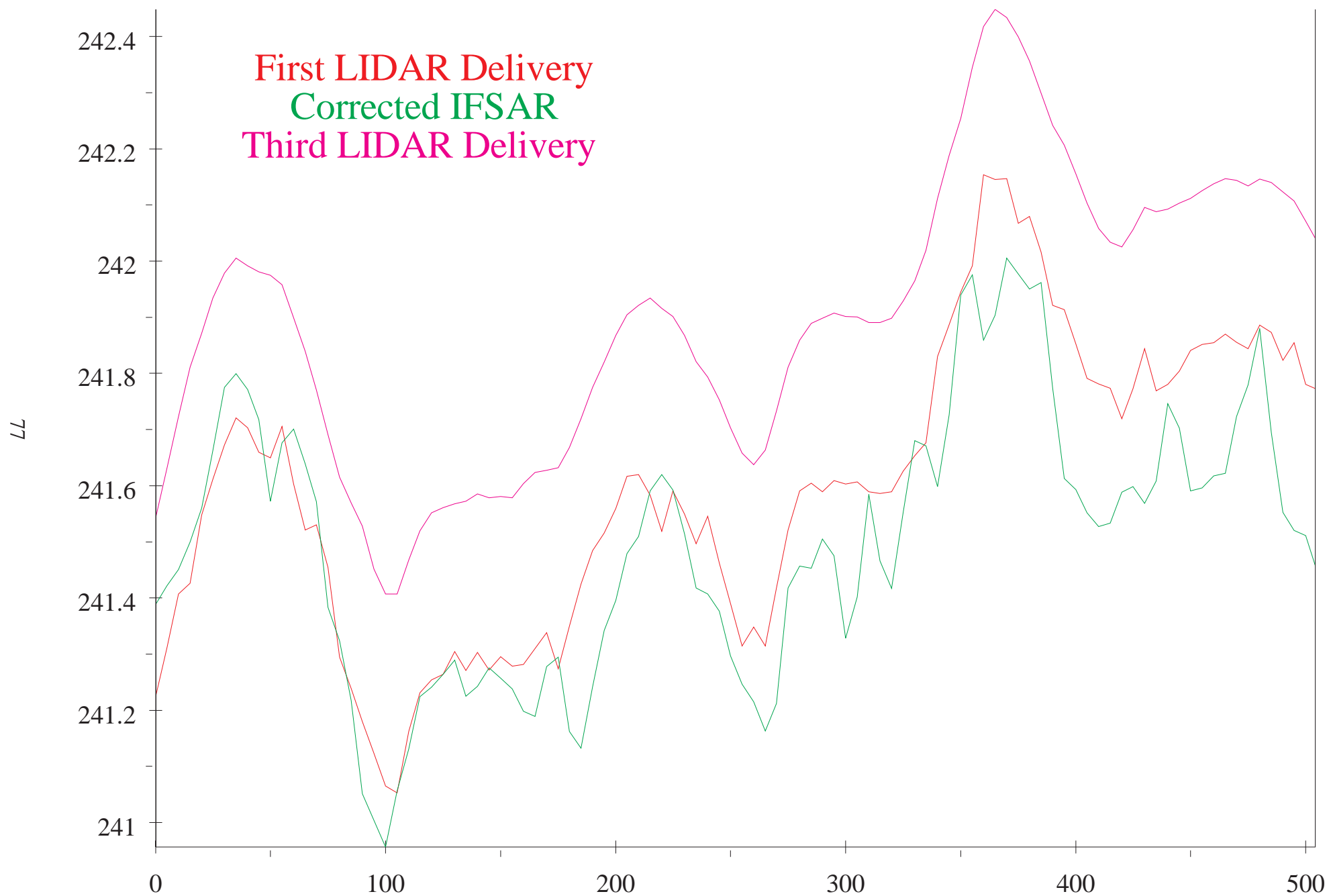
Figure 57. Third LIDAR Delivery Compared with the First LIDAR Delivery and Corrected IFSAR from Figure 24

CONCLUSIONS

LIDAR

The LIDAR DEMs provided a high resolution surface with a narrow area coverage. The LIDAR DEMs provided a bare earth with most of the urban and forested areas removed from the three DEMs. The first LIDAR DEM had a systematic error throughout the DEM surface. However, the first LIDAR DEM had less severe flaws than the second and third LIDAR deliveries. The second LIDAR DEM had data voids making up 1 percent of the total area and a negative 20-m elevation difference. This large elevation difference was due to the lack of a geoid correction being applied to the second LIDAR DEM. The third LIDAR delivery continued to display the systematic error, the DEM had been smoothed when compared to the first LIDAR delivery, and the data voids were quite significant at 1.73 percent of the total area.

The assessment of the LIDAR data using the AeroScan sensor revealed numerous anomalies and errors in the processed bare-earth DEM. While LIDAR technology has the potential to collect higher resolution and more accurate terrain data, there are significant deficiencies in the Earthdata postprocessing software that merges the individual flight lines and feature removal algorithms. The first and third LIDAR deliveries further attest to the unstableness of the postprocessing task by the inconsistent quality and data voids of the two DEMs. The systematic error found in the first LIDAR delivery was still present in the second and third delivery after 8 months of effort to process out the error. This unsuccessful attempt to remove this systematic error cast doubt on the usefulness of the LIDAR bare-earth DEM for hydrologic modeling.

IFSAR

The IFSAR DEM provided a wider area coverage with minor flaws associated with the sensor and processing. It was capable of being lowered to the approximate elevation height of the first LIDAR DEM and allowed for the data fusion of the two DEMs. The IFSAR DEM with vegetation will present an interesting problem for hydrologic tools and software. It did provide a base data set with which to compare the LIDAR DEM, and helped find the systematic error in the LIDAR DEM. A GPS high-accuracy reference network (HARN) using National Geodetic Survey (NGS) standards would provide elevation data that could help bring the IFSAR and LIDAR DEMs down to the actual ground after the data fusion process.

There are differences with the representation of transportation features with the IFSAR and LIDAR collection devices. The LIDAR collection device does represent transportation features really well. On the other hand, the IFSAR collection device represents these transportation features well, but as the transportation feature decreases in width the feature is much less defined.

FEMA 37 Specification

The Federal Emergency Management Agency (FEMA) 37 Specification Appendix 4B, "Airbourne Light Detection and Ranging System," found at http://www.fema.gov/mit/tsd/lidar_4b.htm, defines the acceptable LIDAR collection and deliverables for floodplain mapping. According to A4B-4, "Performance Standards," the spec for section A for deliveries two and three was not met due to data voids, and section B was not met for lack of system calibration, which caused the systematic error in the DEM. The GPS data collected by TEC does not meet the FEMA 37 spec for LIDAR because the data collected was at the 5- to 10-cm accuracy level on roads only and not according to section A4B-5, "GPS Control using NGS standards". According to section A4B-6, "Post-Processing of Data," the minimum point spacing of 5-m was met, and no additional data were delivered other than the LIDAR DEM. According to section A4B-7, "Quality Control/Quality Assurance," the field verification was not done to FEMA 37 spec, and the LIDAR data cannot be verified totally with the GPS data provided to TEC. Additional data were not acquired to support the verification process under vegetation. According to A4B-8, "Deliverables," the LIDAR DEM does not meet the FEMA 37 Specification Appendix 4B. The FEMA 37 Specification Appendix 4B became public as a draft for comments in early 1999 and finalized in May 2000.

According to the Draft FEMA 37 Specification for IFSAR, the Red River IFSAR DEM does not meet the required maximum 15-cm RMSE for vertical accuracy. Currently, Intermap is experimenting to achieve a goal of providing a bare-earth DEM for floodplain analysis at the 30- to 50-cm level, referred to as the GLOBAL Terrain FloodPlain (GTFP). The GTFP product will be made available as an option for customers within the next year after testing is completed.

Costs and Accuracies

The following tabulation summarizes the general range of cost and accuracy of the IFSAR and LIDAR DEM collection capability:

Parameters	IFSAR	LIDAR
Sensor Type	Radar	Laser
Commercially Available	Single Source	Multiple Source
DEM Spacing	5 - 10 m	0.5 - 3 m
Vertical Accuracy	0.6 - 1.5 m	6 cm and up
Typical Cost	$11 - $80 km^2	$225 - $1500 km^2
Post Collection Product Delivery	2 - 3 months	2 - 3 weeks

LIDAR Vendors and Emerging IFSAR Capabilities

To further consider LIDAR technologies to address the IJC Red River Task Force's objectives, other types of LIDAR sensors should be considered and evaluated. Aside from the Earthdata AeroScan system, there are at least three other LIDAR sensor manufacturers (Optech, Topoeye, and Nortech). Aside from these LIDAR manufacturers, John Chance and TerraPoint also operate proprietary LIDAR systems. Appendix H provides a list of the LIDAR manufacturers and a summary of the operating LIDAR vendors in the United States by system.

Currently, Intermap is the sole operator of an IFSAR sensor in the United States. Additionally, Intermap has flown overseas to help supply IFSAR DEMs for floodplain mapping efforts in the United Kingdom (UK) (Galy and Sanders 2000). Intermap is also researching capabilities to produce bare-earth DEMs (Intermap 2000).

Closing Statement

A thorough assessment of IFSAR and LIDAR DEMs in a GIS environment was accomplished. Tools were presented to modify, evaluate, and check the elevation heights of the IFSAR and LIDAR DEMs. Visual analysis and cross sections were employed to assist in the evaluation process. Cross-section information was used to bring the surfaces to a common elevation height for the data fusion process. If not for the systematic error in the LIDAR DEM, the two data sets could be brought closer to achieve the desired goal. The Saint Paul District was delivered a fused DEM data set using the first LIDAR delivery in the summer of 1999, which was achieved using GIS-based tools such as ArcInfo. ArcInfo tools for DEM editing will require major updating to easily handle the new IFSAR and LIDAR floating point data. Data size was not looked into in this report, but should be considered for operational systems using IFSAR and LIDAR DEMs. The smaller cell size of IFSAR and LIDAR DEMs increases the total volume of data on a hard drive. Statistics alone cannot point to systematic errors in these new technologies for DEM production as seen in this report. Other areas may not have an IFSAR DEM for reference to detect anomalies in the future. FEMA has currently produced specifications for LIDAR and IFSAR data collections and deliveries for floodplain mapping, which are the guidelines for the start of all floodplain-related projects involving IFSAR and LIDAR collections.

The contract for the LIDAR DEM data purchase was awarded by the Canadian Government working with the Saint Paul District. Neither the Saint Paul District nor the Canadians were actively involved in interacting with EarthData in the LIDAR redelivery process. The Canadian Government contract monitor was responsible for accepting or rejecting the LIDAR DEM.

REFERENCES

Damron, James J. (1999). "Techniques for Digital Elevation Model (DEM) Fusion using Arc/Info: Using IFSAR and LIDAR DEM Data," *Second Conference on GIS Applications of Remote Sensing for Disaster Management*, Washington, DC, January 19-21, 1999. The George Washington University, 14 pg.

Federal Emergency Management Agency. (2000). "Flood hazard mapping; Appendix 4B, Airborne Light Detection and Ranging Systems," Washington, DC. http://www.fema.gov/mit/tsd/lidar_4b.htm (21 May 2000).

Galy, H. M., and Sanders, R. A. (2000). "Using SAR Imagery for Flood Modeling," Englewood, CO. http://www.intermap.ca/PDF/rgs_paper.pdf (22 February 2000).

Intermap Technologies, Inc. (2000) "BALD EARTH - DEMs," Englewood, CO. http://www.intermap.ca/HTML/research_new_bald.htm (22 November 2000).

Spencer B. Gross, Inc. (2000). "The AeroScan LIDAR System Technical Description," Portland, OR. http://www.sbgmaps.com/lidar.htm (24 October 2000).

APPENDIX A. INTERMAP IFSAR DEM HEADER

Intermap Technologies Inc.
Global Terrain Metadata File (DEM)

File Creation date: Wednesday, June 16, 1999
Tile Identifier #:   GT1N48W097H2V1.bil
Project Area: Red River

Product Description
Product Level: GT1
DEM posting (meters):   5.0
Horizontal Accuracy: 2.5 meters (1 sigma)
Vertical Accuracy: 1 meters (1 sigma)

Sensor
Data Source: Intermap Star-3i Airborne Interferometric SAR
Flying Height: 20,000 ft. Above Mean Ground
Primary Look: North
Alternate (Secondary)Look: South
Mission #(s):   168
Acquisition Date: 11/01/1998 and 11/02/1998
Band: X-Band

Processing
Interpolation: Continuous curvature spline over non-data areas
Phase Unwrapper: Goldstein

Data Format, Parameters, and Coordinates
Format: 32 bit BIL (float)
Projection: UTM
Horizontal Datum: WGS84 Ellipsoid
Vertical Datum: NAVD 88
Geoid Model: GEOID96
Vertical Reference: Mean Sea Level (MSL)
Central Scale: 0.9996
UTM Zone: 14
Central Meridian: 99 degrees West
False Easting (meters):   500,000.0 meters
False Northing (meters):   0.0 meters
UTM Easting (meters):   Min.   627,727.50 Max.   638,947.50
UTM Northing(meters):   Min. 5,411,802.50 Max. 5,431,752.50
Pixel Origin: Center Center
Pixels (columns):   2245
Lines (rows):   3991

Legacy Information

Intermap Project Number: 98065
Flight Acquisition Manager: J. Keith Tennant   403.266.0900
Denver Processing Center: Ken Rath   303.708.0955
Ottawa Processing Center: Ian Isaacs   613.226.5442
Metadata File Creator: Tom Hutt   613.226.5442
Mississippi DHS Center: Ron Birk   228.688.1465
Project Manager: Cliff Holle   228.688.1783
Metadata File Description: www.globalterrain.com
Intermap Information: www.intermaptechnologies.com
ISO 9001 Certification No.   0411-069

APPENDIX B. INTERMAP MAGNITUDE IMAGE HEADER

Intermap Technologies Inc.
Global Terrain Metadata File (ORI)

File Creation date: Friday, June 18, 1999
Tile Identifier #:   IM2N48W097H2V1.tif
Project Area: Red River

Product Description
Product Level: GT1
Image Pixels (meters):   2.5
Horizontal Accuracy: 2.5 meters (1 sigma)

Sensor
Data Source: Intermap Star-3i Airborne Interferometric SAR
Flying Height: 20,000 ft. Above Mean Ground
Primary Look: North
Alternate (Secondary)Look: South
Mission #(s):   168
Acquisition Date: 11/01/1998 and 11/02/1998
Band: X-Band

Processing
Interpolation: Continuous curvature spline over non-data areas
Phase Unwrapper: Goldstein

Data Format, Parameters, and Coordinates
Format: 8 bit GEOTIFF
Projection: UTM
Horizontal Datum: WGS84 Ellipsoid
Vertical Datum: NAVD 88
Geoid Model: GEOID96
Central Scale: 0.9996
UTM Zone: 14
Central Meridian: 99 degrees West
False Easting (meters):   500,000.0 meters
False Northing (meters):   0.0 meters
UTM Easting (meters):   Min.   627,729.50   Max.   638,947.00
UTM Northing(meters):   Min. 5,411,803.50   Max. 5,431,751.00
Pixel Origin: Upper Left
Pixels (columns):   4488
Lines (rows):   7980

Legacy Information
Intermap Project Number: 98065
Flight Acquisition Manager: J. Keith Tennant   403.266.0900

Denver Processing Center: Ken Rath   303.708.0955
Ottawa Processing Center: Ian Isaacs   613.226.5442
Metadata File Creator: Tom Hutt   613.226.5442
Mississippi DHS Center: Ron Birk   228.688.1465
Project Manager: Cliff Holle   228.688.1783
Metadata File Description: www.globalterrain.com
Intermap Information: www.intermaptechnologies.com
ISO 9001 Certification No.   0411-069

APPENDIX C. ELEVEXTRACT.AML

```
/*************************************************************************
/* ELEVEXTRACT.AML  07/12/99
/* James J. Damron
/* U.S. Army Topographic Engineering Center
/* 7701 Telegraph Road
/* Alexandria, VA 22315-3864
/* jdamron@tec.army.mil
/*
/* Extracts elevation data using an x,y ASCII text file for a stack or
/* single grid and dumps xyz values to an ASCII text file
/*
/* filename - ASCII text file created            writefile - output of elevation
/*
/* type - type grid used for extraction          name - name of the grid or stack
/*
/* file - opens x,y ASCII coordinate file  line - selects new line of x,y
/*
/*************************************************************************
&severity &error &ignore
&severity &warning &ignore
display 9999
&term 9999
grid
/* Setting up files and output file name
&sv filename = [ response 'Please enter file name to write to' elev.txt ]
&sv writefile = [open %filename% openstatus -write]
&type
&sv type = [ response 'Please enter type of grid: single or stack' stack ]
&type
&sv name = [ response 'Please enter name of the grid for extraction' grid ]
&type
/* Setting up environment
mape %name%
&sv file := [open [getfile *.txt -file] ok -r]
&sv line = [read %file% readstatus]
&sv count = 1

/* Examining file type and grid
&if %type% = single and [exists %name% -grid] &then
  /* Opening file for processing and output to ASCII
       &do &while %readstatus% eq 0
              &type %line%
              &type
              &sv elev = [ show cellvalue %name% %line% ]
              &if [write %writefile% %line%,%elev%] = 0 &then
              &type Writing file to %filename% ....
```

89

```
            &type
            &type this many finished %count%
            &type
            &sv count = %count% + 1
            &sv line = [read %file% readstatus]
       &end

/* Examining file type and grid
&if %type% = stack and [exists %name% -stack] &then
  /* Opening file for processing and output to ASCII
       &do &while %readstatus% eq 0
            &type %line%
            &type
            &sv elev = [ show cellvalue %name% %line% ]
            &if [write %writefile% %line%,%elev%] = 0 &then
            &type Writing file to %filename% ....
            &type
            &type this many finished %count%
            &type
            &sv count = %count% + 1
            &sv line = [read %file% readstatus]
       &end
&sv count = %count% - 1
&type
&type File %filename% closed and this many files processed %count%.....
&return
```

APPENDIX D. CROSS SECTION AML

```
/*************************************************************************
/* Crosssect.AML  07/15/99
/* James J. Damron
/* U.S. Army Topographic Engineering Center
/* 7701 Telegraph Road
/* Alexandria, VA 22315-3864
/* jdamron@tec.army.mil
/* Plots elevation and any type of data using a vector line or drawn in ArcPlot
/* Surfaceprofile used for graphing one surface
/* Stackprofile used for graphing more than one surface
/*************************************************************************

&severity &error &ignore
&severity &warning &ignore
display 9999
&term 9999

map oldnew3prof
pages 11 8.5
/*shadeset colornames
/*shadesym 27
/*patch 0 0 11 8.5
/*lineset jamesd
linesym 1
box 0 0 11 8.5

maplimits 1.25 0.5 10.75 8.25 /*0.75 0.5 10.5 8.5
mape profile3
mappos cen cen
mapunits meters
mapscale auto
/*linesym 5
/*image baretiff.tif
lineset color
linesym 3

/* Surfaceprofile Plots one surface on a Graph
surface lattice oldnew3diff
surfaceprofile '1.25 0.5 10.75 8.25' profile3 oldnew3 3.0
/* Stackprofile Plots two or more surfaces on a Graph
/*stackprofile '1.25 0.5 10.75 8.25' proline1 stack.txt compall
msel 2
mdel
&return
```

APPENDIX E. XYZ DATA FROM ELEVEXTRACT.AML IFSAR (GT1), FIRST (1ST) AND THIRD (3RD) DELIVERY

x-coord	y-coord	GT1	1st LIDAR	3rd LIDAR
624361.36571	5426862.49698	241.6215	241.0834	241.3604
624835.70737	5426704.38313	240.9554	241.0247	241.3200
625310.04903	5426546.26929	241.6143	241.6180	241.5740
625784.39069	5426388.15544	240.6785	241.1496	241.3790
626258.73235	5426230.04160	240.8938	240.8816	241.1313
626733.07402	5426071.92775	240.3699	240.7580	241.0086
627207.41568	5425913.81391	240.8558	240.7580	241.0440
624123.18727	5426038.79672	241.3883	240.7660	241.0435
624598.17559	5425882.63623	242.2863	241.5286	241.7965
625073.16391	5425726.47574	241.5053	241.3253	241.6030
625548.15223	5425570.31526	241.1147	241.7242	241.7681
626023.14054	5425414.15477	240.4846	240.4670	240.7314
626498.12886	5425257.99428	240.1631	240.6096	240.9111
626973.11718	5425101.83380	241.2237	240.6749	240.9768
623885.00884	5425294.48939	240.3068	240.2293	240.4947
624358.07389	5425132.59603	240.7578	240.1930	240.4782
624831.13893	5424970.70267	240.4404	240.2970	240.6412
625777.26903	5424646.91595	239.2975	240.0535	240.3474
626117.93080	5424530.33393	240.6066	240.5511	240.8817
626485.12272	5423527.99965	240.9044	240.7872	241.0909
626967.98071	5423398.19918	240.0811	240.0066	240.2978
627450.83870	5423268.39872	241.5427	241.1499	241.3457
627933.69669	5423138.59825	239.6863	240.2095	240.5208
628416.55468	5423008.79778	240.6240	240.9076	241.2063
628899.41267	5422878.99731	240.4700	240.8479	241.1361
629253.94598	5422783.69271	240.1096	240.5094	240.7495
626256.86855	5422823.38899	240.6479	240.7086	241.0868
626737.29542	5422684.86093	240.5987	240.7384	241.0637
627217.72229	5422546.33288	241.1431	241.2410	241.5308
627698.14916	5422407.80482	241.7010	242.0959	242.3507
628178.57603	5422269.27677	241.3469	241.5652	241.8709
628659.00290	5422130.74871	240.8542	241.2564	241.4925
629139.42977	5421992.22066	240.9841	241.2657	241.5925
629492.12441	5421890.52339	240.6127	240.9699	241.1720
626117.93080	5422148.54996	240.7911	240.8860	241.2096
626601.69314	5422022.16166	241.3947	241.6932	241.9821
627085.45547	5421895.77335	241.5168	241.9656	242.2366
627569.21781	5421769.38504	241.8706	242.0421	242.5572
628052.98014	5421642.99674	241.6223	242.1307	242.4615
628536.74248	5421516.60843	241.0488	241.4013	241.5510
629020.50481	5421390.22013	240.9959	241.4008	241.5786
629422.65612	5421285.15361	241.6095	241.8381	242.0915
625760.66354	5421751.58603	240.4450	240.8279	240.9720
626238.78672	5421605.30472	241.2863	242.6448	242.4345
626716.90990	5421459.02341	241.3324	241.9445	242.1337
627195.03309	5421312.74210	241.7052	242.2648	242.4465
627673.15627	5421166.46080	242.1877	242.9321	243.1784
628151.27945	5421020.17949	241.5897	242.1677	242.3841
628629.40264	5420873.89818	241.3352	242.0078	242.2201

95

629107.52582	5420727.61687	241.0694	241.7607	242.0216
624629.31616	5421602.72480	241.2540	241.3575	241.6837
625102.09358	5421439.99340	240.7662	241.0793	241.3572
625574.87100	5421277.26200	239.9490	240.1559	240.4484
626047.64843	5421114.53060	240.9050	241.0694	241.3810
626520.42585	5420951.79920	241.6760	241.7821	242.2847
626993.20327	5420789.06780	242.0841	242.2397	242.6117
627368.36701	5420659.93532	242.1195	242.2563	242.5469
624490.37880	5421037.05111	241.2755	241.3721	241.6701
624961.37211	5420869.22590	241.0767	241.3650	241.6613
625432.36543	5420701.40069	239.8955	240.2734	240.5109
625903.35874	5420533.57549	240.8100	241.4786	241.7435
626374.35205	5420365.75028	241.5793	242.0877	242.3710
626845.34536	5420197.92507	241.6617	242.1919	242.4817
627080.56842	5420114.10996	241.9453	242.4776	242.8070
624500.30306	5420520.99796	241.0156	241.7112	241.7832
624968.78251	5420346.27816	240.8700	241.5661	241.6848
625437.26196	5420171.55837	239.2419	239.9652	240.1599
626374.22085	5419822.11877	241.2372	241.9957	242.1424
626842.70030	5419647.39898	241.8994	242.7719	242.9568
623666.67873	5419846.15931	240.7398	241.5469	241.7188
624136.11689	5419674.03198	240.6034	241.2081	241.4502
624605.55504	5419501.90464	240.5346	241.6403	241.8640
625074.99319	5419329.77730	241.3002	242.3207	242.5334
625544.43134	5419157.64996	240.9851	241.7951	241.9540
626013.86950	5418985.52263	241.7076	242.4120	242.6240
626483.30765	5418813.39529	241.8535	242.5837	242.8423
624480.45454	5420044.64128	240.3894	240.4355	240.7389
624944.69289	5419858.94594	241.5780	241.9618	242.2449
625408.93123	5419673.25060	240.6710	241.1048	241.3824
625873.16958	5419487.55527	241.0756	241.7043	242.0317
626337.40792	5419301.85993	242.0848	242.7257	243.0134
626713.37689	5419151.47234	241.6860	242.1389	242.4692
617116.77329	5423269.97346	244.1718	244.4390	244.6658
617590.69573	5423110.60745	243.2785	243.2912	243.6061
618064.61816	5422951.24144	242.7987	243.2432	243.5136
618538.54060	5422791.87543	242.3730	242.6686	242.9727
619012.46303	5422632.50941	242.3433	242.6050	242.8504
619486.38547	5422473.14340	241.5880	242.0474	242.3468
619960.30790	5422313.77739	241.1627	241.7814	242.0458
620434.23034	5422154.41138	241.4033	241.6765	241.9833
621855.99764	5421676.31334	240.8398	240.9253	241.1967
622329.92008	5421516.94733	240.5299	240.8585	241.1151
622803.84251	5421357.58132	240.4726	240.8901	241.0976
623277.76495	5421198.21531	240.6284	240.9486	241.1570
623751.68738	5421038.84930	240.5723	241.3830	241.6130
616888.51903	5422783.69233	243.5547	243.9723	244.1630
617362.56815	5422624.70355	242.9538	243.1063	243.3431
618784.71550	5422147.73720	242.0441	242.2245	242.4569
619258.76462	5421988.74842	241.7128	241.9447	242.2182
619732.81374	5421829.75963	240.8321	241.1143	241.3648
620206.86286	5421670.77085	241.0959	241.2756	241.5834
621154.96110	5421352.79329	240.7347	240.8638	241.1371
622103.05933	5421034.81572	240.9062	241.1930	241.3998

622577.10845	5420875.82694	240.4815	240.6761	240.9538
623339.18305	5420620.23885	240.8205	241.3550	241.6099
604404.00152	5426971.66193	253.6264	253.5044	253.7996
604878.94244	5426815.35735	253.1365	253.5224	253.7889
606778.70612	5426190.13903	250.9801	251.2145	251.6045
607253.64704	5426033.83444	251.3714	251.7526	252.1850
607728.58796	5425877.52986	251.3341	250.8590	251.2099
608203.52888	5425721.22528	250.9281	250.8320	251.1164
608678.46980	5425564.92070	250.2456	250.1917	250.5040
609153.41072	5425408.61612	250.7823	250.4337	250.7553
609628.35164	5425252.31153	249.5551	249.8954	250.2339
610103.29256	5425096.00695	249.3996	249.5144	249.7834
610578.23348	5424939.70237	249.0797	248.9846	249.3062
611053.17440	5424783.39779	248.4413	248.4782	248.7513
611528.11532	5424627.09321	247.9655	248.1632	248.4806
612003.05624	5424470.78862	247.6990	248.1186	248.4718
612477.99716	5424314.48404	247.1234	247.7022	247.9902
612952.93808	5424158.17946	247.0106	247.1002	247.4351
613427.87900	5424001.87488	246.6841	247.0512	247.3514
613902.81992	5423845.57030	246.9604	246.6961	246.9951
614377.76084	5423689.26572	246.6001	246.7804	247.1076
614852.70176	5423532.96113	246.1707	246.5540	246.8224
615327.64268	5423376.65655	245.8854	245.9963	246.2915
616134.28620	5423111.18758	245.0783	245.5525	245.7942
604195.59452	5426326.59531	253.5140	253.3675	253.6805
604670.01227	5426168.70989	252.7596	252.8131	253.0894
605144.43001	5426010.82447	253.3160	253.2201	253.1772
605618.84775	5425852.93905	252.3916	252.1300	252.5161
606093.26549	5425695.05363	251.0570	251.7470	252.0686
606567.68323	5425537.16821	251.9822	251.9298	252.1776
608465.35420	5424905.62653	250.6316	250.6825	250.9164
609414.18969	5424589.85569	250.3131	250.1000	250.3971
610363.02517	5424274.08485	248.6925	248.9445	249.3034
610837.44292	5424116.19943	248.4300	249.0870	249.4356
611311.86066	5423958.31401	247.9447	248.2507	248.4773
611786.27840	5423800.42859	247.4932	247.7712	247.9949
612260.69614	5423642.54317	247.1550	247.7754	248.0162
612735.11389	5423484.65775	246.6659	246.8217	247.0909
613209.53163	5423326.77233	245.8804	245.9469	246.3049
614158.36711	5423011.00149	244.6489	245.1640	245.3878
614632.78485	5422853.11607	244.5824	244.9646	245.2362
615107.20260	5422695.23065	244.6652	245.0628	245.3473
615581.62034	5422537.34523	244.4184	244.6938	245.0529
616056.03808	5422379.45981	244.0994	244.0543	244.3356
616530.45582	5422221.57439	242.9209	243.3340	243.5827
617004.87357	5422063.68897	242.9725	243.2141	243.4395
617479.29131	5421905.80355	242.7895	243.1478	243.3696
618428.12679	5421590.03272	241.7847	242.1726	242.3363
618902.54454	5421432.14730	242.3195	242.7186	242.9352
619376.96228	5421274.26188	241.7015	242.0431	242.3764
619851.38002	5421116.37646	241.2482	241.6892	241.9806
620325.79776	5420958.49104	240.6435	240.9107	241.1586
620800.21551	5420800.60562	240.3627	240.7968	241.0567
621274.63325	5420642.72020	240.9926	241.1827	241.4212

621749.05099	5420484.83478	240.7903	241.3882	241.6084
622223.46873	5420326.94936	240.5663	241.5672	241.7442
617841.23095	5423547.84760	243.6625	243.7971	243.9595
618313.69655	5423384.21307	242.8041	243.3832	243.5251
618786.16215	5423220.57854	242.0511	242.8708	243.0598
619258.62774	5423056.94401	242.3024	242.7117	242.8748
619731.09334	5422893.30949	241.9751	242.3253	242.5337
622009.35242	5422168.39752	240.8343	241.2959	241.4396
622483.08715	5422008.47442	240.9615	241.3147	241.4786
622956.82189	5421848.55131	240.8451	241.3528	241.4124
623430.55663	5421688.62820	241.1511	241.4204	241.5940
623567.43613	5421642.42050	241.3711	241.8062	241.8357
605396.41077	5429829.80258	251.7975	252.3868	252.6835
605871.47859	5429673.88411	251.5105	251.9841	252.2958
606346.54640	5429517.96564	251.0213	251.4369	251.7522
606821.61422	5429362.04717	250.5777	250.7493	251.0670
607296.68204	5429206.12870	250.2540	250.5160	250.8556
607771.74985	5429050.21022	250.3507	250.7129	250.9901
608246.81767	5428894.29175	250.0974	250.3013	250.5827
608721.88548	5428738.37328	249.7090	249.8337	250.1474
609196.95330	5428582.45481	248.9174	250.7102	250.6323
609672.02112	5428426.53634	249.2467	249.5076	249.8074
610147.08893	5428270.61786	248.4930	249.0153	249.3305
610622.15675	5428114.69939	248.0087	248.2828	248.5680
611097.22457	5427958.78092	247.7782	247.8367	248.1238
611572.29238	5427802.86245	247.7977	247.5890	247.9471
612047.36020	5427646.94397	246.8407	246.9096	247.2932
612522.42801	5427491.02550	246.9306	246.4657	246.8330
612997.49583	5427335.10703	244.6915	245.0494	245.4399
613472.56365	5427179.18856	245.8159	245.1737	245.4974
613947.63146	5427023.27009	245.1677	244.7687	245.0775
614422.69928	5426867.35161	245.3910	245.0377	245.3507
614897.76710	5426711.43314	245.3551	245.2681	245.5720
615372.83491	5426555.51467	245.5002	245.3281	245.6655
615847.90273	5426399.59620	244.7383	244.5980	244.9764
616322.97054	5426243.67773	244.8672	244.5442	244.8689
616798.03836	5426087.75925	244.7303	244.3559	244.6975
617273.10618	5425931.84078	243.2160	243.0710	243.3565
617748.17399	5425775.92231	242.5093	242.3406	242.6536
618223.24181	5425620.00384	242.0587	242.2870	242.5726
618698.30963	5425464.08537	242.2725	241.9708	242.3130
619173.37744	5425308.16689	241.0807	241.4925	241.8936
619648.44526	5425152.24842	241.1992	241.1226	241.3057
620123.51307	5424996.32995	240.9704	240.6272	240.9563
620598.58089	5424840.41148	239.5242	239.8176	240.1561
621548.71652	5424528.57453	240.2088	240.3986	240.7374
622023.78434	5424372.65606	241.3545	241.0934	241.4305
622973.91997	5424060.81912	240.9407	241.1657	241.3750
623448.98779	5423904.90064	240.3837	240.6529	240.9496
623924.05560	5423748.98217	239.7330	239.8426	240.1456
624874.19124	5423437.14523	240.8220	240.9526	241.1450
625349.25905	5423281.22676	240.2979	241.1787	241.4383
616938.13765	5426723.55981	243.6298	243.7071	244.0275
617411.78527	5426563.37887	242.7444	242.8623	243.1928

617885.43289	5426403.19793	242.3281	242.0536	242.3350
618359.08050	5426243.01698	242.0566	242.1801	242.1139
618832.72812	5426082.83604	241.4012	241.0014	241.2653
619306.37574	5425922.65509	241.1855	240.6627	240.9933
619780.02335	5425762.47415	240.9098	240.6245	241.0011
620253.67097	5425602.29320	241.3267	240.5041	240.8267
620727.31859	5425442.11226	241.1136	240.1407	240.5363
621200.96620	5425281.93131	240.8157	240.0431	240.3895
621674.61382	5425121.75037	241.4183	241.4628	241.5213
622621.90905	5424801.38848	241.0962	240.9697	241.2291
623095.55667	5424641.20754	241.3000	240.8967	241.1951
623569.20429	5424481.02659	240.5122	240.3559	240.5719
624042.85191	5424320.84565	240.6069	240.3225	240.6161
624516.49952	5424160.66470	240.0851	240.4284	240.7232
624990.14714	5424000.48376	239.5822	239.2961	239.6462
625463.79476	5423840.30281	241.0997	240.5908	240.8570
625800.35761	5423726.48200	240.9485	240.8818	241.1660
605654.43672	5429016.02697	251.4673	251.8649	252.0983
606130.72749	5428863.88524	251.0705	251.3173	251.5952
606607.01825	5428711.74351	250.8763	251.2191	251.4977
607083.30902	5428559.60178	251.0163	251.7675	252.0161
607559.59979	5428407.46005	250.5325	250.6404	250.9376
608035.89055	5428255.31832	250.4742	250.6926	250.9683
608512.18132	5428103.17659	250.0271	250.2926	250.6071
608988.47209	5427951.03486	250.2907	250.1521	250.4520
609464.76285	5427798.89313	249.6346	249.7704	250.0439
609941.05362	5427646.75141	249.6833	249.8071	249.9502
610417.34438	5427494.60968	249.0349	248.9677	249.3003
610893.63515	5427342.46795	248.4953	248.3215	248.6503
611369.92592	5427190.32622	248.2181	248.3125	248.6000
611846.21668	5427038.18449	248.4284	248.1364	248.4331
612322.50745	5426886.04276	247.3357	247.9250	248.1738
612798.79822	5426733.90103	247.2623	247.4956	247.7800
613275.08898	5426581.75930	246.2994	246.8127	247.0682
613751.37975	5426429.61757	246.2157	246.1886	246.4807
614227.67052	5426277.47584	246.6512	246.3028	246.5821
614703.96128	5426125.33411	245.7733	245.9850	246.2497
615180.25205	5425973.19239	246.0246	246.3820	246.6121
616609.12435	5425516.76720	244.3762	244.7913	245.0347
617085.41512	5425364.62547	243.2862	243.5297	243.7649
617561.70588	5425212.48374	242.9317	243.3716	243.5595
618037.99665	5425060.34201	243.2666	243.1838	243.3325
618514.28742	5424908.20028	242.3731	242.7727	242.9069
618990.57818	5424756.05855	242.3656	242.9235	243.4705
619466.86895	5424603.91682	241.6818	241.8053	241.9716
619943.15971	5424451.77509	241.2075	241.4365	241.6305
620419.45048	5424299.63336	240.7281	240.9701	241.0699
620895.74125	5424147.49164	240.8131	240.9535	241.2494
621372.03201	5423995.34991	239.8621	240.1754	240.3894
621848.32278	5423843.20818	239.7092	240.3903	240.4630
622324.61355	5423691.06645	240.7737	241.0419	241.1998
622800.90431	5423538.92472	240.9337	241.1313	241.2449
623277.19508	5423386.78299	241.1859	241.4528	241.5515
623753.48585	5423234.64126	240.6663	241.0988	241.1816

624706.06738	5422930.35780	241.0327	241.2618	241.4172
625165.21433	5422783.69233	241.0915	241.6800	241.7713
605674.28395	5428271.71868	251.8130	251.8523	252.1843
606150.49601	5428119.33080	251.8123	251.9260	252.2490
606626.70808	5427966.94292	251.3390	251.6693	251.9848
607102.92015	5427814.55504	251.0247	251.4258	251.7106
607579.13222	5427662.16716	251.4288	251.3680	251.6356
608055.34429	5427509.77928	252.1078	252.2957	252.6109
608531.55636	5427357.39140	251.9197	251.7380	252.0269
609007.76842	5427205.00352	250.6184	250.4113	250.7987
609483.98049	5427052.61564	249.8816	250.2357	250.5151
609960.19256	5426900.22776	250.6449	250.4270	250.6906
604026.88323	5425522.74318	254.3342	254.2984	254.6667
604499.85449	5425360.57604	253.1997	253.2117	253.5135
604972.82576	5425198.40889	252.8217	252.8419	253.1624
605445.79702	5425036.24175	252.2858	252.4164	252.7062
605918.76829	5424874.07461	252.2651	251.6628	252.0163
606391.73955	5424711.90746	250.9858	251.0597	251.3324
607337.68208	5424387.57317	250.5742	250.3105	250.6647
607810.65335	5424225.40603	249.9236	250.0464	250.3551
608283.62461	5424063.23889	249.7787	250.0463	250.3861
608756.59588	5423901.07174	250.7538	250.3366	250.5784
609702.53841	5423576.73745	249.2754	249.2389	249.5919
610648.48094	5423252.40317	247.6304	247.6251	248.1613
611121.45220	5423090.23602	247.4458	247.2466	247.5562
611594.42347	5422928.06888	247.3849	247.1886	247.4870
612540.36600	5422603.73459	245.8335	245.9156	246.3992
613013.33726	5422441.56745	245.6081	245.6456	245.9758
613486.30852	5422279.40030	245.3598	245.4659	245.7979
613959.27979	5422117.23316	245.6444	245.5082	245.8742
614432.25105	5421955.06601	245.2773	245.2839	245.5923
614905.22232	5421792.89887	244.6730	244.6525	244.9190
606802.44844	5426534.17336	251.1535	252.4266	252.6215
607277.53408	5426378.30922	251.4888	252.2140	252.3548
607752.61972	5426222.44507	251.5144	251.8432	252.0484
608227.70537	5426066.58093	250.5700	251.6284	251.6943
608702.79101	5425910.71678	250.6960	251.5159	251.5801
609177.87665	5425754.85264	250.7668	251.0377	251.1320
609652.96230	5425598.98849	249.9620	250.7765	250.8960
610128.04794	5425443.12435	249.1997	250.1236	250.3087
610603.13358	5425287.26021	249.3708	249.8921	249.9747
611078.21923	5425131.39606	248.9349	249.3144	249.4081
611553.30487	5424975.53192	248.5179	248.8123	248.9043
612028.39051	5424819.66777	248.7167	249.4346	249.5704
612503.47616	5424663.80363	248.3828	248.9229	249.0201
612978.56180	5424507.93949	247.3583	247.9766	248.1036
613453.64744	5424352.07534	247.9317	248.1691	248.2969
613928.73309	5424196.21120	247.3141	247.7531	247.9600
616173.52241	5425652.15471	245.0895	245.8357	246.0689
625589.38367	5423179.02228	241.2531	241.2858	241.6159
629543.90485	5420584.04508	240.8986	241.7229	242.0894
627414.69142	5425830.38641	240.8599	241.1225	241.3546
627140.12229	5425026.53448	240.3776	240.3546	240.6477
610315.60910	5426786.13753	250.0438	250.1877	250.4826

605203.25524	5426693.57160	252.5785	252.7902	253.0865
607045.23912	5425429.49220	251.3402	251.1880	251.4795
607535.34733	5425337.50666	251.0482	251.2729	251.5633
607947.00309	5424969.36929	249.9230	250.3870	250.6350
608892.70055	5424779.12192	250.6240	250.8788	250.9625
609778.77443	5424155.81832	249.3650	249.5938	249.8760
609204.46237	5423556.89543	250.3132	250.4853	250.7864
610219.44292	5423467.91786	248.7912	248.9038	249.2154
612145.84693	5422731.38273	247.0532	247.0426	247.3209
613812.61098	5423099.84889	245.8819	246.0420	246.2784
614231.35162	5424069.55774	246.8409	247.4518	247.4687
615156.84297	5421696.04724	244.6917	244.6283	244.9591
615790.03128	5423119.93314	245.4881	245.3568	245.6231
617692.26519	5422497.09569	242.7681	242.8191	243.1012
617897.22348	5421638.08495	242.9867	242.8627	243.1566
618414.22335	5422275.34505	242.2118	242.7695	243.0204
620013.74718	5422774.19803	242.0336	242.2615	242.4569
622547.25812	5420212.99719	240.7764	241.5110	241.7248
623013.50060	5420848.63791	240.6118	241.1944	241.3849
623233.27752	5419739.57760	240.2042	240.5965	240.8873
623988.05587	5420950.28305	241.3221	241.5470	241.8403
627103.79246	5419552.00517	241.5271	242.4757	242.6207
625830.42747	5420040.77182	241.4126	242.1898	242.3566
626763.15565	5418691.74661	241.8835	242.5911	242.8342
622574.16634	5424185.35678	241.0112	241.2530	241.4953
622085.49982	5424983.53605	242.0826	241.1595	241.5286
615628.30003	5425877.53623	245.8261	245.8270	246.0176
629304.09422	5424789.46037	237.6239	237.6307	237.8957
629162.88028	5424475.65145	238.7409	238.9065	239.1320
629018.52809	5424092.80451	238.5465	238.8909	239.1904
628861.62369	5423731.92420	240.6227	240.8100	241.0765
628513.29570	5423468.32464	240.1791	240.3570	240.6316
627935.88721	5423499.70556	239.5797	240.3704	240.5342
627568.73074	5423725.64804	240.4357	240.4408	240.6679
631277.95311	5425037.36941	239.7329	239.2929	239.6646
631196.36264	5424764.35573	239.3995	239.5605	239.6653
631067.70103	5424400.33727	239.5073	238.9758	239.2956
630942.17732	5423973.55708	239.8147	240.5391	240.6778
630810.37781	5423490.29120	240.8494	241.4799	241.7959
630653.47317	5422988.19689	240.8044	240.7418	241.1009
630537.36388	5422655.55937	240.3019	240.5892	240.8001
630430.66889	5422344.88847	239.1639	239.4325	239.7537
630333.38821	5422065.59850	238.6059	238.9257	239.2043
630236.10740	5421830.24178	238.4680	239.2311	239.2607
629809.32721	5421161.82859	239.5449	240.1011	240.1195
629969.36975	5420477.72502	240.1970	240.7616	241.0042
630163.93136	5421023.75261	239.7789	239.8953	239.9219
630280.04047	5425175.44521	241.0120	241.0856	241.3771
630182.75979	5424877.32675	240.5137	240.4195	240.6565
622955.73971	5422919.15888	240.8345	241.4273	241.7078
623721.43364	5422686.94018	240.8801	241.1817	241.5040
623846.95724	5422197.39819	241.4057	241.9081	242.1659
624747.58888	5422071.87460	241.2100	241.8529	241.9103
625073.95025	5421867.89875	240.4354	241.0955	241.2536

619983.96888	5423961.00446	241.9684	242.3001	242.5878
621079.16226	5423509.11950	240.9209	241.4903	241.7651
622011.17496	5423258.07232	241.6574	242.0532	242.3438
618644.00489	5423797.82365	243.3940	243.2973	243.6256
619315.55598	5423393.01009	242.6177	242.9109	243.2137
616086.46184	5423986.10898	245.9300	246.0978	246.3846
616208.84730	5424158.70397	245.5814	246.0544	246.1377
616321.81850	5424315.60849	245.3934	245.6884	245.8995
616459.89448	5424481.92719	244.7969	244.6993	245.0206
616535.20872	5424560.37951	244.2564	244.5879	244.9084
616654.45603	5424711.00787	244.1958	244.8702	245.0674
616754.87497	5424823.97889	244.3657	244.6154	244.7778
616880.39857	5424962.05493	243.5009	244.2089	244.4513
616980.81751	5425096.99270	243.9669	243.5119	243.8432
613739.17081	5425630.46788	247.4538	247.9095	248.2291
614636.66444	5425219.37815	246.9840	247.1592	247.4117
615844.82921	5424999.71184	245.4630	246.0694	246.3326
604958.79607	5428166.04424	252.3349	252.9456	253.1399
631318.74972	5425162.89174	239.8576	239.3429	239.6597
631234.02124	5424914.98258	239.7437	239.6987	239.8962
631152.43090	5424626.27831	238.9290	239.3954	239.7029
631105.35950	5424500.75471	239.6256	239.3467	239.6747
631033.18359	5424281.08834	238.9963	239.0913	239.3370
630967.28359	5424061.42214	239.5981	240.2160	240.3396
630913.93604	5423857.44629	240.0296	240.5763	240.8427
630882.55523	5423735.06078	240.8589	241.0342	241.3473
630848.03628	5423618.95149	240.8703	240.9223	241.2017
630785.27442	5423383.59474	241.4348	241.7347	241.9749
630744.47944	5423251.79491	240.8737	241.3961	241.5785
630703.68420	5423129.40946	240.7602	241.3153	241.5228
630590.71294	5422843.84327	240.3090	240.5201	240.8162
630562.47027	5422746.56246	240.0979	240.5157	240.7906
630505.98445	5422558.27707	239.2384	239.9132	239.8900
630484.01783	5422470.41057	238.3267	238.9148	239.0136
630399.28947	5422257.02048	239.2761	239.3769	239.7178
630371.04668	5422153.46353	238.7182	238.9529	239.2558
630311.42296	5421990.28283	238.5592	239.0852	239.3174
630270.62786	5421899.27831	238.7179	239.0972	239.3228

APPENDIX F. RESULTS FROM MINITAB

C3 - Corrected IFSAR
C4 - First LIDAR Delivery
C5 - Third LIDAR Delivery

Paired T-Test and Confidence Interval

Paired T for C3 - C4

	N	Mean	StDev	SE Mean
C3	410	244.042	4.147	0.205
C4	410	244.276	4.124	0.204
Difference	410	-0.2336	0.3642	0.0180

95% CI for mean difference: (-0.2689, -0.1982)
T-Test of mean difference = 0 (vs not = 0): T-Value = -12.99 P-Value = 0.000

Paired T-Test and Confidence Interval

Paired T for C3 - C5

	N	Mean	StDev	SE Mean
C3	410	244.042	4.147	0.205
C5	410	244.533	4.134	0.204
Difference	410	-0.4902	0.3326	0.0164

95% CI for mean difference: (-0.5225, -0.4579)
T-Test of mean difference = 0 (vs not = 0): T-Value = -29.84 P-Value = 0.000

Paired T-Test and Confidence Interval

Paired T for C4 - C5

	N	Mean	StDev	SE Mean
C4	410	244.276	4.124	0.204
C5	410	244.533	4.134	0.204
Difference	410	-0.25666	0.09121	0.00450

95% CI for mean difference: (-0.26551, -0.24780)
T-Test of mean difference = 0 (vs not = 0): T-Value = -56.98 P-Value = 0.000

Wilcoxon Signed Rank Confidence Interval

			Estimated Achieved	
	N	Median	Confidence	Confidence Interval
C3	410	243.8	95.0 (	243.3, 244.4)
C4	410	244.1	95.0 (	243.5, 244.6)
C5	410	244.3	95.0 (	243.7, 244.9)

Mann-Whitney Confidence Interval and Test

C3   N = 410   Median =   242.00
C4   N = 410   Median =   242.29
Point estimate for ETA1-ETA2 is   -0.25
95.0 Percent CI for ETA1-ETA2 is (-0.58,0.08)
W = 163223.0
Test of ETA1 = ETA2 vs ETA1 not = ETA2 is significant at 0.1340
The test is significant at 0.1340 (adjusted for ties)

Cannot reject at alpha = 0.05

Mann-Whitney Confidence Interval and Test

C3   N = 410   Median =   242.00
C5   N = 410   Median =   242.55
Point estimate for ETA1-ETA2 is   -0.50
95.0 Percent CI for ETA1-ETA2 is (-0.82,-0.18)
W = 158191.5
Test of ETA1 = ETA2 vs ETA1 not = ETA2 is significant at 0.0029
The test is significant at 0.0029 (adjusted for ties)

Mann-Whitney Confidence Interval and Test

C4   N = 410   Median =   242.29
C5   N = 410   Median =   242.55
Point estimate for ETA1-ETA2 is   -0.25
95.0 Percent CI for ETA1-ETA2 is (-0.59,0.09)
W = 163362.0
Test of ETA1 = ETA2 vs ETA1 not = ETA2 is significant at 0.1450
The test is significant at 0.1450 (adjusted for ties)

Cannot reject at alpha = 0.05

Runs Test

  C3

  K = 244.0425

The observed number of runs = 19
The expected number of runs = 197.3951
163 Observations above K 247 below
        The test is significant at 0.0000

Runs Test

   C4

   K =   244.2761

   The observed number of runs = 19
   The expected number of runs = 196.9805
   162 Observations above K 248 below
        The test is significant at 0.0000

Runs Test

   C5

   K =   244.5327

   The observed number of runs = 19
   The expected number of runs = 196.9805
   162 Observations above K 248 below
        The test is significant at 0.0000

Regression Analysis

The regression equation is
C3 = - 0.60 + 1.00 C4

Predictor   Coef   StDev   T   P
Constant   -0.595   1.068   -0.56   0.578
C4   1.00148   0.00437   229.14   0.000

S = 0.3646   R-Sq = 99.2%   R-Sq(adj) = 99.2%

Analysis of Variance

Source   DF   SS   MS   F   P
Regression   1   6978.2   6978.2 52502.96   0.000
Residual Error 408   54.2   0.1
Total   409   7032.4

Unusual Observations

Obs	C4	C3	Fit	StDev Fit	Residual	St Resid
7	241	241.388	240.527	0.024	0.861	2.37R
8	242	242.286	241.291	0.022	0.995	2.74R
13	241	241.224	240.436	0.024	0.788	2.17R
15	240	240.758	239.953	0.025	0.804	2.21R
43	243	241.286	242.409	0.019	-1.123	-3.08R
71	242	240.535	241.403	0.021	-0.868	-2.39R
72	242	241.300	242.084	0.020	-0.784	-2.15R
105	254	253.626	253.284	0.044	0.342	0.94 X
106	254	253.136	253.303	0.044	-0.166	-0.46 X
158	242	240.566	241.330	0.022	-0.763	-2.10R
177	251	248.917	250.486	0.033	-1.569	-4.32R
186	245	245.816	244.941	0.018	0.874	2.40R
214	241	241.185	240.424	0.024	0.762	2.09R
216	241	241.327	240.265	0.024	1.062	2.92R
217	240	241.114	239.901	0.026	1.213	3.33R
218	240	240.816	239.803	0.026	1.012	2.78R
226	241	241.100	240.352	0.024	0.748	2.06R
277	254	254.334	254.080	0.047	0.255	0.70 X
281	252	252.265	251.440	0.037	0.825	2.27R
297	252	251.154	252.205	0.040	-1.052	-2.90R
300	252	250.570	251.406	0.037	-0.836	-2.30R
344	241	242.083	240.921	0.023	1.161	3.19R
355	239	239.507	238.734	0.029	0.773	2.13R
391	239	239.858	239.102	0.028	0.756	2.08R

R denotes an observation with a large standardized residual
X denotes an observation whose X value gives it large influence.

Durbin-Watson statistic = 1.23

Regression Analysis

The regression equation is
C3 = - 0.416 + 1.00 C5

Predictor	Coef	StDev	T	P
Constant	-0.4157	0.9741	-0.43	0.670
C5	0.999695	0.003983	250.99	0.000

S = 0.3330   R-Sq = 99.4%   R-Sq(adj) = 99.4%

Analysis of Variance

Source	DF	SS	MS	F	P
Regression	1	6987.1	6987.1	62995.04	0.000

Residual Error   408   45.3   0.1
Total   409   7032.4

Unusual Observations

Obs	C5	C3	Fit	StDev Fit	Residual	St Resid
7	241	241.388	240.554	0.022	0.834	2.51R
8	242	242.286	241.307	0.020	0.979	2.95R
13	241	241.224	240.488	0.022	0.736	2.21R
15	240	240.758	239.989	0.023	0.769	2.31R
21	241	241.543	240.856	0.021	0.686	2.06R
71	242	240.535	241.375	0.020	-0.840	-2.53R
72	243	241.300	242.044	0.018	-0.744	-2.24R
105	254	253.626	253.307	0.040	0.320	0.97 X
106	254	253.136	253.296	0.040	-0.159	-0.48 X
158	242	240.566	241.255	0.020	-0.689	-2.07R
177	251	248.917	250.140	0.029	-1.223	-3.69R
186	245	245.816	245.007	0.017	0.809	2.43R
214	241	241.185	240.504	0.022	0.681	2.05R
216	241	241.327	240.338	0.022	0.989	2.98R
217	241	241.114	240.047	0.023	1.066	3.21R
218	240	240.816	239.901	0.023	0.915	2.75R
226	241	241.100	240.368	0.022	0.732	2.20R
277	255	254.334	254.173	0.044	0.161	0.49 X
281	252	252.265	251.524	0.034	0.741	2.24R
286	251	250.754	250.086	0.029	0.667	2.01R
297	253	251.154	252.129	0.036	-0.975	-2.95R
315	242	240.899	241.600	0.019	-0.701	-2.11R
344	242	242.083	241.039	0.020	1.043	3.14R
355	239	239.507	238.807	0.027	0.700	2.11R
391	240	239.858	239.171	0.025	0.687	2.07R

R denotes an observation with a large standardized residual
X denotes an observation whose X value gives it large influence.

Durbin-Watson statistic = 1.31

Regression Analysis

The regression equation is
C4 = 0.395 + 0.997 C5

Predictor	Coef	StDev	T	P
Constant	0.3948	0.2652	1.49	0.137
C5	0.997336	0.001084	919.91	0.000

S = 0.09065   R-Sq = 100.0%   R-Sq(adj) = 100.0%

Analysis of Variance

Source	DF	SS	MS	F	P
Regression	1	6954.2	6954.2	846227.53	0.000
Residual Error	408	3.4	0.0		
Total	409	6957.6			

Unusual Observations

Obs	C5	C4	Fit	StDev Fit	Residual	St Resid
2	242	241.618	241.325	0.006	0.293	3.24R
10	242	241.724	241.519	0.005	0.205	2.27R
37	243	242.042	242.306	0.005	-0.264	-2.91R
43	242	242.645	242.183	0.005	0.461	5.10R
54	242	241.782	242.034	0.005	-0.252	-2.78R
105	254	253.504	253.518	0.011	-0.014	-0.15 X
106	254	253.522	253.508	0.011	0.015	0.16 X
129	253	253.220	252.898	0.010	0.323	3.58R
166	241	241.353	241.164	0.006	0.189	2.09R
168	242	241.806	241.586	0.005	0.220	2.43R
177	251	250.710	250.359	0.008	0.351	3.88R
212	242	242.180	241.864	0.005	0.316	3.50R
219	242	241.463	241.273	0.006	0.190	2.10R
254	243	242.923	243.217	0.005	-0.293	-3.24R
277	255	254.298	254.383	0.012	-0.085	-0.94 X
288	248	247.625	247.895	0.006	-0.270	-2.98R
291	246	245.916	246.138	0.005	-0.222	-2.45R
300	252	251.628	251.419	0.009	0.210	2.33R
301	252	251.516	251.305	0.009	0.211	2.34R
305	250	249.892	249.704	0.007	0.189	2.09R
323	251	250.879	250.689	0.008	0.190	2.11R
329	247	247.452	247.204	0.005	0.248	2.74R
362	239	239.231	239.018	0.007	0.213	2.36R
363	240	240.101	239.875	0.007	0.226	2.51R
365	240	239.895	239.678	0.007	0.218	2.41R
371	242	241.853	241.661	0.005	0.192	2.12R
405	240	239.913	239.646	0.007	0.267	2.96R

R denotes an observation with a large standardized residual
X denotes an observation whose X value gives it large influence.

Durbin-Watson statistic = 1.39

APPENDIX G. RESULTS OF SPLUS K-S TESTS

RESULTS OF SPLUS K-S TESTS FOR NORMALITY AND DISTRIBUTIONS

> ks.gof(check411a$V3,distribution="normal")

One sample Kolmogorov-Smirnov Test of Composite
Normality

data: check411a$V3
ks = 0.2059, p-value = 0
alternative hypothesis:
   True cdf is not the normal distn. with estimated parameters
sample estimates:
 mean of x standard deviation of x
  244.0366   4.143243

> ks.gof(check411a$V4,distribution="normal")

One sample Kolmogorov-Smirnov Test of Composite
Normality

data: check411a$V4
ks = 0.1909, p-value = 0
alternative hypothesis:
   True cdf is not the normal distn. with estimated parameters
sample estimates:
 mean of x standard deviation of x
  244.2683   4.122435

> ks.gof(check411a$V5,distribution="normal")

One sample Kolmogorov-Smirnov Test of Composite
Normality

data: check411a$V5
ks = 0.1931, p-value = 0
alternative hypothesis:
   True cdf is not the normal distn. with estimated parameters
sample estimates:
 mean of x standard deviation of x
  244.525   4.132398

> ks.gof(check411a$V3,check411a$V4)

Two-Sample Kolmogorov-Smirnov Test

data: check411a$V3 and check411a$V4
ks = 0.0876, p-value = 0.0754
alternative hypothesis:
  cdf of check411a$V3 does not equal the
          cdf of check411a$V4 for at least one sample point.

> ks.gof(check411a$V3,check411a$V5)

        Two-Sample Kolmogorov-Smirnov Test

data: check411a$V3 and check411a$V5
ks = 0.1557, p-value = 0.0001
alternative hypothesis:
  cdf of check411a$V3 does not equal the
          cdf of check411a$V5 for at least one sample point.

> ks.gof(check411a$V4,check411a$V5)

        Two-Sample Kolmogorov-Smirnov Test

data: check411a$V4 and check411a$V5
ks = 0.0779, p-value = 0.1481
alternative hypothesis:
  cdf of check411a$V4 does not equal the
          cdf of check411a$V5 for at least one sample point.

>

Appendix H. LIDAR Vendors

Proprietary Systems

Company	Location	Sensor
John Chance	LA	FLI-MAP
TerraPoint	TX	ALTMS

FLI-MAP - Fast Laser Imaging and Mapping Airborne Platform (Helicopter Based System)
ALTMS - Airborne Lidar Topographic Mapping System

LIDAR Sensor Manufactures

Company	Location	Sensor	Number U.S. Operating
Optech	Canada	ALTM	6
Azimuth	U.S.	AeroScan	5
Nortech	Canada	ATLAS	1
TopoEye	Sweden	TopoEye	1

ALTM - Airborne Laser Terrain Maper
ATLAS- All Terrain Laser Acquisition System

U.S. Based Companies Operating Optec's ALTM Sensor

Company	Location
Airborne 1	CA
Analytical Surveys Inc.	IN
Atlantic Technologies	AL
Laser Mapping Specialists	MS
Waggoner Engineering	MS
Woolpert	OH

U.S. Based Companies Operating Customized Variations of the Azimuth's AeroScan System

Company	Location
3001: The Spatial Data	LA
EagleScan	CO
EarthData	MD
EnerQuest	CO
Spencer B. Gross	OR

U.S. Based Companies Operating the Following LIDAR Sensors

Sensor	Company	Location
TopoEye	Aerotec	LA
Nortech ATLAS	Magnolia Group	TX